WIDEBAND NON-LINEAR PIEZOELECTRIC VIBRATION ENERGY HARVESTING

WAN AHMAD FAIZ BIN WAN HASHIM

UNIVERSITI TEKNIKAL MALAYSIA MELAKA

WIDEBAND NON-LINEAR PIEZOELECTRIC VIBRATION ENERGY HARVESTING

WAN AHMAD FAIZ BIN WAN HASHIM

**This report is submitted
in fulfillment of the requirement for the degree of
Bachelor of Mechanical Engineering**

Faculty of Mechanical Engineering

UNIVERSITI TEKNIKAL MALAYSIA MELAKA

2019

DECLARATION

I declare that this project report entitled "Wideband Non-linear Piezoelectric Vibration Energy Harvesting" is the result of my own work except as cited in the references.

Signature : ....

Name : ....

Date : ....

APPROVAL

I hereby declare that I have read this project report and in my opinion this report is sufficient in terms of scope and quality for the award of the degree of Bachelor of Mechanical Engineering.

Signature : ....

Name of Supervisor : ....

Date : ....

DEDICATION

To my beloved mother and father

ABSTRACT

Kinetic energy exists in the form of vibrations, forces and any random displacements. Harvesting the kinetic energy is needed in order to generate electricity and prevent it to be wasted. Energy harvesting can be defined as processes that capture the freely available energy in environment and converting it in electrical energy that can be used or stored. Piezoelectric is used to convert mechanical energy to electrical energy. Piezoelectric produces charge when piezoelectric material compressed or mechanically stressed. Basically, energy harvesters are designed as a linear system in order to achieve optimal performance but most ambient energy is sensitive and having different frequency. Due to that, the linear energy harvesters need to tune for every application in order to prevent from narrow bandwidth. To solve this problem, a non-linear mechanism is suggested, which is wider bandwidth can be obtained in one mechanism. In addition, by using non-linear energy harvesting, it able to produce wider bandwidth without any adjustment. A non-linear energy harvester is designed as a cantilever beam with mechanical stopper at upper and bottom side of the beam. The piezoelectric is attached on the beam so that it will deflect along with the beam. The aim of this mechanism is to provide a wider bandwidth with maximum power harvested. The experimental results for the linear and non-linear device are obtained by using quasi-static and dynamic measurement. The quasi-static measurement is used to measure the restoring force against the deflection of beam. Meanwhile, dynamic measurement is used to measure the dynamic response for characterisation of the device. The performance of open circuit and closed circuit of system are also investigated. The system is varied by changing the length of the beam, position of the stopper and input level.

ABSTRAK

Tenaga kinetik wujud dalam bentuk getaran, daya dan sebarang pengalihan secara rawak. Untuk menjana tenaga elektrik, penuaian tenaga kinetik diperlukan atau sebaliknya tenaga kinetik tersebut akan terbuang. Penuaian tenaga boleh ditakrifkan sebagai proses yang menangkap tenaga bebas yang terdapat di persekitaran dan mengubahnya kepada tenaga elektrik yang boleh digunakan atau disimpan. Piezoelektrik digunakan untuk menukar tenaga mekanikal kepada tenaga elektrik. Piezoelektrik menghasilkan caj apabila bahan piezoelektrik dimampatkan atau ditekan secara mekanikal. Pada asasnya, penuai tenaga direka dalam bentuk linear bagi mencapai prestasi optimum tetapi tenaga bebas yang terdapat di persekitaran adalah sensitif dan mempunyai frekuensi yang berbeza-beza. Oleh itu, penuai tenaga linear perlu menyesuaikan diri untuk setiap aplikasi untuk mengelakkan dari lebar jalur menjadi sempit. Untuk menyelesaikan masalah ini, satu mekanisma bukan linear dicadangkan, yang merupakan jalur lebar yang lebih luas boleh diperolehi dalam satu mekanisma. Di samping itu, dengan menggunakan penuaian tenaga bukan linear, ia dapat menghasilkan jalur lebar yang lebih luas tanpa sebarang pelarasan. Penuai tenaga bukan linear direka sebagai rasuk penyangga dengan penahan mekanikal di sebelah atas dan bawah rasuk. Piezoelektrik dipasang pada rasuk supaya ia memesong bersama rasuk. Matlamat mekanisma ini adalah untuk menyediakan jalur lebar yang lebih luas dengan kuasa maksimum dituai. Keputusan eksperimen untuk peranti linear dan bukan linear diperoleh dengan menggunakan pengukuran kuasi statik dan dinamik. Pengukuran kuasi statik digunakan untuk mengukur daya pengembalian terhadap pesongan rasuk. Sementara itu, pengukuran dinamik digunakan untuk mengukur tindak balas dinamik untuk pencirian peranti. Prestasi litar terbuka dan sistem litar tertutup juga disiasat. Sistem ini diubah dengan mengubah panjang rasuk, kedudukan penahan dan tahap input.

ACKNOWLEDGEMENTS

Alhamdulillah, by the grace of Al-Mighty that I have finally completed my final year project report. I would like to take this opportunity to gratitude to all people who guide me in all aspect towards the completion of this project. Not forgetting to my supervisor on this project, Prof Madya Dr. Roszaidi Bin Ramlan for his guidance, patience, motivation and idea throughout my final year project. Besides that, I would like to thank my beloved parents who never stopped praying for my welfare and always supported me morally as well as economically. Last but not least, special thanks to everyone especially to all my friends who supported me directly or indirectly for letting me to finish this report effectively.

TABLE OF CONTENT

LIST OF FIGURES

LIST OF TABLES

CHAPTER 1

INTRODUCTION

1.1 Background

Energy is the capacity to do work. It may appear in many forms such as potential energy, thermal energy, kinetic energy and more. Basically, energy is associated with motion and can be converted to another form in various ways. For example, kinetic energy generators able to convert energy in the form of mechanical movement present in application environment into electrical energy. Kinetic energy exists in the form of vibrations, forces and any random displacements. Kinetic energy could produce motion, sound, thermal energy and electrical energy. In order to generate a clean electricity, harvesting the kinetic energy are needed or otherwise it be wasted.

Energy harvesting can be defined as the sum of all those processes that allow capturing the freely available energy in environment and converting it in electrical energy that can be used or stored. Harvesting energy is one of the most promising techniques in response to global energy problem. Nowadays, most vibration-based energy harvesters are designed as linear resonators that only work efficiently with limited bandwidth near their resonant frequencies. Unfortunately, in the vast majority of practical scenarios, ambient vibrations are frequency-varying or aimless with energy distributed over a wide frequency range. Therefore, increasing the bandwidth of vibration energy harvesters has become one of the most critical issues before these harvesters can be widely deployed in practice.

1.2 Problem Statement

In linear energy harvesting system, maximum power can be obtain when device is operated at the natural frequency of the system, ($\omega_{system} = \omega_n$). But, if the harvester is mistuned, a slight shift of excitation frequency will drop the performance of the system. Most ambient energy is frequency-varying and sensitive. Due to that, the linear energy harvesters need to adjust for every application in order to prevent from narrow frequency range. To solve this problem, a non-linear mechanism is suggested, which is a wide frequency range can be obtained in one mechanism. Furthermore, by using non-linear energy harvester, there is no need to adjust or tune towards wider bandwidth. So, the device can cover the bandwidth and optimize the performance. The harvester should be carefully designed in accordance with prescribed procedure.

1.3 Objectives

The objectives of this project are:

a) To characterise the linear and non-linear mechanism in energy harvesters.

b) To design and develop the non-linear energy harvester.

c) To investigate the performance of the non-linear piezoelectric energy harvester.

1.4 Scope

This research is studies the effect of non-linear energy harvester with appearance of piezoelectric. A non-linear energy harvester can be simply design as a cantilever beam with rectangular cross-section. A pair of mechanical stopper is added at upper and bottom side of the beam. The gap between stopper and beam is expected to inherit the features of resonant peaks and hardening dynamics for bandwidth widening. The experiment will be conducted by two types of measurement, which are quasi-static measurement and dynamic measurement. The system is varied by changing the length of the beam, position of the stopper and the input level.

CHAPTER 2

LITERATURE REVIEW

There is energy in everything and energy is used in everything. Energy is the ability to do work and it fall in two categories: non-renewable and renewable. Non-renewable energy is energy that comes from the ground and it is not replaced in relatively short amount of time. For examples, energy generated from combustion of fossil fuels, coal, natural gas and etc. Most of fossil fuels such as oil, natural gas and coal are considered as non-renewable resources. Their used is not sustainable because their formation takes a billion years. The term of non-renewable resources also refers to minerals and metals from the earth, such as gold, silver and iron, which is similarly formed as long-term results of geological processes such as plate tectonics. These resources often cost to mine, as they are usually deep within the earth but there are more abundant than fossil fuels. Some types of groundwater are considered as non-renewable resources, if the aquifer is unable to be replenished at the same rate at which it is drained. Also, nuclear materials such as uranium are referring as non-renewable resources. Meanwhile, renewable energy can be generated continuously practically without of decay of source. Some of examples are solar energy, wind energy, hydro energy, geothermal energy and kinetic energy. Renewable sources of energy are better than non-renewable sources because they refill themselves over a short period time while non-renewable resources have a limited quantity and it will be run out. The world is taking a serious look at ways to make a renewable source of energy.

It is all begin with the sun. Solar power is energy from the sun and without its presence, all life in earth will end. Solar energy is a powerful source of energy. Radiant energy is produced by the sun and able to convert to useful energy such as electricity. Radiation from the sun can be visible (light) and invisible (infrared, ultraviolet and etc.). Radiant light and heat from the sun is harnessed by solar collection method such as solar cell, solar heating, solar architecture, photovoltaic and more. Solar energy technology is used widely to provide electricity, light, heat, hot water even cooling for homes, business and industries. Solar panel converts the radiant light into usable energy using N-type and P-type semiconductor material. When sunlight is absorbed by these materials, the solar energy knocks electron loose from their atoms, allowing the electron to flow through the material to produce electricity. Currently, solar panel converts most of the visible light spectrum and about half of the ultraviolet (UV) and infrared light spectrum to usable solar energy. This process converting light (photons) to electricity (voltage) is called photovoltaic (PV) effect. The Solar Photovoltaic is the largest growing renewable energy employer worldwide with an increasing need for experts than can support this growth. Figure 2.1 shows an example of solar photovoltaic system. Solar energy is the cleanest, does not produce any noise and most well-supplied renewable energy source available.

Figure 2.1: Solar photovoltaic system.

Wind is the movement of air or gases on a large scale from areas of high pressure to areas of low pressure. In meteorology, winds are often to refer to their strength and direction of the wind blowing. Winds had been used as energy resources in a long time. The main source that drives the wind is the sun. The sun warms the earth and creates wind. Wind energy is a renewable energy source that uses wind power to generate electricity. Wind power is obtain due to the speed of the air flow through to turn the blades of huge turbines which spin generators and create electricity. Wind turbine (Figure 2.2) is the most popular source for wind energy including the windmills. There are many types of wind turbines such as vertically axis wind turbine, horizontally axis wind turbine and more. Wind energy is a clean energy because it produces no emissions, no pollutants and does not produce carbon dioxide (CO2), so it is does not contribute to the greenhouse effect. Meanwhile, the turbines may be ugly to look at and affect wild bird population. They can be a danger to flying animals. Wind farms require large tracts of land and produce negative visual impact on the landscape. Though the wind is free, the installation of wind energy system may be very expensive.

Figure 2.2: Wind turbines.

Hydro means water. Meanwhile, hydropower is an energy come from the force moving water. The water has mass and it flow and falls downward due to gravitational force. Hydroelectric energy is the production of energy power through the use of gravitational force of flowing or falling water. Form Figure 2.3, the water is stored or moving through the reservoirs, flowing rivers, streams, waterfall and etc. The water flowing has kinetic energy and it can generate electrical energy. Usually, the dam need to build and let the water fall or flow it gradually. The dam is used to control and stabilize water flow. Meanwhile, it can help to restore the water levels of inland lakes and seas. The energy is obtained by the flow or fall of water from a height a level below which causes the movement of hydraulic or turbine wheels. The water can be stored and be used whenever the energy needed. There is no pollution in hydro energy because nothing gets burn. The disadvantages of using hydro energy are a lot of money needed to build a dam and the dam can ruin the environment, because it changes where the natural water flows and some animals and plants may die.

Figure 2.3: Sayano-Shushenskaya hydropower plant.

The word geothermal originated from the Greek roots, *geo* means earth and *thermos* means heat. In simple means, geothermal energy is energy extract from heat stored in the earth. Thermal energy is the energy that is related to the temperature of matter. Geothermal energy is the exploitation of heat energy from the molten core of the earth. The deeper region of the earth crust is very hot. The heat melts rocks from the molten core of the earth and form magma. The magma moves up and collects at below some places called hot spots. The underground water in contact with hot spot gets heated and produces steam at high pressure. In crust region, holes can be drilled into hot-rocks and make the steam coming out from the ground water. Then, the steam drive the generators (rotates the turbines) to produce electricity. Geothermal power plants are power plants that use the Earth‟s core to produce electricity. The source is the almost unlimited amount of heat generated by the Earth‟s core. The main advantage of using geothermal energy is that it does not create any pollution. Therefore, it has helped in reducing global warming. Some of disadvantages are high start-up cost and the source is close to volcanic activity.

Kinetic energy is one of the main types of energy. Kinetic energy also one of the newest emerging sources for clean energy. Kinetic energy is associated with object in motion and not all kinetic energy is produced by physical objects. It is defined as energy in motion of waves, electrons, atoms, molecules and substances. Energy due to motion depends on mass and speed of object. The greater speed and mass, the greater kinetic energy produced. Kinetic energy could produce motion, sound, thermal energy and electrical energy. For example, about a brake pad on a bicycle wheel, the movement of the wheels is progressively stopped using friction and the kinetic energy is transformed to heat (thermal energy). Kinetic energy can be made by many different types of movement such as translation, rotation and vibration. Translation is a movement from place to place. Rotation is a movement about an axis while vibration is a repetitive "back to forth motion".

The production of the kinetic energy is the simplest among all energies. It is only required a movement from any object while the solar power generator need a complicated designed to collect the radiation from the sun. Same goes to the dam from hydro power, windmills from wind power and geothermal power plant, all of them were hard to handle. Kinetic energy makes up almost all of the energy in motion throughout the world. In order to generate a clean electricity, harvesting the kinetic energy are needed or otherwise it be wasted.

2.1 General resonant generator theory

This section will discuss the fundamental of kinetic energy harvesting. Energy harvesting is the process of taking the wasted energy from natural energy sources, collecting and save it for later use [1]. Kazmierski and Beeby [2] define that energy harvesting is the conversion of ambient energy that exist in the environment and convert into electrical energy. Harvesting energy is one of the most promising techniques in response to global energy problem without lowering the resources. Williams and Yates [3, 4] were the first developers that define the generic model for kinetic energy harvesters. Kinetic energy harvesting (mainly in form vibrations) is converting the movement to electricity. Vibration energy is well suited to inertial generators with the mechanical component that attached to inertial frame which acts as the fixed references. Second-order spring and mass system with the linear damper is used as the general analysis. The system presents a draft of resonant generators and its focus to important aspects that are applicable to all transduction mechanism. Figure 2.4 shows a general example of a system.

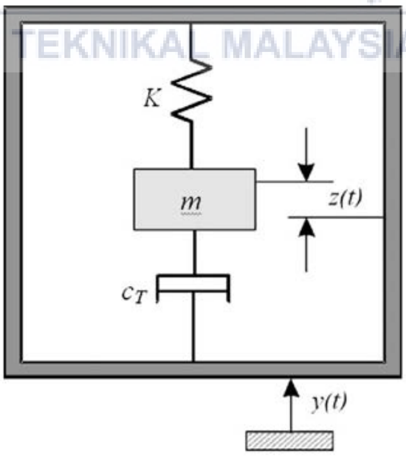

Figure 2.4: Base excitation of spring-mass-damper.

The system is based on a seismic mass, m, and on a stiffness of the spring, k. Energy losses in system are considered to be as damping coefficient, c_T. Damping coefficient, c_T, is consists of parasitic loss mechanisms, c_p and electric energy extracted by the transduction mechanism, c_e. The generator is driven by a harmonic base excitation, $y(t) = Y\sin(\omega t)$, it will move out of phase with the mass at resonance resulting in net displacement, $z(t)$, between the mass and frame. All documents about theory of inertial-based generator can be taken from [5] and it will be discussed.

The governing equation of motion is given

$$-k(x-y)(t) - c(\dot{x}-\dot{y})(t) = m\ddot{x}(t)$$

where relative displacement is $z = x - y$

$$-k(z)(t) - c(\dot{z})(t) = m(\ddot{z}+\ddot{y})(t)$$

$$m\ddot{z}(t) + c\dot{z}(t) + kz(t) = -m\ddot{y}(t) \qquad (1)$$

For harmonic motion, substitute $z = Ze^{j\omega t}$ and $y = Ye^{j\omega t}$

$$m\left(-\omega^2 Ze^{j\omega t}\right) + c\left(j\omega Ze^{j\omega t}\right) + k\left(Ze^{j\omega t}\right) = -m\left(-\omega^2 Ye^{j\omega t}\right)$$

divide with $e^{j\omega t}$

$$m(-\omega^2 Z) + c(j\omega Z) + k(Z) = m(\omega^2 Y)$$

$$Z(-\omega^2 m + j\omega c + k) = m\omega^2 Y$$

$$\frac{Z}{Y} = \frac{m\omega^2}{\sqrt{(k-\omega^2 m)^2 + c^2\omega^2}} \qquad (2)$$

In order to maximize power output, the excitation frequency must equal with the natural frequency of the system ($\omega_{system} = \omega_n$).

$$\omega_n = \sqrt{\frac{k}{m}} \tag{3}$$

The instantaneous power that absorbed by the damper is

$$P_{inst} = F\,dx = F\,(vdt) = (c\dot{x})(\dot{x}dt) = c\dot{x}^2dt \tag{4}$$

and for $\dot{x} = \omega X cos(\omega t - \boldsymbol{\phi})$, the energy harvester per cycle is

$$\begin{aligned} E_{cycle} &= \int_0^{\tau=\frac{2\pi}{\omega}} P_{inst}\,dt \\ &= \int c[\omega X cos(\omega t - \boldsymbol{\phi})]^2\,dt \\ &= c\omega^2X^2 \int cos^2(\omega t - \boldsymbol{\phi})\,dt \\ &= c\omega^2X^2 \int \left[\frac{cos2(\omega t - \phi)}{2} + \frac{1}{2}\right] dt \\ &= c\omega^2X^2 \left[\frac{sin2(\omega t - \phi)}{2}\cdot\frac{1}{2} + \frac{t}{2}\right]_0^{\frac{2\pi}{\omega}} \\ &= c\omega^2X^2 \left[\left(\frac{\pi}{\omega}\right) - 0\right] \\ &= \pi c\omega X^2 \end{aligned} \tag{5}$$

where $\tau = 2\pi/\omega$ and averaged power flow in the system is defined as

$$P_{ave} = \frac{E_{cycle}}{\tau} = \frac{\pi c \omega X^2}{(2\pi/\omega)} = \frac{c\omega^2 X^2}{2} \tag{6}$$

substitute X with Z from Equation (2),

$$\begin{aligned} P_{ave} &= \frac{c\omega^2 X^2}{2} = \frac{c\omega^2 Z^2}{2} \\ &= \frac{c\omega^2}{2}\left[\frac{m\omega^2 Y}{\sqrt{(k-\omega^2 m)^2 + c^2\omega^2}}\right]^2 \\ &= \frac{cm^2\omega^6 Y^2}{2[(k-\omega^2 m)^2 + c^2\omega^2]} \end{aligned} \tag{7}$$

in dimensionless form, the equation for the average power dissipated behaviour within the damper (i.e. the power extracted by transduction mechanism and the power lost through parasitic damping mechanism) is given in Equation (8) by [4].

$$P_{ave} = \frac{m\zeta_T Y^2 (\frac{\omega}{\omega_n})^3 \omega^3}{[1-\left(\frac{\omega}{\omega_n}\right)^2]^2 - [2\zeta_T(\frac{\omega}{\omega_n})]^2} \tag{8}$$

where ζ_T is total damping factor given by $\zeta_T = c_T/2m\omega_n$. The unit for average power is energy per second. Maximum power can be obtain when device is operated at the natural frequency of the system, ω_n. For this case, P_{ave} is given

$$P_{ave} = \frac{mY^2{\omega_n}^3}{4\zeta_T} \tag{9}$$

Since the peak of acceleration of the base, A, is given by $A = \omega^2 Y$ and damping factor is related to the damping coefficient, $c_T = 2m\omega_n\zeta_T$, Equation (9) can be written in form:

$$P_{ave} = \frac{(mA)^2}{2c_T} \tag{10}$$

Incorporating the parasitic and electrical damping into Equation (8), it gives the average power delivered to the electrical domain as:

$$P_{ave} = \frac{m\zeta_e A^2}{4\omega_n(\zeta_e + \zeta_p)^2} \tag{11}$$

Maximum power is delivered to electrical domain when damping arising from electrical domain equal to mechanical losses, $\zeta_e = \zeta_p$. This applies when *z(t)* less than or equal z_{max}. In this case, Equation (11) can be simplifies to:

$$P_{max} = \frac{mA^2}{16\omega_n\zeta_p} \tag{12}$$

2.1.1 Transduction damping coefficients

Energy sources such as human activities [6] are considered for harvesting by employing electromagnetic, electrostatic and piezoelectric transduction methods [7-9]. All of them are the main transduction mechanisms in energy harvesting. Electricity can be obtained through transduction mechanisms by exploiting the mechanical strain or relative displacement occurs in the system. The effect from the strain exploits a deformation and employs active materials in order to generate electrical energy. Every transduction mechanism has the same output (electricity) but different in damping characteristic. These differences should be taken into consideration and it need to be carefully in modelling the generators.

Not all the energy transduced into electrical domain, some will be delivered into the load. For example coil losses in electromagnetic transduction, some of the power delivered to electrical domain is lost within the coil. The actual power in the load is a function of the coil and load resistances, as shown in Equation (13) [10].

$$P_{max} = \frac{mA^2}{16\omega_n \zeta_p} \left(\frac{R_{Load}}{R_{Coil} + R_{Load}} \right) \tag{13}$$

At the same time, the coil and the load resistance also affect the damping factor arising from electromagnetic transduction, c_e. The damping coefficient arising from electromagnetic transduction, c_e can be estimated from Equation (14) [11].

$$c_e = \frac{(NlB)^2}{R_{Coil} + R_{Load} + j\omega L_{Coil}} \tag{14}$$

where N is the number of turns in the generator coil, l is the side length of the coil (assumed square) and B is the flux density to which is subjected. R_{Coil} is represented as coil resistance, R_{Load} is load resistance and L_{Coil} is coil inductance.

Next, an expression for the damping coefficient arising from piezoelectric transducer can be estimated from Equation (15) [12].

$$c_{piezo} = \frac{2m\omega_n^2 k^2}{2\sqrt{\omega_n^2 + [1/(C_{Load}R_{Load})^2]}} \tag{15}$$

where k represented as the piezoelectric material electromechanical coupling factor while C_{Load} is load capacitance and R_{Load} is load resistance. Same as before, R_{Load} can be used to optimize the ζ_e and optimum value can be construct from Equation (16). When $\zeta_e = \zeta_p$, the maximum power is obtained.

$$R_{opt} = \frac{1}{\omega_n C}\frac{2\zeta_p}{\sqrt{4\zeta_p^2 + k^4}} \tag{16}$$

Furthermore, electrostatic transduction is represented by a constant force damping effect, indicated as Coulomb damping and the basic system is shown in Figure 2.5 [13].

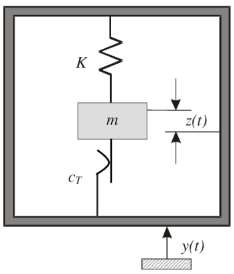

Figure 2.5: Model of an electrostatic resonant generator

The energy dissipated within the damper of the system and the power is given by the force-distance of the product. The expression for the power in electrostatic transduction is shown in Equation (17) where $\omega_c = \omega/\omega_n$ and $U = \sin(\pi/\omega_c)/[1+\cos(\pi/\ \omega_c)]$.

$$P = \frac{4y_o F\omega\omega_c^2}{2\pi}[\frac{1}{1-\omega_c^2} - \left(\frac{FU}{mY_o\omega^2\omega_c}\right)^2]^{1/2} \tag{17}$$

and Equation (18) shows the optimum damping force in electrostatic transduction.

$$F_{opt} = \frac{y_o\omega^2 m}{\sqrt{2}}\frac{\omega_c}{|(1-\omega_c^2)U|} \tag{18}$$

The paper by Mitcheson *et al.* [13] can be as a reference for further details.

2.2 Generators

Basically, a vibration generator is a type of electric generator that converts vibration (kinetic energy) to electricity. There are three main approaches that can be used to implement a vibration-powered generator and those were electromagnetic, electrostatic and piezoelectric generator. All of the three generators will be discuss on the other section.

2.2.1 Electromagnetic generators

Electromagnetic principles deal with the relationship between electricity and magnetism, as well as the relationship between magnetism and electricity. The production of electric current across a conductor when exposed to a changing magnetic field is known as electromagnetic induction. The current is induced in the coil due to relative motion between magnet and coil. In principle, either the coil or magnet will be placed on the beam while the other will remain fixed. The amount of electricity produces depends on the using stronger magnet (strength of the magnetic field), the speed of motion between magnet-coil, length of wire and the using a coil of wire consisting more turns or a larger area. Figure 2.4 can be used to describe the operation of electromagnetic generator. The electromagnetic transduction depends on the damper, *c*. The implementation of this method can be made either in micro scale (wafer-scale) and macro scale.

Beeby *et al.* [14] have developed a silicon-based generator consisted of micromachined paddle, four NeFeB magnets and a wire-wound coil, as shown in Figure 2.6. Two of thagnets are placed within etched recesses in the two Pyrex wafers, which are anodically bonded to each face of the silicon wafer. The coil is placed on a silicon cantilevered paddle, which is designed to vibrate laterally in the plane of the wafer. The resonant frequency is obtained at 9.5 kHz and generated 21 nW of the electrical power from 1.92 ms^{-2} rms.

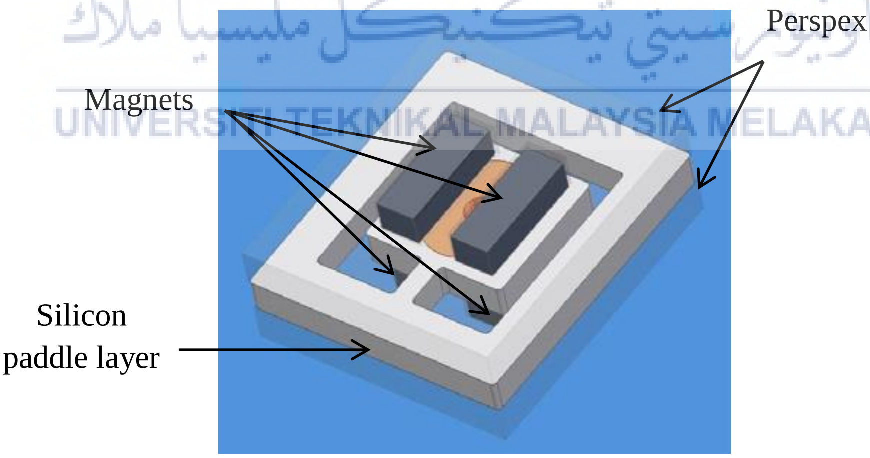

Figure 2.6: A silicon electromagnetic generator by Beeby *et al.* [14].

Huang *et al.* [15] proposed an electromagnetic harvester consisted of a planar copper coil, a nickel-iron spring element and a magnet. A „finger tap" action can produces 100 Hz and capable to generates 0.16µW. Perez-Rodriguez *et al.* [16] also used a similar design that used a polyimide film as the spring, a NdFeB magnets and a planar coil that made from 1.5 µm thick aluminium layer. Figure 2.7 shows a cross-section of the device. A displacement of 10µm produces a resonant frequency of 400 Hz and generates power at 1.44µW.

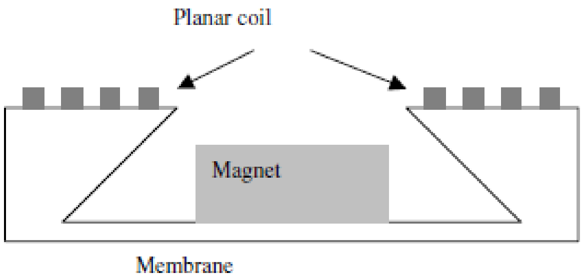

Figure 2.7: A cross-section of inertial generator by Perez-Rodriguez *et al* [16].

For macro-scale implementations, El-Hami *et al.* [11] proposed a vibration-based power generator comprises a cantilever beam (spring), fixed at one end and supporting a pair of NdFeB magnets (mass) on a c-shaped core at free end. The coil is made up of enamelled copper with many turns and fixed in between the poles of the magnets, as shown in Figure 2.8. The power generation is dissipating at 1mW for a volume of 240 mm^3 at a frequency of 320 Hz.

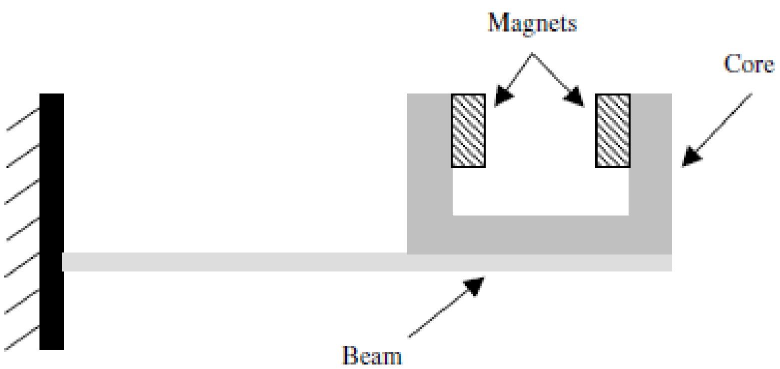

Figure 2.8: The electromagnetic generator proposed by El-Hami *et al.* [11].

Glynne-Jones *et al.* [17] followed the previous work by El-Hami *et al.* [11]. A system using different magnet configuration (different combinations of the magnets and the coils) and two prototypes have been found. The first prototype was based on a moving coil between two fixed magnets and had an overall volume of 0.84 cm^3 while the second prototype used four magnets and having a volume of 3.15 cm^3, as shown in Figure 2.9. The improvement of the magnetic coupling between magnets and coils makes the second prototype generates more power than first one.

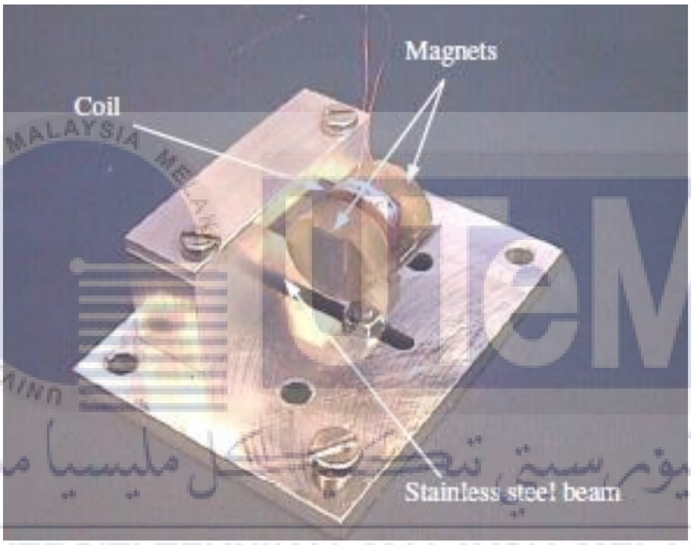

Figure 2.9: An electromagnetic resonator by Glynne-Jones *et al.* [17].

2.2.2 Electrostatic generators

Next, this section will discuss about the basic concepts and operating principle system in electrostatic generators. Electrostatics transduction exploits the relative movement between two dielectrically isolated electrodes (capacitor). The plates are charged by periodic connection to a voltage source or by the use of electrets. The electrostatic potential energy is stored in capacitors. Firstly, the definition of capacitance is given by

$$C = \frac{Q}{V} \tag{19}$$

where C the capacitance in farads, Q is the charge in coulombs and V is voltages on plates in volts. For parallel plate capacitor, C is given by

$$C = \varepsilon \frac{A}{d} \tag{20}$$

where ε is the permittivity of the material between the plates in Fm^{-1}, A is the area of the plates in m^2 and d is the distance separation between the plates in m. Equation (20) can be expressed in terms of the dielectric constant, $k = \varepsilon/\varepsilon_o$ with the permittivity of the material of free space, ε_o, of the insulator material, as shown in Equation (21).

$$C = k\varepsilon_o \frac{A}{d} \tag{21}$$

The voltage across the plate capacitor is given by

$$V = \frac{Qd}{\varepsilon_o A} \tag{22}$$

The energy stored in a capacitor, with the plate charge, Q and potential difference, V is given by

$$E = \frac{1}{2}QV = \frac{1}{2}CV^2 = \frac{1}{2}\frac{Q^2}{C} \tag{23}$$

If the charge on the plates is held constant, the perpendicular force between the plates is shown in Equation (24).

$$F = \frac{Qd}{\varepsilon A} \tag{24}$$

If the voltage between the plates is held constant the perpendicular force between the plates is given by

$$F = \frac{1}{2}\frac{\varepsilon AV^2}{d^2} \tag{25}$$

Harvested energy is obtained from the work done against the electrostatic force between the plates. In microelctromechanical systems (MEMS), the separation between the two plates is typically very small (nm to µm range). Electrostatic generators can be categorized into three types [18] and the first type is in plane overlap varying as shown in Figure 2.10. Second, out plane gap closing, as shown in Figure 2.11 and the third is in plane gap closing, as shown in Figure 2.12.

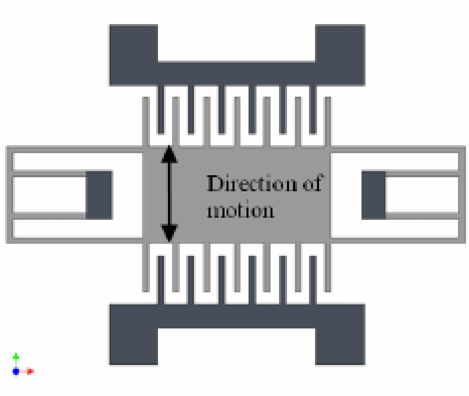

Figure 2.10: In plane overlap varying

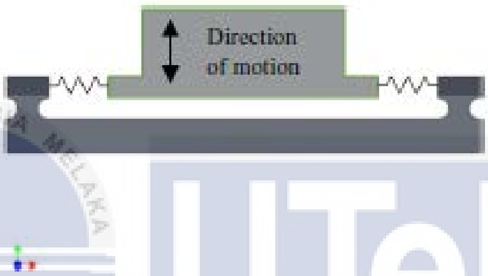

Figure 2.11: Out of plane gap closing

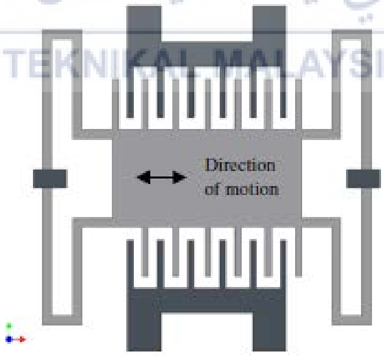

Figure 2.12: In plane gap closing

Note that both in plane configurations create two variable capacitors with the capacitances 180^{o} out of phase. All three approaches can be operated either in charge constrained or voltage constrained cycles. Voltage constrained approach more energy than the charge constrained. Nevertheless, by incorporating a capacitor in parallel with the energy harvesting capacitor, the energy from the charge constrained system can approach that of the voltage constrained system as the parallel capacitance approaches infinity. This parallel capacitor effectively constrains the voltage on the energy harvesting capacitor [19].

Table 1 provides the electrostatic force variation for the three configurations where *x* is the displacement of the internal mass [20]. For a high damping configuration the electrostatic damping force has to be counter balanced almost entirely by mechanical spring force.

Table 1: Electrostatic force variation for the three configurations

Structure	Charge constrained	Voltage constrained
In plane overlap varying	$F_e \sim \frac{1}{x^2}$	$F_e = \text{constant}$
Out plane gap closing	$F_e = \text{constant}$	$F_e \sim \frac{1}{x}$
In plane gap closing	$F_e \sim x^2$	$F_e \sim \frac{1}{x^2}$

In plane gap closing generates the highest power output with an optimized design producing 100μW cm^{-3}, follow by out plane gap closing and the lowest is by in plane overlap varying. These ranking is provided by Roundy [12]. Maximum power generation exists for very small dielectric gaps.

2.2.3 Piezoelectric generators

Piezo literally means to squeeze or press in Greek. Piezoelectric is a material that able to generate electric potential (voltage) when mechanical stress is applied. In piezoelectric material, an internal charge can be produced when mechanical stress (pressure) or strain (deformation) is applied. This charge can be described as electrical potential energy (voltage) that can be used like other source. Piezoelectric materials are applicable in many forms. For example, single crystal (e.g. quartz), piezoceramic such as lead zirconate titanate or PZT (Figure 2.13), thin film (e.g. zinc oxide) and polymeric materials such as polyvinylidenefluoride (PVDF) [21].

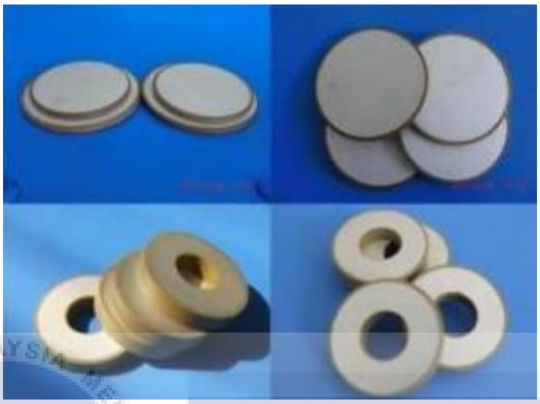

Figure 2.13: Lead zirconate titanate or PZT

Since piezoelectric materials are anisotropic, their physical constants (elasticity, permittivity and etc.) were tensor quantities and related to both the direction of the applied stress, electric field and to the directions perpendicular to these. The level of piezoelectric activity of a material is defined by symbol and notation [22]. The rectangular coordinate system for notation of axes is shown in Figure 2.14.

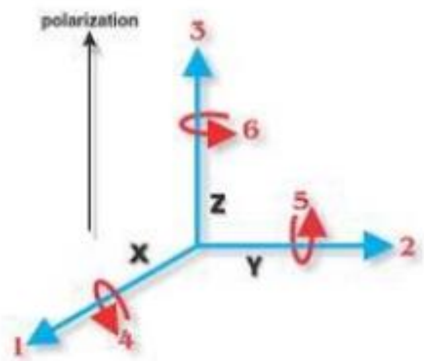

Figure 2.14: Notation of axes

The direction of positive polarization is usually in Z- axis. Furthermore, the direction of X, Y and Z are represented 1, 2 and 3 respectively. Then, the axes by 4, 5 and 6 are about the shear. A series of constants used in conjunction with the axes and notation. The permittivity, ε, for a piezoceramic material is the dielectric displacements per unit electric field. Next, the piezoelectric charges constant, d, is the polarization generated per unit of mechanical stress applied to a piezoelectric material or, alternatively, is the mechanical strain experienced by a piezoelectric material per unit of electric field applied.

$$d = \frac{Charge}{Applied\ Stress}\ \ (C/N) \tag{26}$$

$$d = \frac{Strain\ Developed}{Applied\ Field}\ \ (m/V) \tag{27}$$

Other relevant piezoelectric constants include the piezoelectric voltage constant, g, which is defined as the electric field generated per unit of mechanical stress applied or, alternatively, the mechanical strain experienced per unit of electric displacement applied. Lastly, the electro-mechanical coupling factor, k, is an indicator of effectiveness with which a piezoelectric material converts electrical energy into a mechanical energy, or converts mechanical energy to electrical energy. This defined in Equation (28).

$$k^2 = \frac{Energy\ Converted}{Input\ Energy} = \frac{Electrical\ Energy\ Stored}{Mechanical\ Input\ Energy} = \frac{W^e}{W^m} \tag{28}$$

These constants are anisotropic and the constants are generally given two subscripts indices which refer to the direction of the two relative quantities (e.g. stress and strain for elasticity, displacement and electric field for permittivity). Furthermore, a superscript is used to indicate a quantity that constants. For a brief explanation of the constants the reader is referred to the IEEE standards [23]. Table 2 provides the coefficients of common piezoelectric materials such as hard lead zirconate titanate piezoceramics (PZT-5A), soft lead zirconate titanate piezoceramics (PZT-5H), barium titanate ($BaTiO_3$) and polyvinylidenefluoride (PVDF).

Table 2: Coefficients of several piezoelectric materials [24, 25].

Property	PVDF	$BaTiO_3$	PZT-5A	PZT-5H
$d_{33}(10^{-12}CN^{-1})$	-33	149	374	593
$d_{31}(10^{-12}CN^{-1})$	23	78	-171	-274
$g_{33}(10^{-3}VmN^{-1})$	330	14.1	24.8	19.7
$g_{31}(10^{-3}VmN^{-1})$	216	5	-11.4	-9.1
k_{33}	0.15	0.48	0.71	0.75
k_{31}	0.12	0.21	0.31	0.39
$(\varepsilon/\varepsilon_o)$	12	1700	1700	3400

Cavallier *et al.* [26] has studied the coupling of mechanical impact to a piezoelectric plate (PZT) via a nickel package. The vibrations are transmitted to the piezoelectric element while the impact occurs on the outside of nickel case. This work investigated the optimum mounting positioning for the piezoelectric plate and the inclusion of silicon beam that placed between two PZT plates forms a resonant structure. In order to find how it is, the test was done by dropping a 40g tin ball from 1 cm and 3 cm height (3.92 and 11.7 µJ impact energy respectively). The electrical energy varies linearly with incident energy. The addition of silicon beam between those two plates improve the magnitude and duration of the electrical output compared to PZT plate arrangement. The voltage produced for each 11.7µJ impact with a total package size of 120 mm^3 was 2 V.

Electromagnetic generator is focused on the behaviour of magnetic induction. Electrostatic generator is related to the parallel capacitor plate while piezoelectric generator behaviour is associated with the piezoelectric effect. Piezoelectric is the most common types of transducers that use in vibration analysis. When piezoelectric is compressed or had any mechanical pressure, the charge will produce. Moreover, piezoelectric generator is easy to fabricate (no requirement for having additional components and complex geometries) than electromagnetic and electrostatic generator. So that, piezoelectric generator is (prefer than electromagnetic and electrostatic generator) befit to use in microengineering and for experimental in studies.

2.3 Tuning techniques

Mostly, energy harvesters were designed as a linear resonator to match their resonance frequencies with the excitation frequencies and achieve optimal output power. Nevertheless, when the excitation frequency varies in different operational conditions, the energy harvester may not able to obtain optimal output power. Therefore, an energy harvester is looked for a resonance tuning mechanism to increase its functionality. Roundy and Zhang [27] stated that, the resonance can be tuned in active and passive mode. Active mode need a continuous power input for resonance tuning while in passive mode, a discontinuous power input required for resonance tuning and there is no power needed when frequency matching is already achieved, until the excitation frequency varies again. There are three tuning methods with different tuning mechanisms such as mechanical, magnetic and piezoelectric method. All these method will be discussed.

The resonance of a system can be tune by changing the mass and the stiffness of the system. Commonly, it is more practical to change the stiffness rather than the mass. Leland and Wright [28] proposed a method to tune the resonance of their harvester by applying axial compressive load, which already changed the stiffness of the harvester. Figure 2.15 shows the schematic of a simply supported bimorph energy harvester with applied preload.

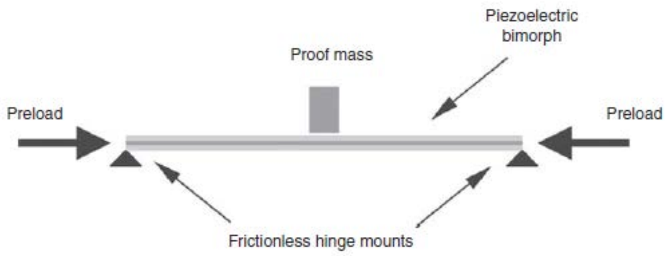

Figure 2.15: Schematic of supported bimorph energy harvester by Leland and Wright [28].

Through their experiment test, they found that before bimorph failure, a compressive axial preload can reduce the resonance frequency of vibration energy scavenger by up to 24% at the same time it increase the damping, as shown in Figure 2.16.

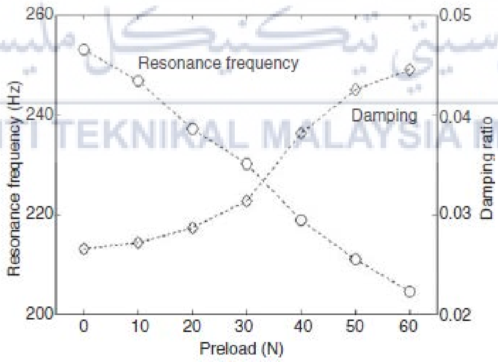

Figure 2.16: Damping and resonance frequency vs compressive preload by Leland and Wright [28].

By using a 7.1 g proof mass attached under the excitation of 1 g acceleration, 300-400 µW can be obtained over the range of 200-250 Hz. The designed presented was planned to operate in „passive" mode, where the device should be manually tuned. But, Leland and Wright [28] was not addressed the tuning procedure. Furthermore, the resonance frequency can only be tuned in uni-directionally.

Eichhorn *et al.* [29] conducted a same study on resonance frequency by using prestress. Figure 2.17 shows generator with arms (upper and bottom sides) and schematic of the entire setup.

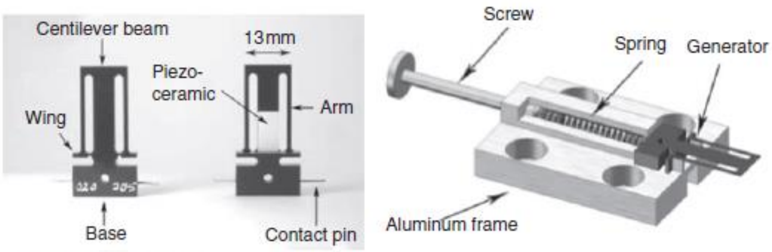

Figure 2.17: Upper side and bottom sides of the generator with schematic of the entire setup by Eichhorn *et al.* [29].

A cantilever tunable energy harvester was designed and fabricated with two wings attached with the tip of the beam and the arms. The revolution of screw generated the compression on the spring, which force applied on the arms. The force forwarded by the wings and finally applied at the end of cantilever. Below the fracture limit, a resonance shift from 380 to 292 Hz was achieved by applying up to 22.75 N preload, as shown in Figure 2.18.

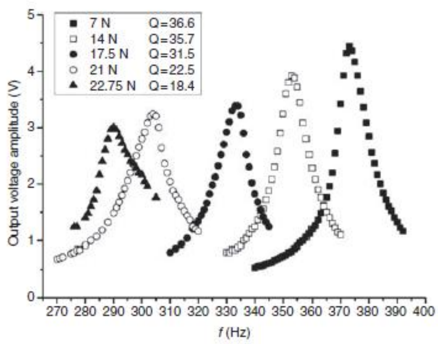

Figure 2.18: Resonances curves with various prestress by Eichhorn *et al.* [29].

The quality factor was decreased, which means the damping arose with increased preload. Moreover, the automatic controller for tuning process was not implemented in the design and the harvester should be tune in manual.

Some tunable resonator is working in bending mode but some researchers also explored on the tunable resonator to work in extensional mode, termed as an extensional mode resonator (XMR; Morris *et al.* [30]; Youngsman *et al.* [31]). Morris *et al.* [30] fabricated XMR prototype by suspending a seismic mass with two piezoelectric membranes (PVDF; polyvinylidene fluoride). Pre-tensioning two membranes (dimensions of $2l \times w \times h$) by a rigid link with length of $2u_p$ and deflecting the link by Δu, as shown in Figure 2.19.

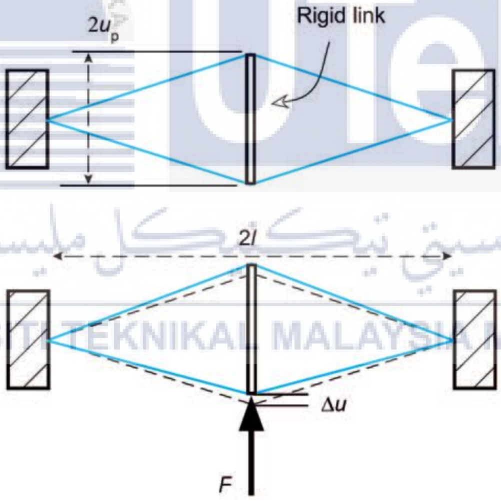

Figure 2.19: Pre-tensioning two membranes by a rigid link. from Morris *et al.* [30].

The force-deflection characteristic of the rigid link is given by:

$$F = \frac{Ewh}{l^3}(6u_p^2\Delta u + 2\Delta u^3) \tag{29}$$

Normalized force-displacement relationship of Equation (29) is shown in Figure 2.20.

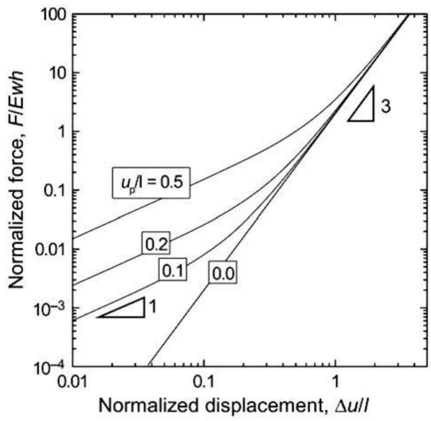

Figure 2.20: Graph normalized force vs normalized displacement for an XMR with rectangular membrane by Morris *et al.* [30].

The natural frequency can be approximated from a sufficient small deflection as

$$f_N = \frac{1}{2\pi}\sqrt{\frac{k}{m}} = \frac{1}{2\pi}\sqrt{\frac{dF}{d(\Delta u)}/m} \approx \ u_p \frac{1}{2\pi}\sqrt{6\frac{Ewh}{ml^3}} \tag{30}$$

Therefore, by adjusting the link length that symmetrically pre-tensions both membranes, the resonance frequency can be tuned. Similar force-deflection relationships and natural frequency expression can be found for other rigidly coupled and transversely loaded membrane. Figure 2.21 shows a XMR prototype with circular configuration.

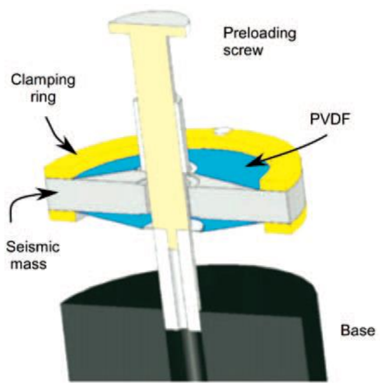

Figure 2.21: Cross-sectional of an assembled XMR prototype by Morris *et al.* [30].

The frequency response functions were come by tuning the preloading screw at three random positions, as shown in Figure 2.22.

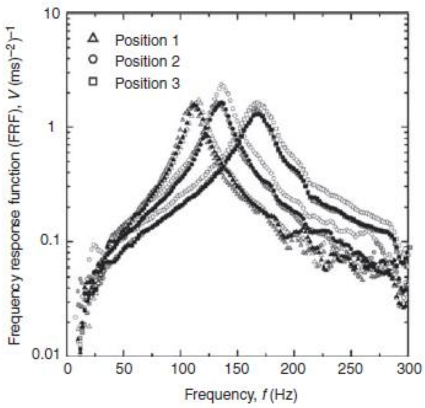

Figure 2.22: Frequency response at three different positions by Morris *et al.* [30].

It seems that, the resonance frequency was repeatable when the tuning screw is adjusted to the same position. It was found that, the resonance frequency shift between 80 and 235 Hz can be easily obtained with the change of pre-tension displacement of around 1.25 mm.

Wu *et al.* [32] demonstrated a tuning techniques by realizing movable tip mass of a cantilever energy harvester. By adjusting the gravity center of the tip mass, the resonance of cantilever can be modified. Figure 2.23 shows a proof mass consisted of fixed part and a movable part.

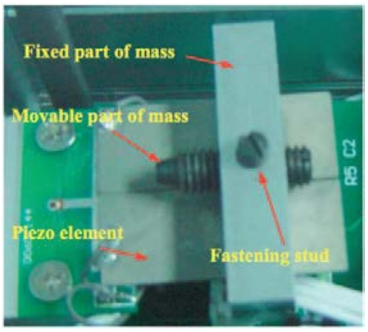

Figure 2.23: A piezoelectric cantilever with a moveable mass by Wu *et al.* [32].

The gravity center of the tip mass can be adjusted by the screw. The fixed part of mass was made of a material of small density and the movable part material was made of larger density. So, the moving distance of the gravity center of proof mass will enlarge the frequency. Observation on the prototype has been made and they claimed that the adjustable resonance frequency range could cover 130 - 180 Hz by tuning the gravity center of the tip mass to 21 mm. Figure 2.24 shows graph of resonance frequency vs the position of the gravity center of moveable mass.

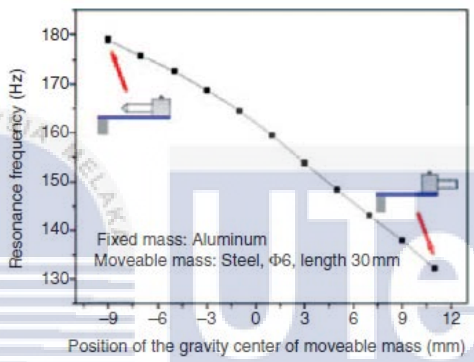

Figure 2.24: Resonance frequency vs the position of the gravity center of moveable mass by Wu *et al.* [32].

Another technique in tuning is by applying magnetic force in the harvester and it will alter the stiffness of the system. Challa *et al.* [33] proposed a tunable harvester as shown in Figure 2.25.

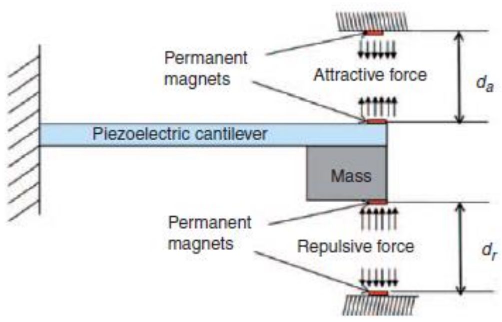

Figure 2.25: Schematic of the resonance tunable harvester by Challa *et al.* [33].

Two magnets were placed and fixed at the free end of the cantilever beam and two magnets were also fixed at the top and the bottom of the device. All the magnets were placed vertically, so that, attract and repel mechanism from the magnetic forces could be generated on each side of the beam. The magnetic force could be altered by tune the distance between the magnets using a spring-screw mechanism, which induced an additional stiffness on the beam and simultaneously adjusted its resonance frequency. The power output was reported to be 240-280 πW at acceleration amplitude of 0.8 ms^{-2} over frequency range of 22-23 Hz. The power output was reduced as the damping increased during the tuning process, as shown in Figure 2.26.

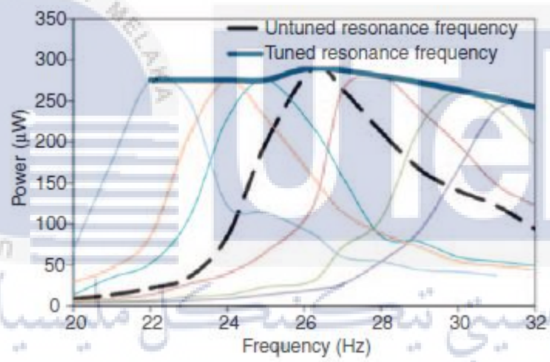

Figure 2.26: Power output vs tuned resonance frequency by Challa *et al.* [33].

From the maximum tuning distance of 3 cm, the energy required was 85 mJ and time taken for each tuning procedure is 320 s. This means that the harvester can only work when the frequency excitation changes slowly.

Reissman *et al.* [34] presented a tuning technique using variable attractive magnetic force, as shown in Figure 2.27.

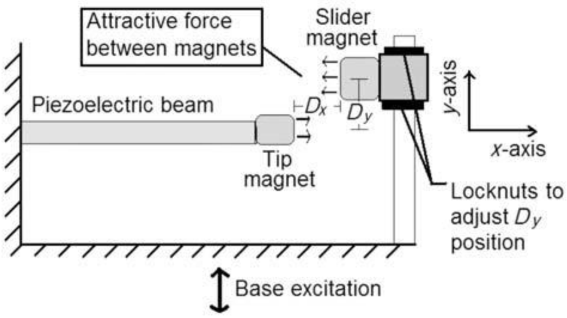

Figure 2.27: Schematic of the resonance tunable harvester by Reissman *et al.* [34].

By adjusting magnetic slider mechanism from the device, the resonance of the piezoelectric energy harvester could be tuned to bi-directional. Previous design by Challa *et al.* [33] is more complicated than this design. The stiffness of the piezoelectric beam was counting on the structural component K_m, the electromechanical component K_e that varied with external resistive loading R_l, and the magnetic stiffness $K_{magnetic}$ that varied with the relative distance D between the two magnets, that is:

$$K = [K_m + K_e (R_l)] + K_{magnetic}(D) \tag{31}$$

According to the concept of a potential energy, by tuning D_y of the two magnets, the resonance could be tune bi-directionally, as shown in Figure 2.28.

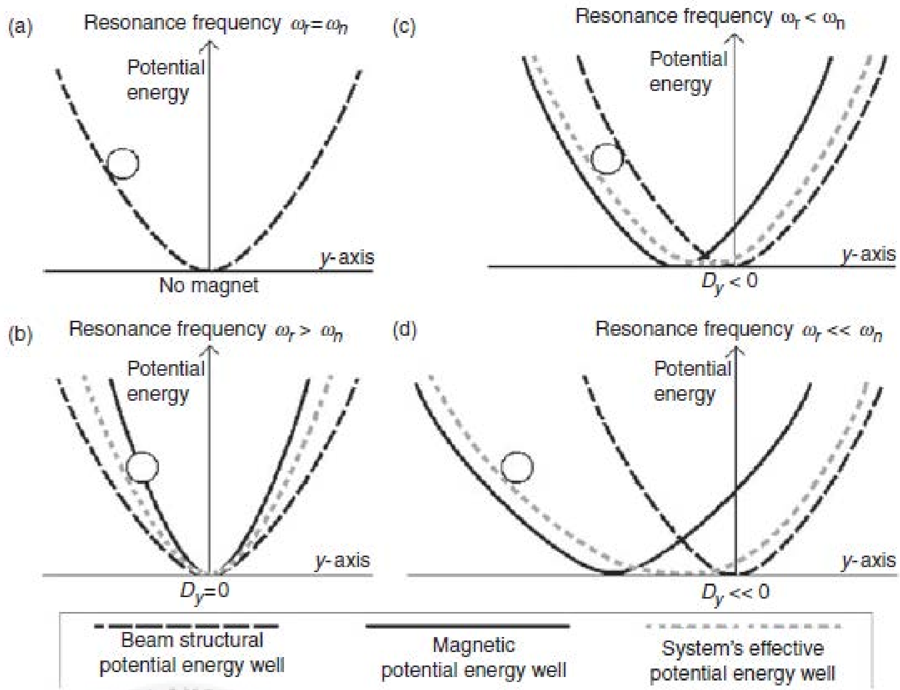

Figure 2.28: Qualitative hypothesis on varying size potential energy wells with respect to the relative displacement of the magnets Reissman *et al.* [34].

For a fixed D_x, the maximum response frequency was obtain at 99.38 Hz, at $D_y = 0$ and at the minimum resonance frequency (88Hz), D_y =1.5 cm. This analytical is shown in Figure 2.29.

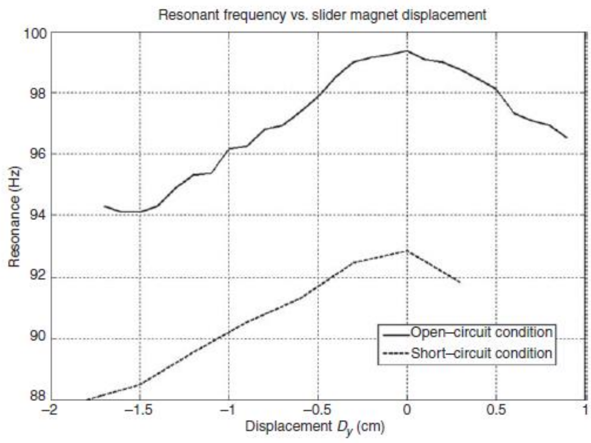

Figure 2.29: Open and short circuit frequencies resonance vs displacement, D_y by Reissman *et al.* [34].

Furthermore, the total bandwidth was 11.38 Hz, including the resonance frequency change from short to open circuit condition due to the piezoelectric coupling.

Zhu *et al.* [35] proposed a setup using magnets with a smart controller for tuning procedure. Figure 2.30 shows a schematic of the tuning mechanism (a linear actuator).

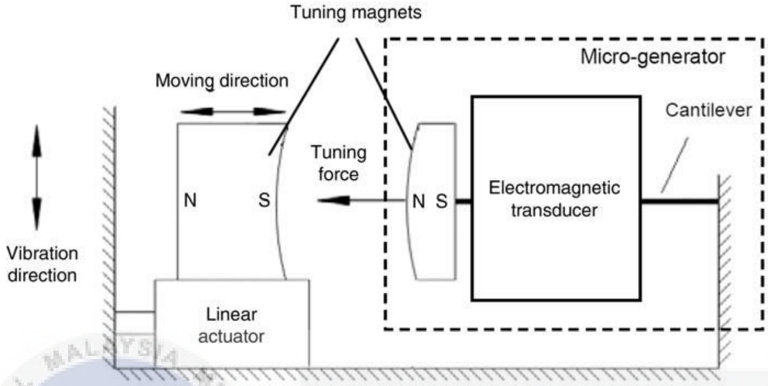

Figure 2.30: A schematic of tuning mechanism by Zhu *et al.* [35].

The tuning process is conducted by a mircrocontroller, which woke up periodically, detected the output voltage of the generator and provided instructions to drive the actuator. In experimental test, frequency can be tuned from 67.6 Hz to 98 Hz by adjusting the distance between two magnets from 5 mm to 1.2 mm, as shown in Figure 2.31.

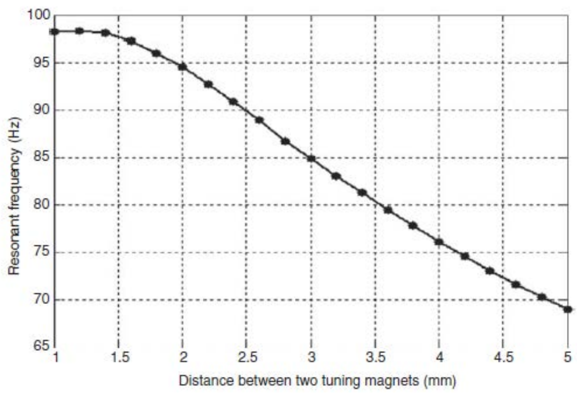

Figure 2.31: Resonance frequency vs distance between two magnets by Zhu *et al.* [35].

The power output of 61.6 µW - 156.6 µW over tuning range can be obtained when at a constant acceleration level of 0.558 m/s^2, as shown in Figure 2.32. From study, it was found that the damping of the microgenerator was not affected by the tuning mechanism and it was increased while the power output was less than predicted.

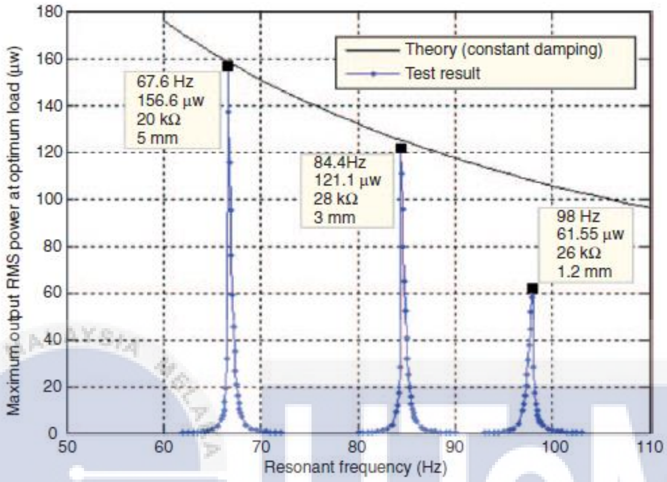

Figure 2.32: Maximum output RMS power at optimum load vs resonance frequency by Zhu *et al.* [35].

The stiffness of a device can be changed by piezoelectric actuator. In point of fact, the stiffness of the piezoelectric material itself can be varied with different electrical loads attached. However, piezoelectric transducers give another option for resonance tuning. The notion of piezoelectric methods refers to the methods for resonance tuning using piezoelectric transducers.

Wu *et al.* [36] proposed a piezoelectric bimorph (PB) generator. The upper piezoelectric layer was used for tuning purpose by connecting with the various capacitive loads. The lower layer was for energy harvesting to charge a supercapacitor. After tuning process, the bandwidth of the generator was narrow than other designs. The tunable bandwidth was 3 Hz from 91.5 to 94.5 Hz. Two demo tests have been done. The device was excited under chirp and random vibration from 80 to 115 Hz. The average power of

1.53 and 1.95 mW was obtained when in the real-time tuning system. These results corresponded to respective 13.4% and 27.4% increases, as compared with output when the turning system was turned off. A microcontroller was used to sample the external frequency and modified the capacitive load to match the external vibration frequency in real-time. In order words, the device was tuned in „active" way and the continual power required by the microcontroller system was in µW level. Figure 2.33 shows the setup of the tunable energy harvesting system by Wu *et al.* [36].

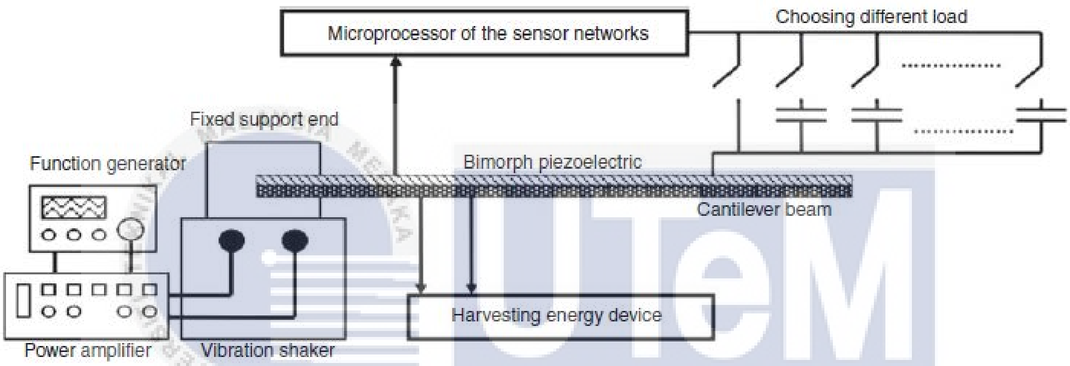

Figure 2.33: The setup of the tunable energy harvesting system by Wu *et al.* [36].

Peters *et al.* [37] provide another idea to tune the resonator, which is through two piezoelectric actuators. The free actuator swings around the axis of rotation with a deflection angle α, as shown in Figure 2.34. If the voltage is apply on the actuators, the both ends of the actuators will deflect by Δy (V_{op}), as shown in Figure 2.35.

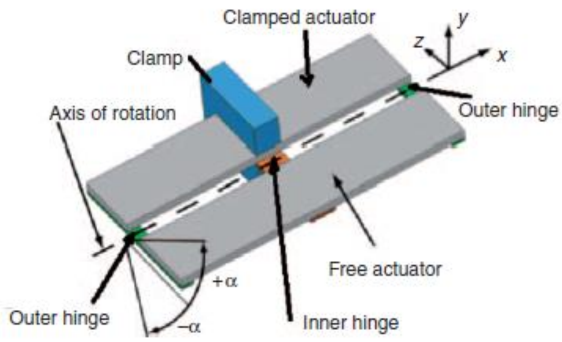

Figure 2.34: Tunable resonator with one clamped and one free actuator

by Peters *et al.* [37].

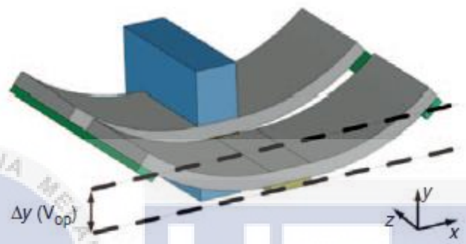

Figure 2.35: Both ends of actuator are deflected by Δy (V_{op}) with applied

tuning voltage by Peters *et al.* [37].

A tuning range over 30% from initial frequency of 78 Hz was achieved by tuning voltage of only ±5V, as shown in Figure 2.36. A discrete control circuit was implemented to resonator and control the resonance tuning of the system. The power output was obtained around 150 mW which significantly outweighed the harvested power (1.4μW).

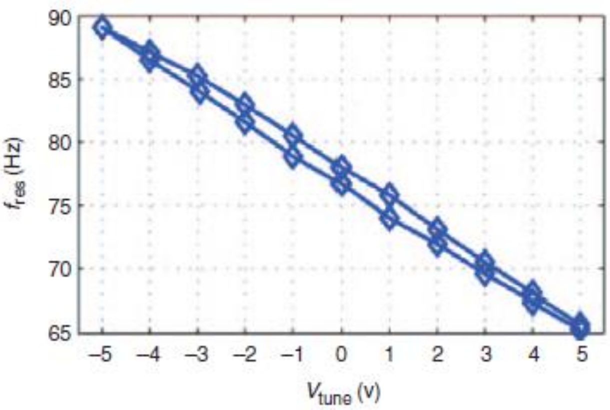

Figure 2.36: Resonance frequency vs applied tuning voltage by Peters *et al.* [37].

Roundy and Zhang [27] investigated the feasibility of active mechanism. Analytically, an active tuning actuator never resulted in net increase in power output. The piezoelectric generator with an active tuning actuator is shown in Figure 2.37.

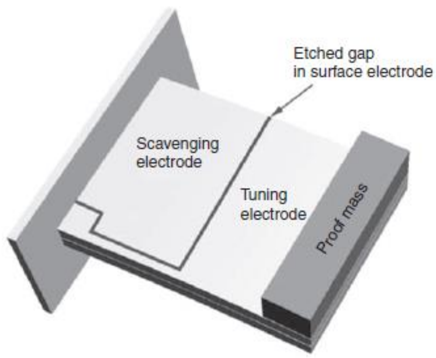

Figure 2.37: Schematic of a piezoelectric bender by Roundy and Zhang [27].

The electrode was etched on the surface to create a scavenging and tuning part. Through several experiment tests, the change of power output (82µW) was smaller than the power needed to continuously drive the actuator (440µW). Then, the passive tuning was suggested and worth more attention.

Mostly, an active tuning is implemented by piezoelectric methods. It requires more power input than passive tuning and it outweighs the power in most of designs, except for Wu *et al.* [36]. The passive tuning only needs less power to adjust the frequency, which is suitable when the excitation frequency varies slowly. But, if the harvester is in the active tuning, the harvester can cover the non-stop power for tuning and work under fast-varying, frequency or random excitation.

2.4 Multimodal energy harvesting

Multimodal harvester is a distributed parameter system or a multi-degree-of-freedom system. A certain vibration mode can be excited when the driving frequency approaches one natural frequency of the harvester. But, if multiple vibration modes are used, power can be harvested over multiple frequency spectra and the bandwidth will become wider. A multimodal energy harvesting techniques is another way to obtain wider bandwidth for efficient energy harvesting produced.

2.4.1 Hybrid energy harvesting scheme

Hybrid energy harvesting scheme is a scenario when two different schemes were combined in one system assisting each other for vibration energy harvesting, such as combining the piezoelectric and electromagnetic method (MacCurdy *et al.* [38]; Challa *et al.* [39]; Tadesse *et al.* [40]). Tadesse *et al.* [40] presented an example in designing a multimodal energy harvester, as shown in Figure 2.38.

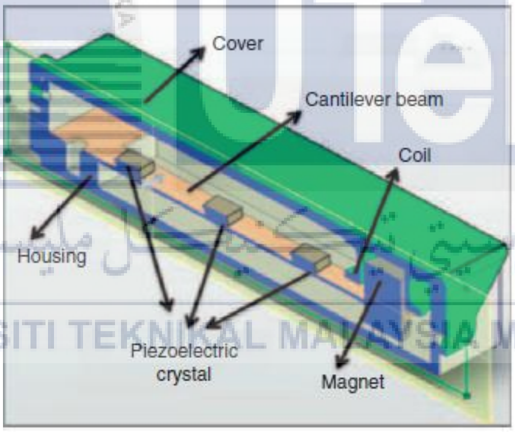

Figure 2.38: A multimodal energy harvesting device by Tadesse *et al.* [40].

The device consists of a cantilever beam with piezoelectric plates bonded and a permanent magnet attached at the tip, which oscillates within a stationary coil fixed to the housing. Electromagnetic scheme generates high output power at low frequency (first mode), while the piezoelectric scheme is use to generates high power at higher frequency. The blend of electromagnetic and piezoelectric scheme could produce significant power output will covering the multiple frequency spectra.

2.4.2 Cantilever array

A continuous wide bandwidth also can be obtained by using a multiple cantilevers in one device. Yang and Yang [41] suggested to connect or coupled bimorph cantilever beams for energy harvesting, whose resonant frequencies were very close to each other and were adjustable. A schematic of the design is shown in Figure 2.39.

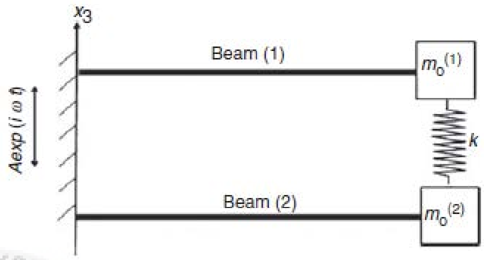

Figure 2.39: Schematic of two beams with two end masses elastically connected by Yang and Yang [41].

Figure 2.40 shows the power output versus frequency for different end mass pairs with fixed spring stiffness and Figure 2.41 presents the power output versus frequency for different spring stiffness with a fixed mass pair.

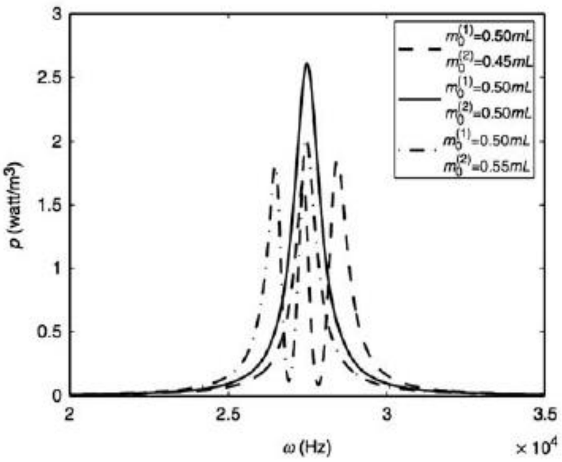

Figure 2.40: Power density vs frequency for different end mass pairs with a fixed spring stiffness by Yang and Yang [41].

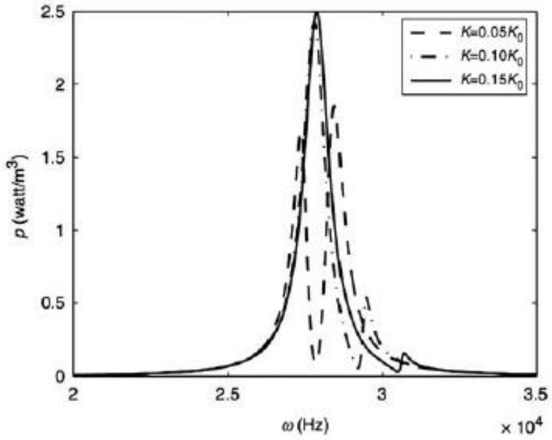

Figure 2.41: Power density vs frequency for different spring stiffness with a fixed mass Yang and Yang [41].

A proper design of the end masses and spring able to attain vibration energy over a wider frequency range than a single beam harvester. The amplitude and resonances location were easily affected to the end masses and end spring. The disadvantage of the connected structure was the reduced peak power with unequal end mas, as set side by side with the structure with equal end masses. Anyhow, unequal end masses in such connected structure are essential for wider bandwidth purpose.

Next, using quasi-uncoupled cantilevers also can be another option for getting a wider bandwidth. Each cantilever is noticed as one substructure of the harvester and the first mode of each cantilever is one of vibration modes of the harvester. Shahruz [42, 43] designed an energy harvester which comprised piezoelectric cantilevers with various lengths and tip masses attached to a common base. It was able resonating at various frequencies without any adjustment. Each cantilever had their own resonant frequency and the combination into a single device is called „mechanical band-pass filters‟, as shown in Figure 2.42. Selecting the length and tip mass of each beam must do properly, so that the voltage response over a wider frequency can be approach as shown in Figure 2.43.

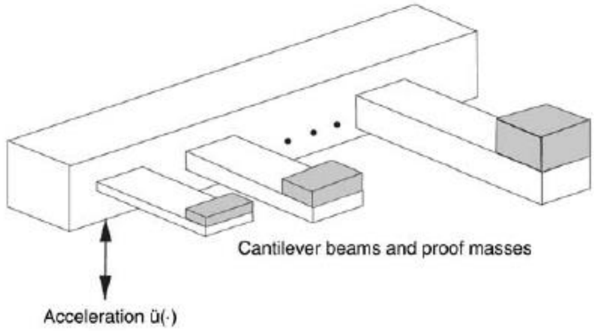

Figure 2.42: Band-pass filter by Shahruz [42].

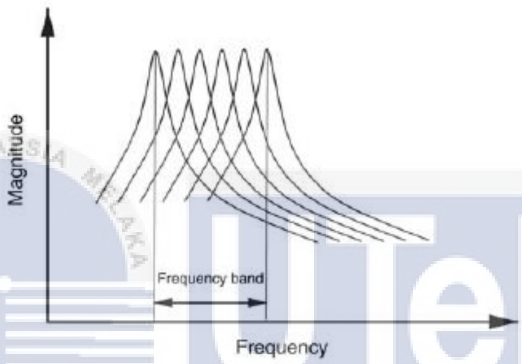

Figure 2.43: Transfer function of the device by Shahruz [42].

Xue *et al.* [44] proposed a designed of broadband energy harvester using multiple piezoelectric bimorph (PBs) with different thicknesses of piezoelectric layers, as shown in Figure 2.44.

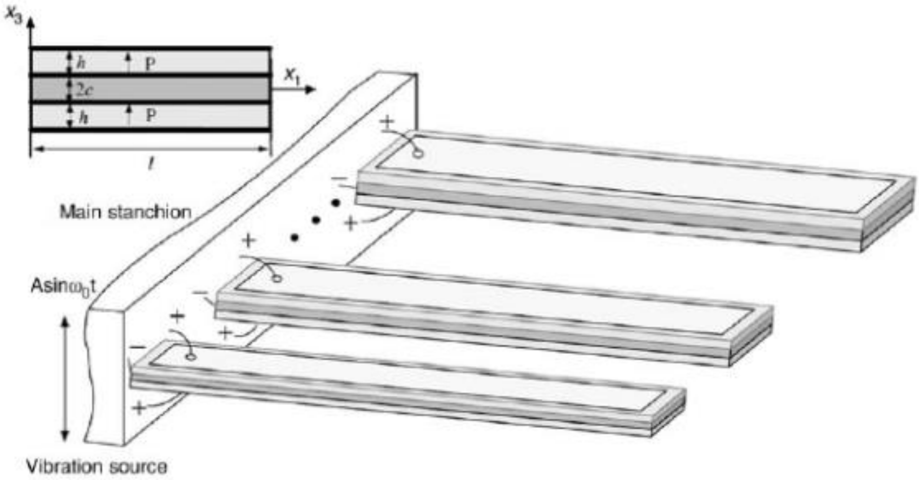

Figure 2.44: A harvester with multiple PBs by Xue *et al.* [44].

When using multiple PBs in series, the output power is increased and the bandwidth becomes wider. Figure 2.45 shows the difference of using single PB and ten PBs connected in series with various thicknesses. However, by changing the number of PBs in parallel, the bandwidth could be shifted to the dominant frequency range.

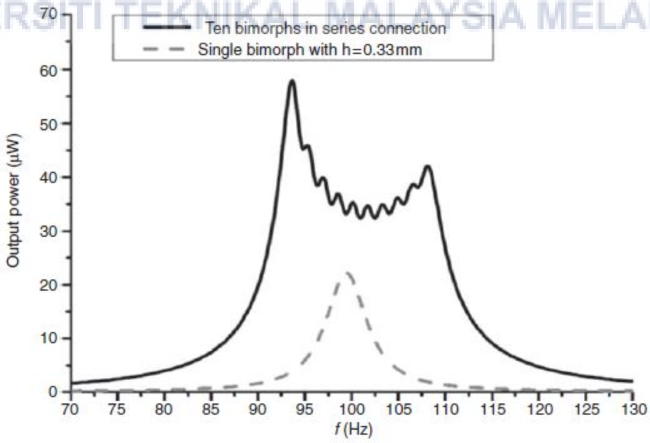

Figure 2.45: Output power vs frequency for a single PB and 10 PBs connected in series with various thicknesses by Xue *et al.* [44].

Broadband energy harvester with cantilever array also can be implemented with current standard microelctromechanical systems (MEMS) fabrication techniques. Liu *et al.* [45] implemented a MEMS-based broadband energy harvester as shown in Figure 2.46.

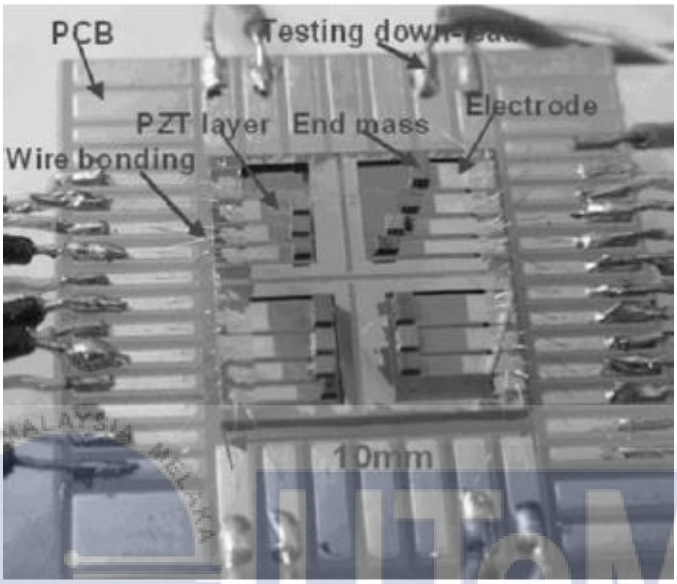

Figure 2.46: Schematic of array prototype by Liu *et al.* [45]

The alternating current (AC) output from the three cantilevers in array and their direct serial connection is shown in Figure 2.47.

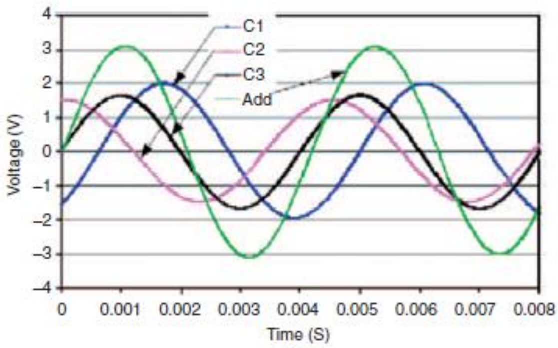

Figure 2.47: AC output of three cantilevers in an array and the direct serial connection by Liu *et al.* [45].

An observation had been made through the phase difference which impaired the electrical accumulation of all three cantilevers. The direct current (DC) voltage across the capacitor after rectification was only 2.51 V. The maximum DC power was 3.15 mW. By solving this problem, a rectifier was attached to each cantilever, as shown in Figure 2.48 and it increase the DC voltage to 3.93 V and the maximum DC power output is at 3.98 μW. The rectification circuit consumed more electrical energy.

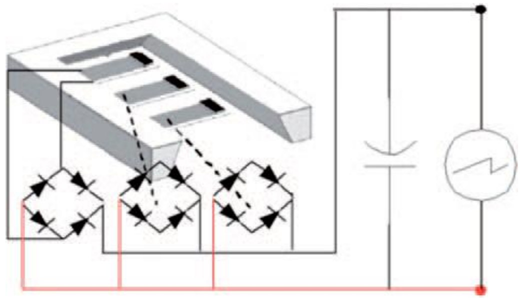

Figure 2.48: Electrical connection after AC-DC rectification Liu *et al.* [45].

To conclude that, by implementing multiple modes or with cantilever array in one device, a multimodal energy harvester will be produced. The multimodal energy harvester does not require any tuning methods compared with the resonance tuning techniques, which is much easier to implement. So, a wide bandwidth can be obtained without any tuning methods.

2.5 Frequency up-conversion

Most practical cases create an ambient vibration at low frequency such as by human motion. However, the low frequency may boost-up, even in a microenergy harvester. A frequency-robust solution for vibration energy harvester is used to amplify the source vibration frequency, so that the power can be harnessed at low frequency excitation situations.

The frequency up-conversion technique had been stated in the novel microvibration energy harvester by Lee *et al.* [46]. The device consists of a sharp probe, microridges, microslider and PB cantilever is shown in Figure 2.49.

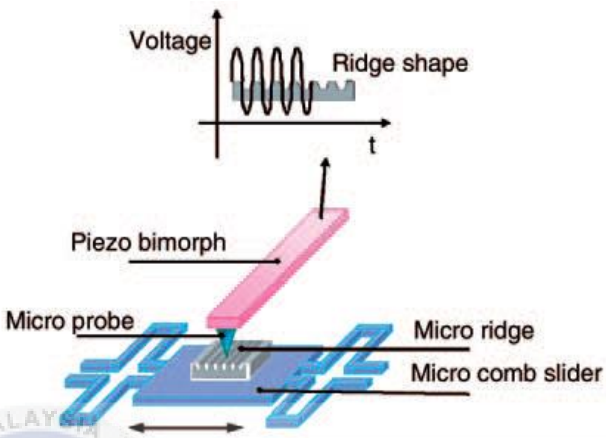

Figure 2.49: Concept of microenergy harvesting device by Lee *et al.* [46].

The microridges were attached onto microslider mechanism while probe tip was attached on the edge of piezoelectric cantilever along the ridges. In experiment, the cantilever was vibrated and produces 225μW/cm^2 with 7 rectifications at 60 Hz, which larger than the conventional resonance approaches.

Kulah and Najafi [47] stated another frequency up-conversion technique and proposed a design of microelectromagnetic generator. The schematic of the generator is shown in Figure 2.50.

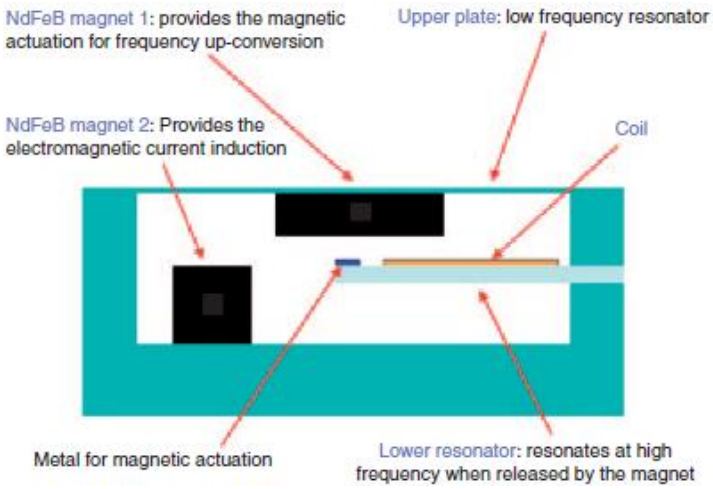

Figure 2.50: A cross-sectional view of the generator by Kulah and Najafi [47].

The permanent magnet at the top is easily deflected in 1-100Hz range due to soft springs and large size. Arrays of beams (cantilever beam) with high frequency were placed at the bottom. A magnetic tip that placed on the beam could be excited with the top magnet. A coil that attached on the beam and the bottom of the permanent magnet will produce electromagnetic current induction. All the setup is shown in Figure 2.51. When the top magnet resonated at low frequency vibration, the cantilever at the bottom will support by resonated at its high natural frequency (1-20 kHz).

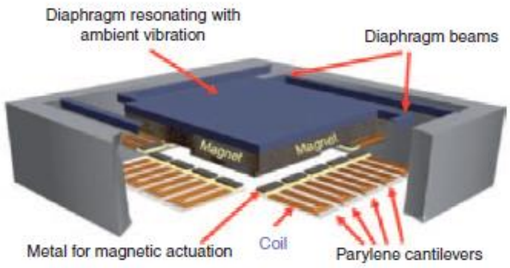

Figure 2.51: Microgenerator structure in three-dimensional view for micro-scale implementation by Kulah and Najafi [47].

All in all, frequency up-conversion techniques can be applied by using a two-stage design. In the two-stage design, the low excitation frequency can be improved to the high natural frequency of the cantilever beam. The performances of the harvester are unresponsive to the excitation frequency, until it is less than the resonance frequency of the harvester. One of the advantages of this technique is the bandwidth still remain behind and this is because of the zigzag structure of the harvesting at low excitation frequency.

2.6 Non-linear techniques

As reported, most of energy harvesters were designed as a linear resonator. The purpose of every design is to match the resonance frequencies with the excitation frequencies and achieve optimal output power. Even though the linear resonator can provides a good performance through some techniques and adjustment, but they still have their own drawbacks. For example, the tuning techniques in linear resonator required many adjustments and tuning part to produce a wide bandwidth and for better performance. A cantilever array needs to produce a lot of peaks in order to create wider bandwidth. However, a wide bandwidth can be created by using non- linear system in one mechanism. Instead of using linear resonator to obtain a wide bandwidth, the non-linear resonator also can be used to obtain good result with wider frequency range.

To tune the resonance of the system, a several techniques by using magnet (Challa *et al*. [33]; Reissman *et al*. [34]; Zhu *et al*. [35]) is used to generate a non-linear stiffness. So that, there could be frequency-robust in frequency variable situations. However, the performance of the energy harvester also can be improved by the non-linearity of the system itself, and a wider bandwidth is produced. The non-linearities of energy harvester are considered to two perspectives. That is, non-linear stiffness (Mann and Sims [48]; Stanton *et al*. [49]; Lin *et al*. [50]; Ramlan *et al*. [51]; Erturk *et al*. [52]) and non-linear piezoelectric coupling. The non-linear stiffness of energy harvester is easier to achieved and control rather than the non-linear piezoelectric coupling. The next section will reviewed on the systems with non-linear stiffness and the benefits on performance broadband energy harvesting. The dynamics of a general oscillator can be described as:

$$\ddot{x} = -\frac{dU(x)}{dx} - \gamma\dot{x} + f(t) \tag{32}$$

where x is the position of the oscillator, γ the viscous friction coefficient, $f(t)$ the force input from the ambient vibration and $U(x)$ the potential function. If the electromagnetic generator is considered, then γ also includes the viscous damping caused by electromagnetic coupling.

For a piezoelectric generator, Erturk and Inman [53] state that the damping caused by piezoelectricity cannot be modelled as a viscous damper. Hence, by adding coupling term (κV), Equation (32) should be modified as

$$\ddot{x} = -\frac{dU(x)}{dx} - \gamma\dot{x} + f(t) + \kappa V \tag{33}$$

where κ is the electromechanical coupling coefficient and V is the voltage on the electrical load. The circuit equations for the piezoelectric and the electromagnetic harvester have a different due to their own impedances. (Gammaitoni *et al*. [54], Cottone *et al*. [55]) stated that the potential energy function, $U(x)$ can be presented in a quadratic form as

$$U(x) = -\frac{1}{2}ax^2 + \frac{1}{4}bx^4 \tag{34}$$

From Equation (35), the potential function, $U(x)$ is symmetric and if $a > 0$, it is consider as bistable. When $a \leq 0$, it is considered as monostable. In bistable case, two minima at $x_m = \pm\sqrt{a/b}$ are separated by barrier at $x = 0$. Both monostable and bistable cases have their own benefits on enhancing the bandwidth of the vibration energy harvester and it will be discussed on the next section.

2.6.1 Monostable non-linear energy harvesters

Duffing"s equation is widely used in modelling non-linear energy harvester (Mann and Sims [48]; Ramlan *et al*. [51]; Moehlis *et al*. [56]). By substitute Equation (34) to Equation (33), Duffing"s equation can be obtained, as shown in Equation (35).

$$f(t) = \ddot{x} + \gamma\dot{x} - ax + bx^3 \tag{35}$$

It is described as monostable when $a \leq 0$. A hardening system response will achieve when $b > 0$, while a softening response was stated when $b < 0$. Investigation on hardening mechanism has been done by Ramlan *et al*. [51] and it was found that, the maximum amount of power in harvesting with a hardening stiffness was same as the maximum power energy harvesting in linear system, irrespective of degree of non-linearity. However, this might occur at a different frequency depending on the degree of non-linearity as shown Figure 2.52. The power can be harvested due to the shift in the resonance frequency.

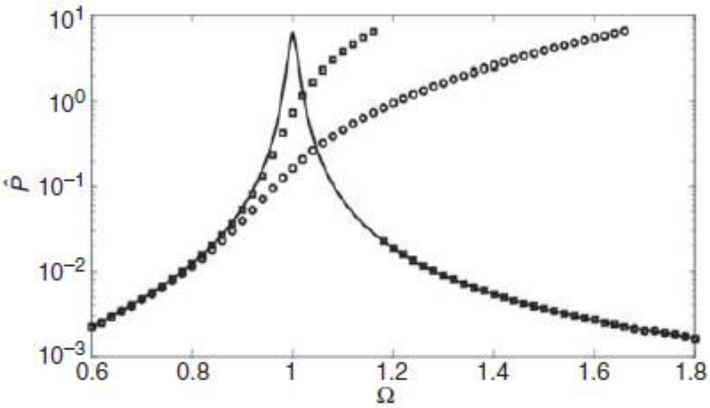

Figure 2.52: Numerical solution for non-dimensional power harvester with damping ratio ζ= 0.01 and amplitude Y= 0.5 by Ramlan *et al*. [51].

Mann and Sims [48] designed an electromagnetic energy harvesting from the non-linear oscillation of magnetic levitation, as shown in Figure 2.53. A system where two magnets are oriented to repel the center magnet, so, suspended it with a non-linear restoring force.

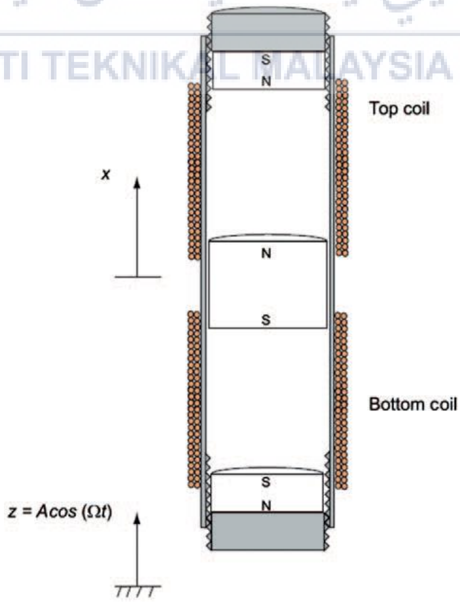

Figure 2.53: Schematic diagram of the magnetic levitation system by Mann and Sims [48].

The derived governing equation for the device is similar with Equation (35). The experimental velocity response and theoretical predictions under low and high excitation levels are shown in Figure 2.54 and Figure 2.55.

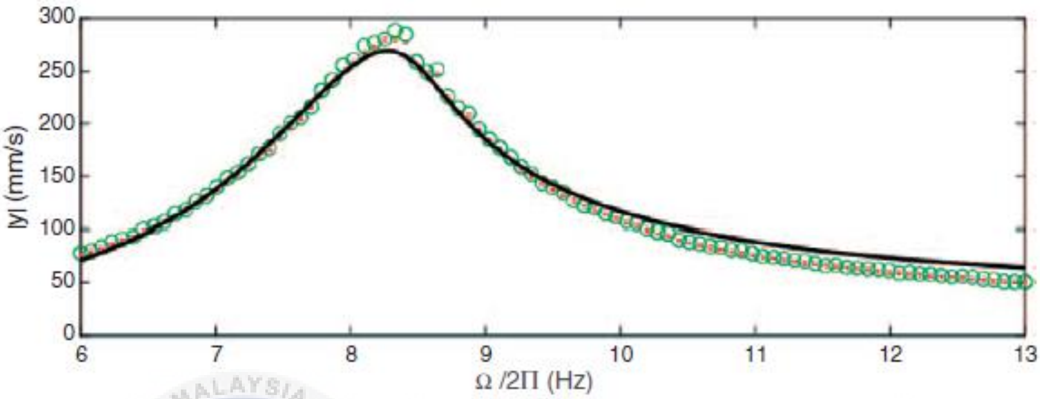

Figure 2.54: Theoretical predictions and experimental velocity response from forward (red dots) and reverse (green circles) frequency sweep under two excitation level at 2.1 ms^{-2} by Mann and Sims [48].

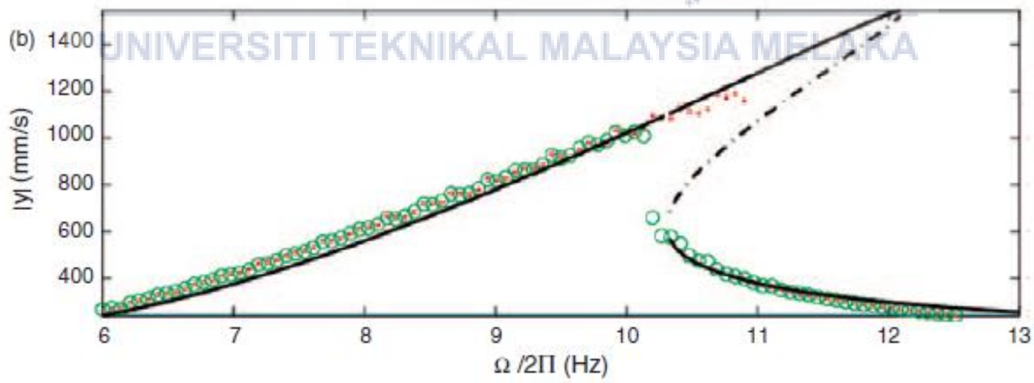

Figure 2.55: Theoretical predictions and experimental velocity response from forward (red dots) and reverse (green circles) frequency sweep under two excitation level at 8.4 ms^{-2} by Mann and Sims [48].

At low excitation level, the frequency response was same as response in linear system. While at high excitation level, the response curve was bent to the right and creates large amplitudes over a wider frequency range. However, the peak responses can only shifts to the right direction.

Another monostable non-linear energy harvester device through piezoelectric effect was proposed by Stanton *et al*. [49] and a schematic diagram of the device is shown in Figure 2.56.

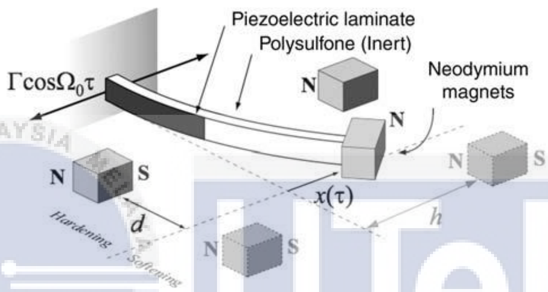

Figure 2.56: Schematic diagram of non-linear harvester by Stanton *et al*. [49].

The device consists of a piezoelectric beam with magnetic field end mass, which have a relation with the field of oppositely poled stationary magnets. The system was modelled by an electromechanically coupled. Duffin‟s equation was same with Equation (35), except that piezoelectric coupling term (κV) should be added such as Equation (33). By tuning the non-linear magnetic interactions around the end mass, d, the hardening and softening response will appears as shown in Figure 2.57 and Figure 2.58.

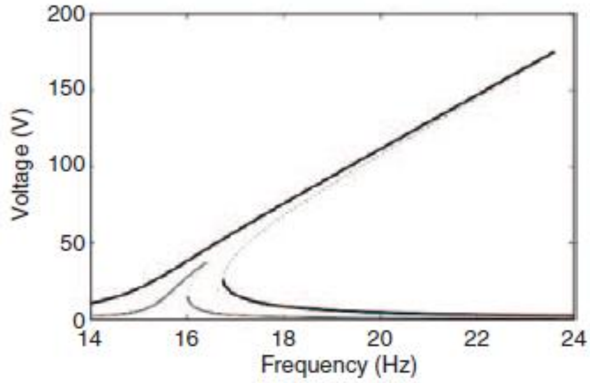

Figure 2.57: Predicted response amplitudes of output voltage for *d* = -2 mm

(Hardening response) by Stanton *et al*.[49].

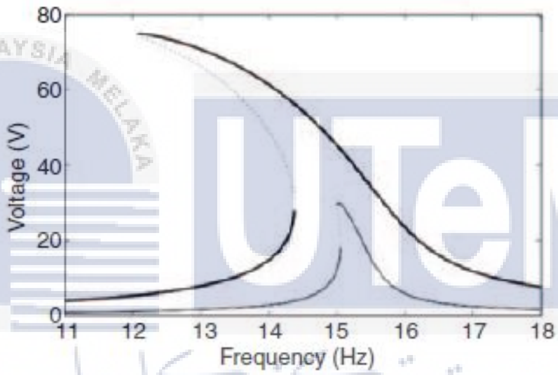

Figure 2.58: Predicted response amplitudes of output voltage for *d* = 5 mm

(Softening response) by Stanton *et al*. [49].

The system allows the frequency response to be broadened bi-directionally. From the experiment, softening response produced a linear decreasing frequency sweep and a comparison between non-linear and linear configuration had been made by removing those two magnets. The power against frequency of the device is shown in Figure 2.59. Wider bandwidth and better performance could be obtained through the non-linear configuration than the linear configuration.

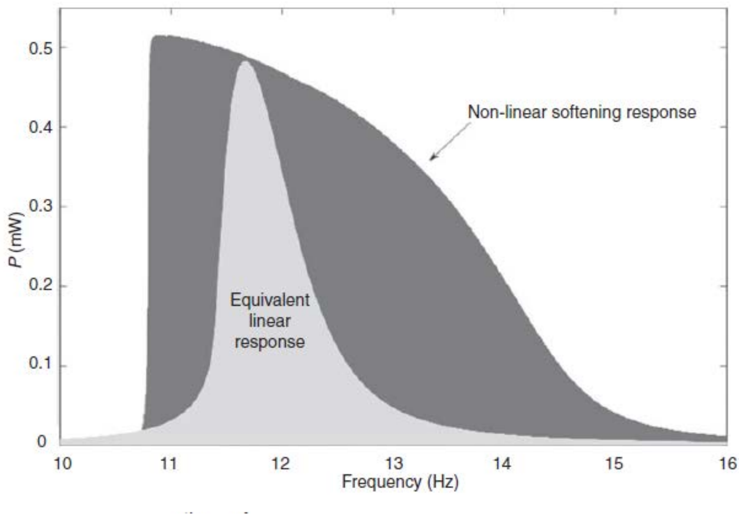

Figure 2.59: The comparison between non-linear and linear configurations under the same excitation amplitude by Stanton *et al*. [49].

Stanton *et al*. [49] stated that, the benefit imparted in the non-linearity hangs on realizing the high-energy attractor. A linearly increasing or decreasing frequency sweep provides the high energy attractor and it enhance the output power and bandwidth in hardening and softening case, respectively.

2.6.2 Bistable non-linear energy harvesters

From Equation (36), if $a > 0$, it is described as a bistable system. A bistable system can undergo with periodic forcing or stochastic forcing. A periodically forced oscillator is subject to many types of large-amplitude oscillations such as chaotic oscillation, large-amplitude periodic oscillation and large-amplitude quasi-periodic oscillation. The behaviour of the system relies upon the pattern of the design, the frequency and the amplitude of the forcing and the damping (Moehlis *et al*. [56]).

An example of bistable oscillator under periodic forcing had been presented by Moehlis *et al*. [56] with the following governing equation:

$$\ddot{x} + 0.1\dot{x} - x + x^3 = \cos(\omega t) \tag{36}$$

In the bifurcation analysis of this forced Duffing"s oscillator (plotting the instantaneous values of x whenever $\dot{x} = 0$ for each ω by getting rid of transients), it was found that large amplitude response ($x > 1$ and $x < -1$) raised over a wide range of frequencies and even extended to very low frequencies.

Ramlan *et al*. [51] proposed an energy harvester with non-linear bistable stiffness and it termed as *snap-through* mechanism. The device consisted of two linear oblique springs connected with a mass and a damper, as shown in Figure 2.60, and the non-linear restoring force is yielding in *x*-direction.

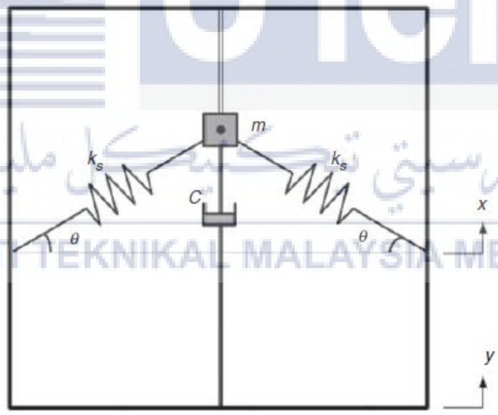

Figure 2.60: *Snap-through* generator by Ramlan *et al*. [51].

This mechanism has the effect of steepening the displacement response of the mass as a function of time and performing a higher velocity for given input excitation. From analytical results, this mechanism could provide a better performance than linear mechanism, when the excitation frequency was less than the natural frequency.

Erturk *et al.* [52] attend with a method in designing a broadband piezomagnetoelastic generator since non-linear bistable stiffness can be made by using magnets. The piezomagnetoelastic generator is shown in Figure 2.61.

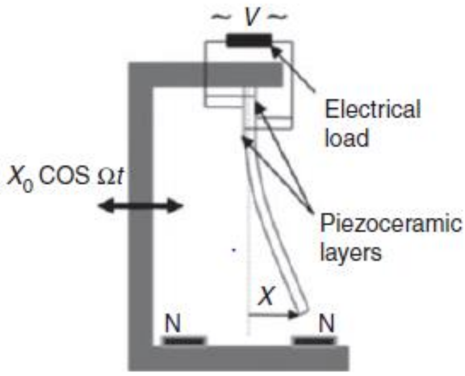

Figure 2.61: The piezomagnetoelastic generator by Erturk *et al.* [52].

The setup consisted of a ferromagnetic cantilevered beam with two permanent magnets (located symmetrically near to the free end) and subjected to harmonic base excitation. Two piezoceramic layers were attached to the root of cantilever. For an initial deflection at equilibrium, the voltage response could be chaotic strange attractor motion or larger amplitude periodic motion, under small or large excitation amplitude, as shown in Figure 2.62 and Figure 2.63. Due to disturbance is obtained under small excitation level, the large-amplitude periodic motion is shown in Figure 2.64.

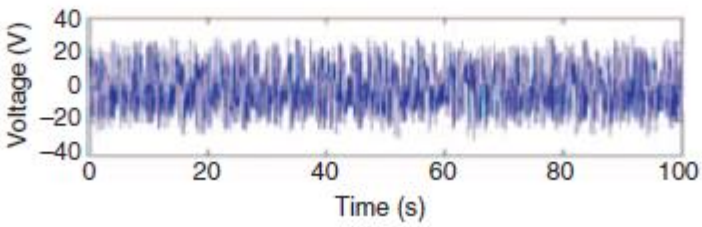

Figure 2.62: Chaotic strange attractor motion (excitation: 05 g at 8 Hz)

by Erturk *et al.* [52].

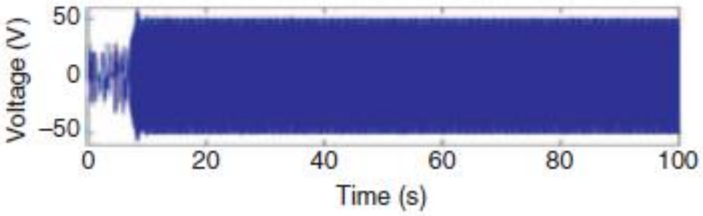

Figure 2.63: Large amplitude periodic motion due to the excitation amplitude (excitation: 0.8 g at 8 Hz) by Erturk *et al*. [52].

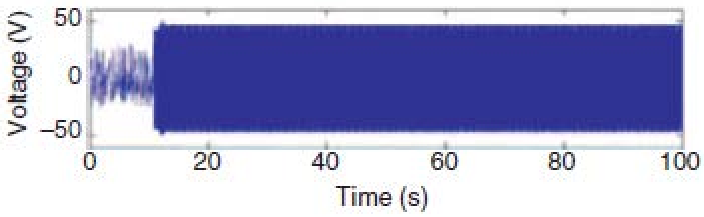

Figure 2.64: Large amplitude periodic motion due to disturbance at 11 s (excitation: 0.5 g at 8 Hz) by Erturk *et al*. [52].

From Figure 2.65, it shows that broadband performance from piezomagnetoelastic is better than the linear piezoelastic configuration (with two magnets remove).

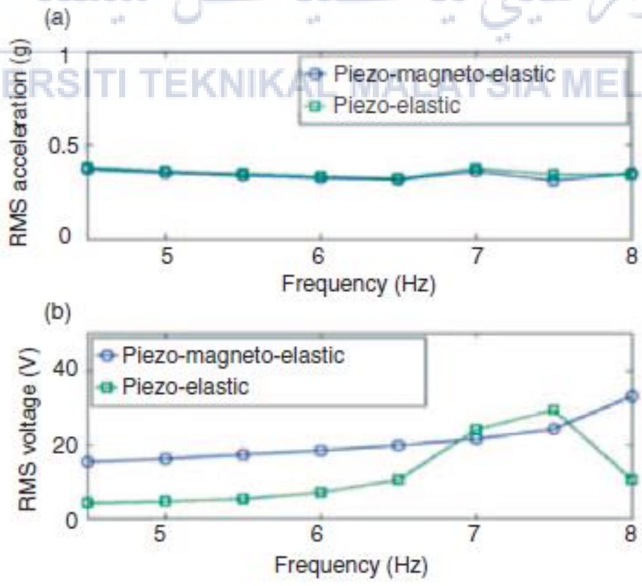

Figure 2.65: a) Root mean square acceleration at differences frequency and b) Root mean square voltage output over a wide frequency range by Erturk *et al*. [52].

In bistable system, stochastic forcing able to induce transitions between the equilibrium of the system and produces large-amplitude oscillations. An experiment has been done by Cottone *et al*. [55] and the schematic of the system is shown in Figure 2.66. Cottone *et al*. [55] stated that, by using the bistable mechanism, a piezoelectric able to flip-flop the pendulum.

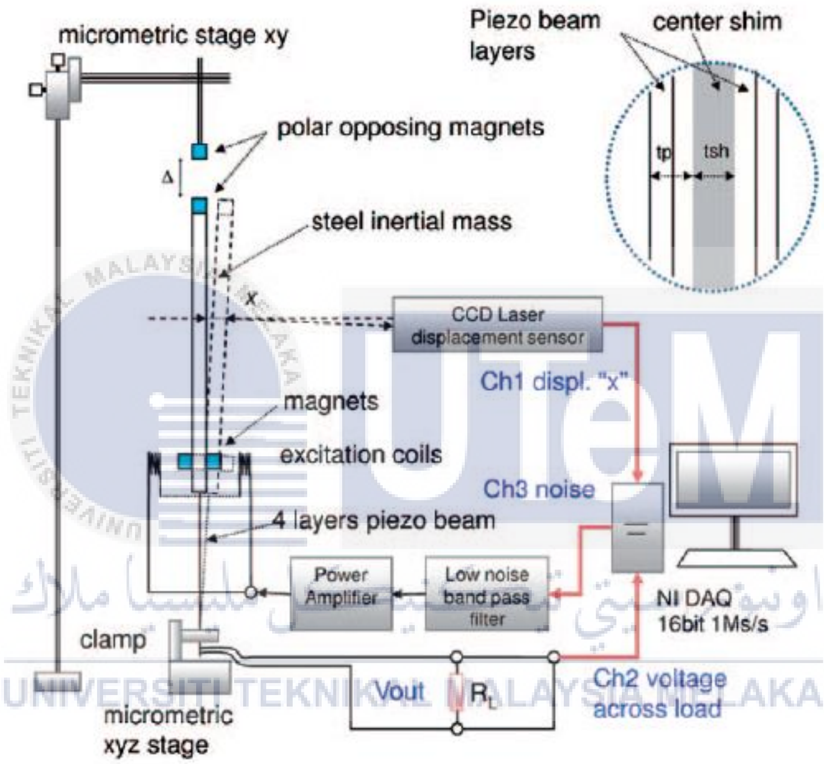

Figure 2.66: Schematic of the experimental apparatus by Cottone *et al*. [55].

Figure 2.67 shows the potential functions of the pendulum in different distances Δ between polar opposing magnets. When Δ was too small, two equilibrium positions come out. The random vibration made the pendulum swing with small oscillations around each equilibrium and large excursions from one and to another. After all, for extremely small Δ, the pronounced barrier of the potential function confined the pendulum swing within one potential well.

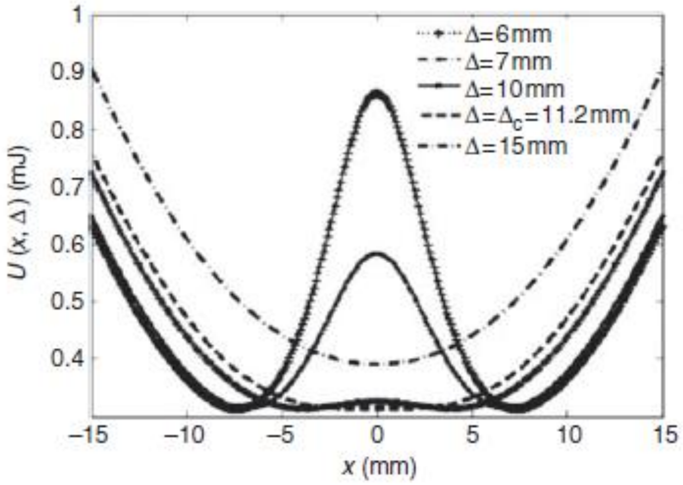

Figure 2.67: Inverted pendulum potential function $U(x)$ with different distances by Cottone *et al*. [55].

Ferrari *et al*. [57] continue the idea by Cottone *et al*. [55] and explored further the energy harvesting performance from wide-spectrum vibrations for a bistable piezoelectric beam by using magnets in opposite poles, as shown in Figure 2.68.

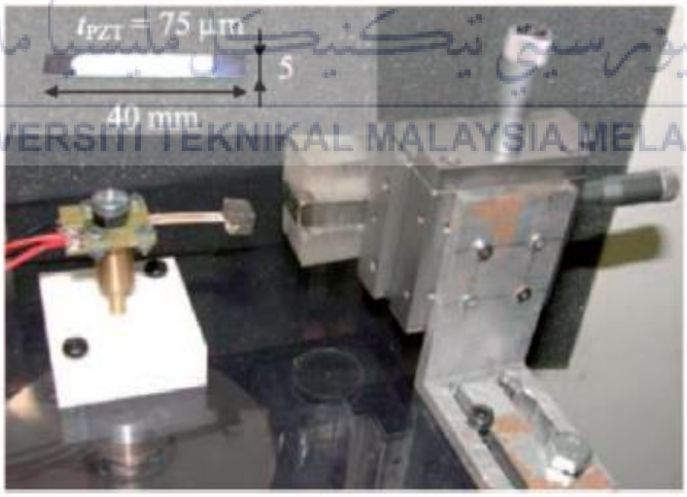

Figure 2.68: Experimental setup by Ferrari *et al*. [57].

Under white-noise excitation, when the magnets come near to each other, transition between two stable states appeared and output voltage is increased, as shown in Figure 2.69.

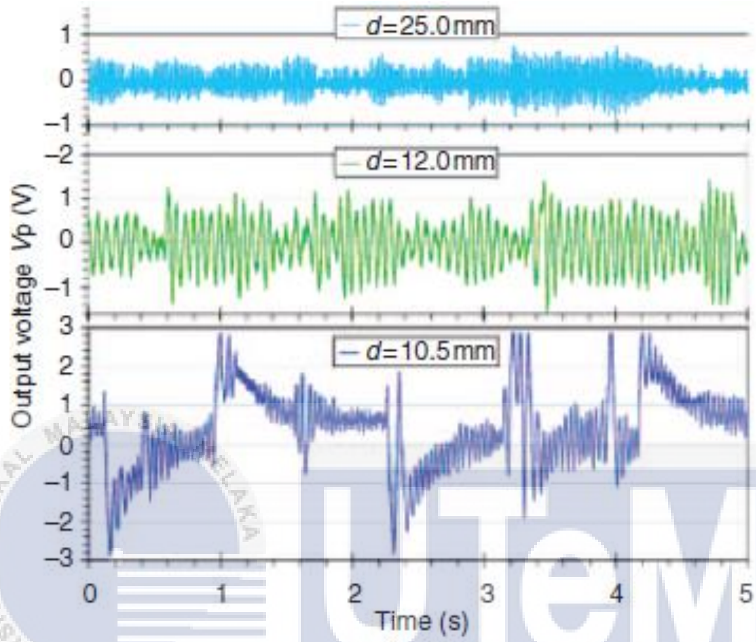

Figure 2.69: Output voltage from the piezoelectric cantilever beam by Ferrari *et al*. [57].

Figure 2.70 (the frequency amplitude spectra of output voltage) shows that spectrum for a bistable configuration (d = 10.5mm) is wider than the quasi-linear case (d = 25.0mm).

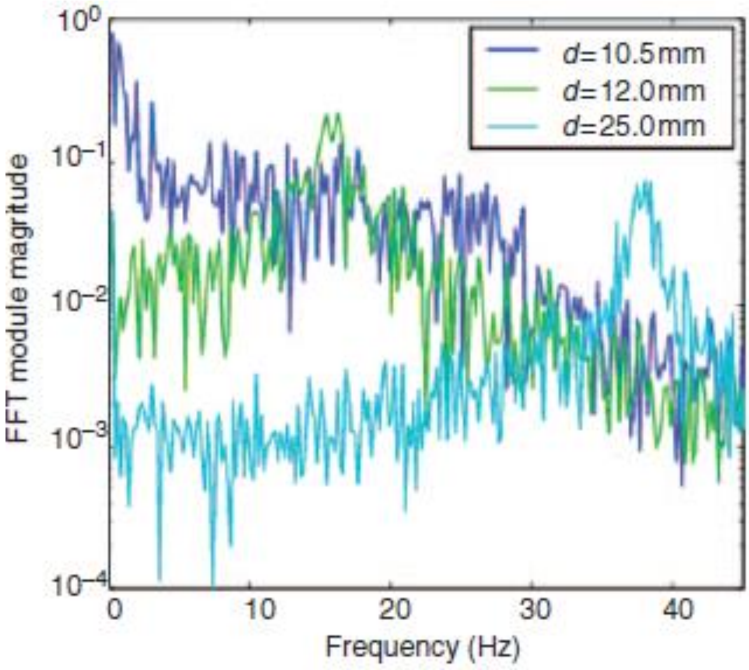

Figure 2.70: Frequency spectra from different distances between magnets by Ferrari *et al*. [57].

Another way to enhance the performance of bistable system is by increase the probability of transition between the potential wells. McInnes *et al*. [58] proposed to exploit the occurrence of stochastic resonance for energy harvesting. If the potential barrier oscillates, the stochastic resonance will exist, and the forcing is matched to the mean time between transitions and inverse Kramer‟s rate (Wellens *et al*. [59]). One degree of freedom bistable model is shown in Figure 2.71 with a beam clamped at both ends. The *snap-through* setup by Ramlan *et al*. [51] is with the model, except the distance *A-A'* can be adjusted at frequency *ω*, therefore, the potential barrier is modified.

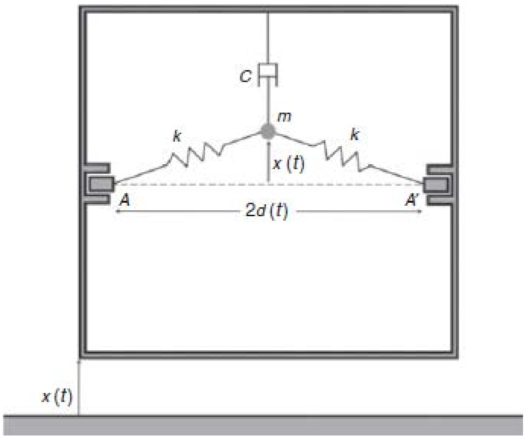

Figure 2.71: Arrangement of one DOF beam model, in which the distance *A-A'* can be adjusted at frequency ω setup by Ramlan *et al*. [51].

All in all, the linearity and non-linearity of system have been studied in this review. The transduction mechanism is an important role to the harvester in generating electricity. Piezoelectric generator is a common transducer that used in vibration analysis. Furthermore, the piezoelectric generator is ease in fabrication (easy to add components and not having complicated geometries) than the other generators. Many methods have been proposed in order to achieve an optimal performance over a wide bandwidth in linear system such as tuning techniques, multimodal techniques and frequency-up conversion techniques. But, drawbacks in linear system open door for non-linear system mechanism to exhibit a wider frequency range in one mechanism. It was found that, a hardening response in non-linear system able to produce large amplitude over a wider frequency range. For further study, an investigation will be done in order to produce wideband in non-linear piezoelectric vibration energy harvesting system.

CHAPTER 3

METHODOLOGY

3.1 Introduction

This chapter will focus on how the objectives are going to be achieved. A few steps have to be taken in order to accomplish all the objectives stated and make the project successful. Figure 3.1 below shows the flow chart of the process.

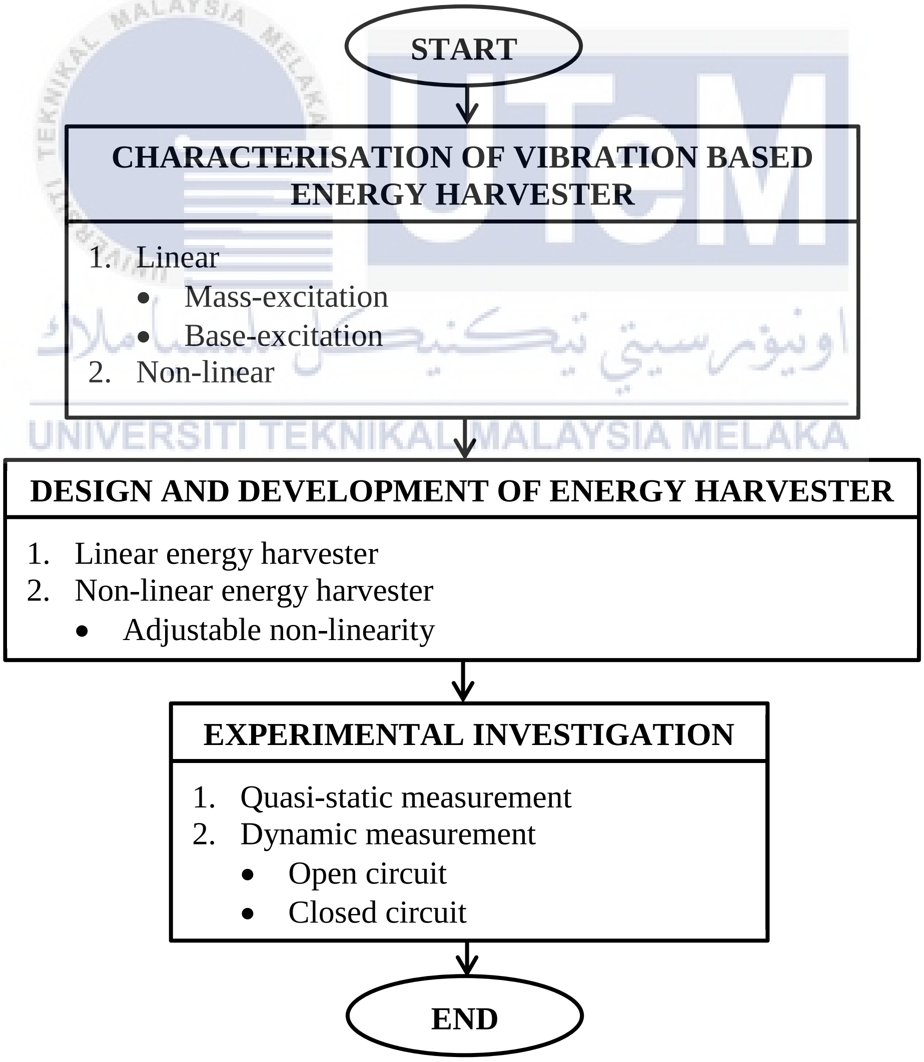

Figure 3.1: Flow chart of the process

3.2 Characterisation of vibration based energy harvester

A vibration system basically consisted of three elements; the mass, the spring and the damper. In vibrating body, there is exchange of energy from one form to another. Energy is stored by the mass in the form of kinetic energy ($1/2\ mv^2$), in the spring in the form of potential energy ($1/2\ kx$) and dissipated in the damper. The power harvested in the system is imitated by the power dissipated in the damper.

3.2.1 Linear system

Linear energy harvesting system is a type of function in the form of $F = k_1 x$ where graph is a straight line on the coordinate plane, as shown in Figure 3.2. k_1 is the linear spring constant and represent as the slope of the line.

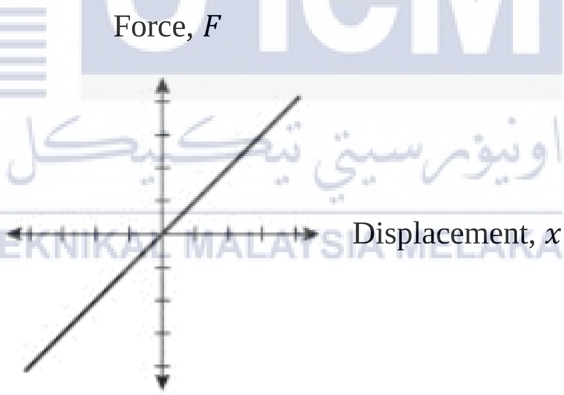

Figure 3.2: A plot of force against displacement in linear system.

The energy enters the system with the application of external force known as excitation. The excitation disturbs the mass from its mean position and the mass moving from the mean position. Two types of forcing that can be applied to the spring-mass-damper system are known as mass-excitation and base-excitation.

3.2.1.1 Mass excitation

Mass excitation is considered as a spring-mass-damper system with applied force at the mass, as shown in Figure 3.3.

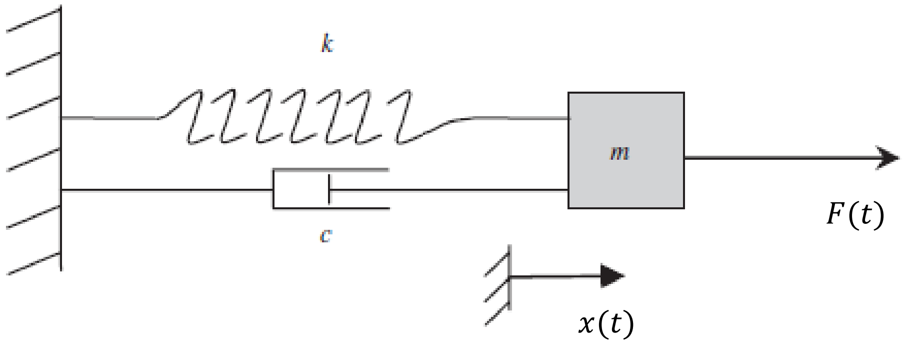

Figure 3.3: Mass-excitation of spring-mass-damper.

For this case, $F(t)$ has the form of sine or cosine function of a single frequency. The force, $F(t)$ will be F sin (ωt) where F the magnitude of the force and ω is the angular frequency of the applied force. The summing forces on the mass in the x-direction yields

$$m\ddot{x} + c\dot{x} + kx = F \sin(\omega t) \tag{37}$$

3.2.1.2 Base excitation

The base is excited and moved by the displacement input function, $y(t)$. This is difference than mass excitation because this case the excitation is at the base not the mass and the excitation is given in terms of displacement not force. Base excitation can be represented as mass connected to base *via* spring and damper, as shown in Figure 3.4.

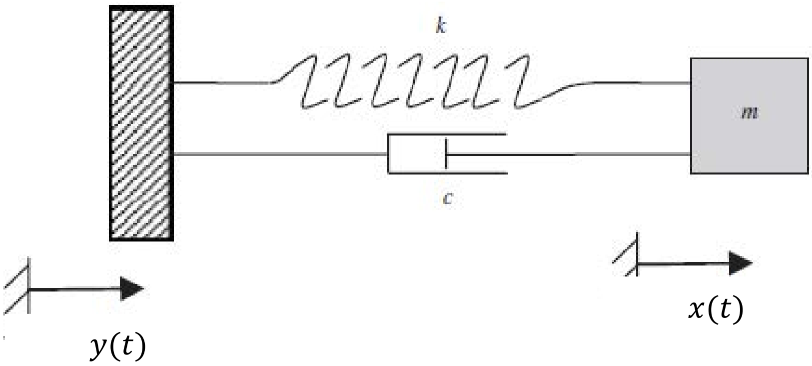

Figure 3.4: Base-excitation of spring-mass-damper.

The equation of motion is given by:

$$-k(x-y)(t)-c(\dot{x}-\dot{y})(t)=m\ddot{x}(t) \tag{38}$$

By addressing the power output as the function of vibration frequency in the linear system, the power harvested is expected to be as shown in Figure 3.5 and indicate that the peak will slightly shifts from the excitation frequency due to narrow in frequency range.

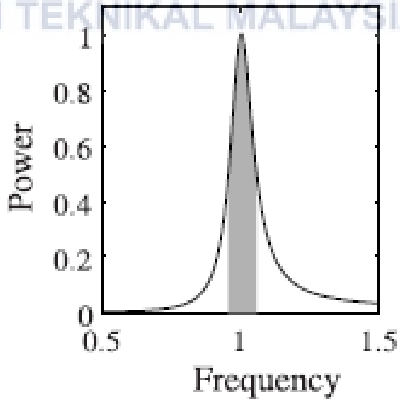

Figure 3.5: A plot of power against frequency in linear energy harvester.

3.2.2 Non-linear system

Non-linear system is a cubic function in the form of $F = k_3x^3 + k_1x$, as shown in Figure 3.6. The non-linearity of the system is depends on the stiffness of k_1 and k_3. Figure 3.6 shows that as displacement increase, the force will increase. But, at certain time, when the displacement continues increase, the force will rapidly increase to the maximum point.

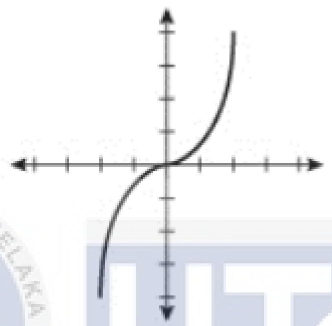

Figure 3.6: A plot of force against displacement in non-linear system.

The system consisted of mass with a combination of damper and non-linear spring whose spring force is in the form $k_3x^3 + k_1x$, where k_1 is the linear spring constant, k_3 is the non-linear spring constant and x the displacement of mass, as shown in Figure 3.7.

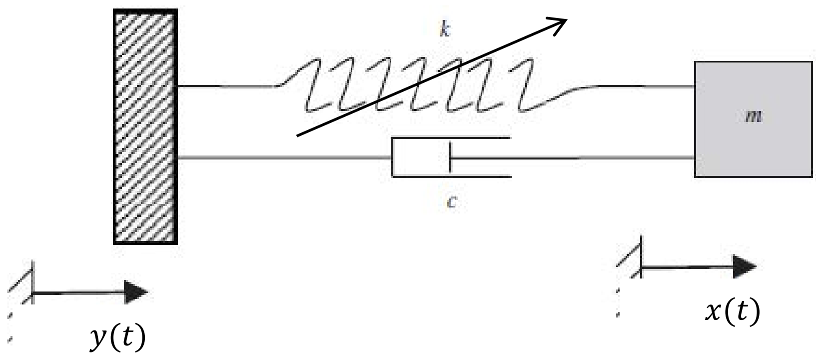

Figure 3.7: Base-excitation of hardening spring-mass-damper.

The equation of motion for a based-excitation of hardening spring-mass-damper is:

$$m\ddot{z} + c\dot{z} + k_1 z + k_3 z^3 = -m\ddot{y} \tag{39}$$

where $z = x - y$, is the relative displacement between mass, x and the base, y.

When k_3 > 0, the system will be in hardening mode. In this mode, the frequency response will bends to the right and exhibits jump phenomena. As the frequency is slowly increased from zero, the amplitude of the response first increases and then jumps down to smaller amplitude value. At high excitation level, the response curve will bends to the right. As the frequency slowly decreased from a high frequency, the amplitude of the response slowly increases and then jumps up to larger amplitude before decreasing. A plot of power against frequency of hardening cases in non-linear system is expected to be as shown in Figure 3.8(a). Non-linear system will exhibit a good result over a wider frequency range than linear system, as shown in Figure 3.8.

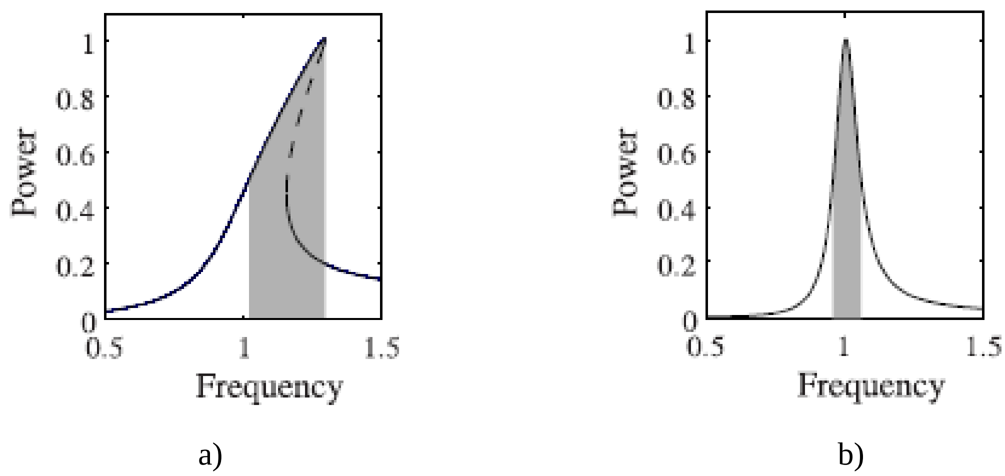

Figure 3.8: A plot of power against frequency of a) hardening response in non-linear energy harvester and b) linear energy harvester.

3.3 Design and development of energy harvester

3.3.1 Linear energy harvester

A linear energy harvester can simply design as a cantilever beam with rectangular cross-section as shown in Figure 3.9. One end is fixed and the other is free. The free end of the beam is attached with mass.

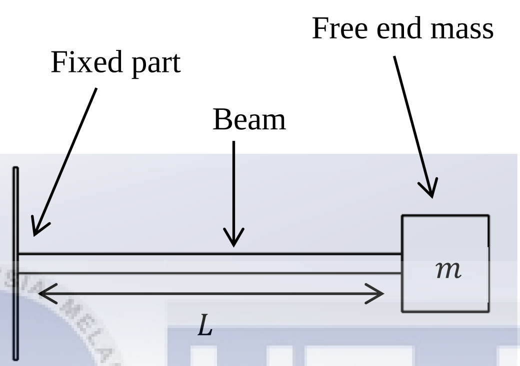

Figure 3.9: A schematic diagram of linear energy harvesting device.

The stiffness of the beam, k is given as

$$k = \frac{3EI}{L^3} \tag{40}$$

where E is the Young‟s modulus of the beam, L is the length of the beam and I is second moment area of the beam. The natural frequency of the system is given as,

$$\omega_n = \sqrt{\frac{k}{m}} \tag{41}$$

By substituting Equation (40) into Equation (41),

$$\omega_n = \sqrt{\frac{3EI}{mL^3}} \tag{42}$$

The second moment area, I is given by

$$I = \frac{bd^3}{12} \tag{43}$$

where b is breadth and d is depth of cross-section of the beam, as shown in Figure 3.10.

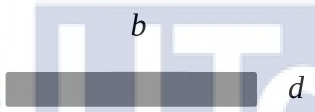

Figure 3.10: A rectangular cross-section of the beam.

The mechanical properties of the device, as shown in Table 3, were determined by weighing, measuring and calculating.

Table 3: The mechanical properties of the device.

Parameter	Value	Unit
Mass, m	0.070	kg
Width of the beam, b	0.026	m
Thickness of the beam, d	0.0075	m
Young modulus of the beam, E	2.69×10^{11}	N/m^2
Second moment area of the beam, I	9.26×10^{-13}	m^4

The photograph of linear energy harvesting device is shown Figure 3.11.

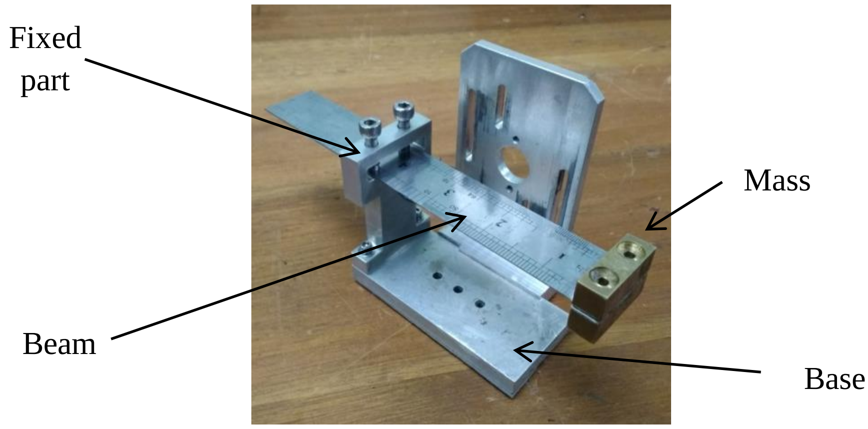

Figure 3.11: Actual photograph of the linear energy harvesting device.

3.3.2 Non-linear energy harvester

In order to design a non-linear energy harvester, a pair of mechanical stopper is added at upper and bottom side of the beam, as shown in Figure 3.12. The stoppers will limit the motion of the beam, which hardens the stiffness of the beam when the motion is beyond the stopper position. The non-linearity can be adjusted by changing the horizontal position of the stopper, x and vertical position of the stopper, y.

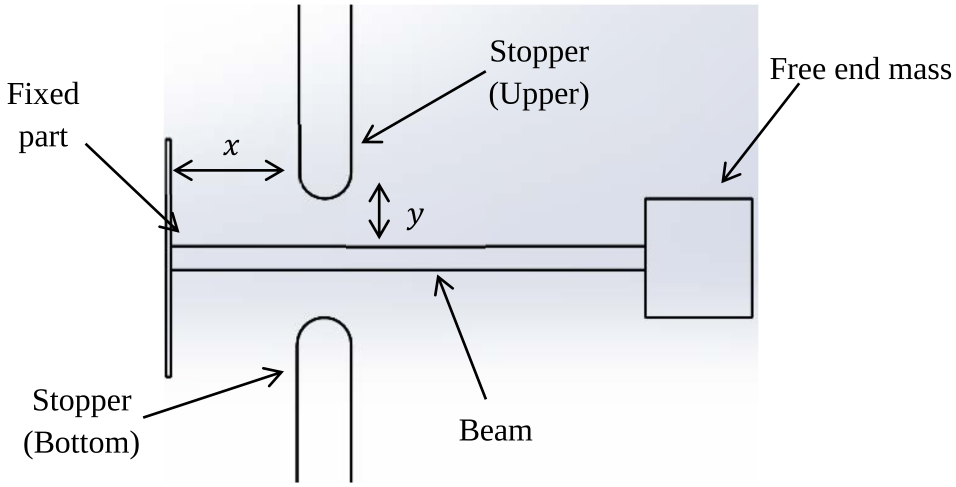

Figure 3.12: A pair of stoppers is added at upper and bottom side of the beam.

The photograph of non-linear energy harvesting device is shown in Figure 3.13.

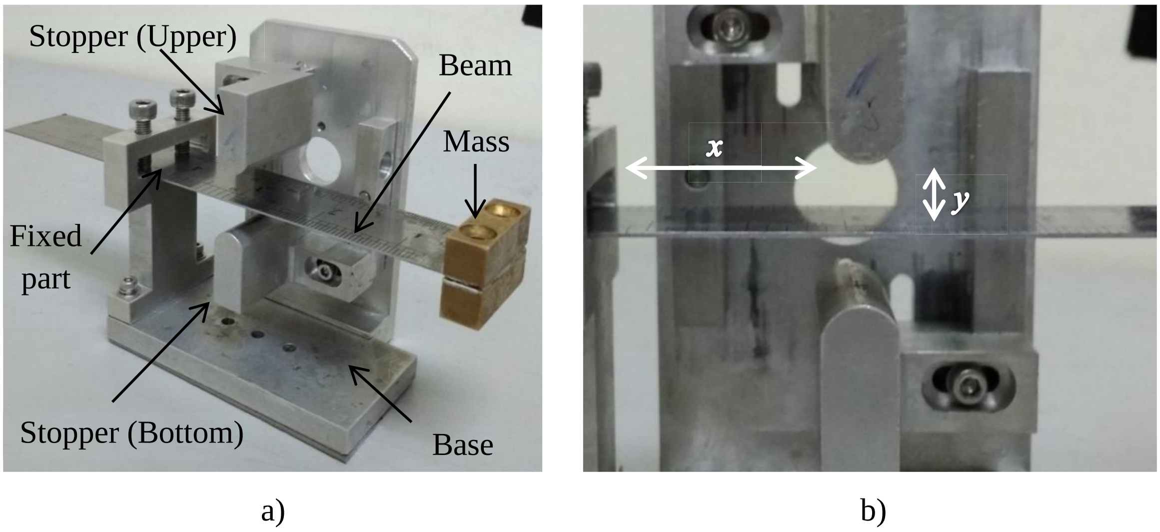

Figure 3.13: a) Actual photograph of non-linear energy harvesting device b) close-up view of the stopper.

3.4 Experimental investigation of non-linear piezoelectric energy harvester

The experiment is separated by two types of measurements. First, quasi-static measurement was conducted to find the relation between restoring force and deflection of the beam. The second measurement was dynamic measurement. Dynamic measurement was tested to measure the dynamic response for characterisation of the device. The result of voltage produce across the piezoelectric and the dynamic response of the mass and the base were recorded.

3.4.1 Quasi-static measurement

The quasi-static measurement is used to measure the restoring force against the deflection of beam, so that, the stiffness of the beam can be determined. The device is placed on the LDS V406 electrodynamic shaker. Shaker was then excited at low frequency of 1 Hz to ensure only small inertia force involved and can be ignored.

Figure 3.14: LDS V406 electrodynamic shaker.

When the base is excited, restoring force of the beam is measured by using Tedea Huntleigh load cell, which is connected to the beam by using stinger. Then, non-contact KEYENCE IL-065 laser sensor is a displacement sensor and used to measure the deflection of beam.

Simply load the Signal Calc 240 software, connect the USB cable between SignalCalc Ace Dynamic signal analyser and PC, and it is ready to begin the measurement. Figure 3.15 shows the actual photograph of PC with Signal Calc 240 software and SignalCalc Ace Dynamic signal analyser.

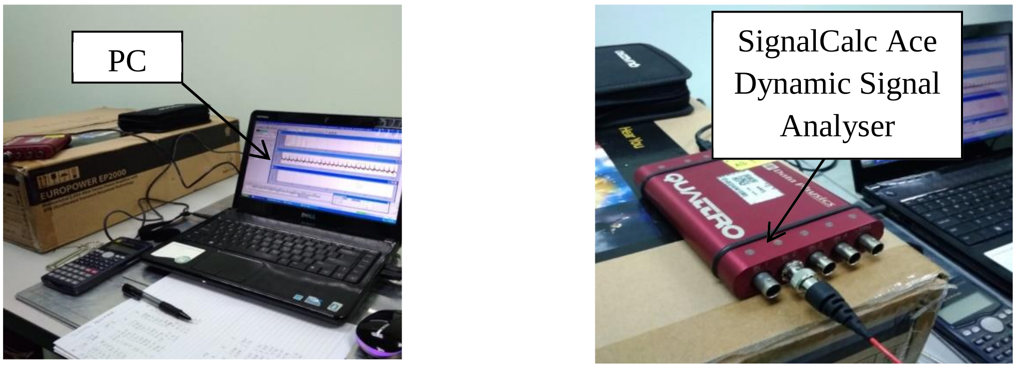

a) b)

Figure 3.15: Actual photograph of a) PC with Signal Calc 240 software and b) SignalCalc Ace Dynamic signal analyser.

The experimental setup for quasi-static measurement is shown in Figure 3.16.

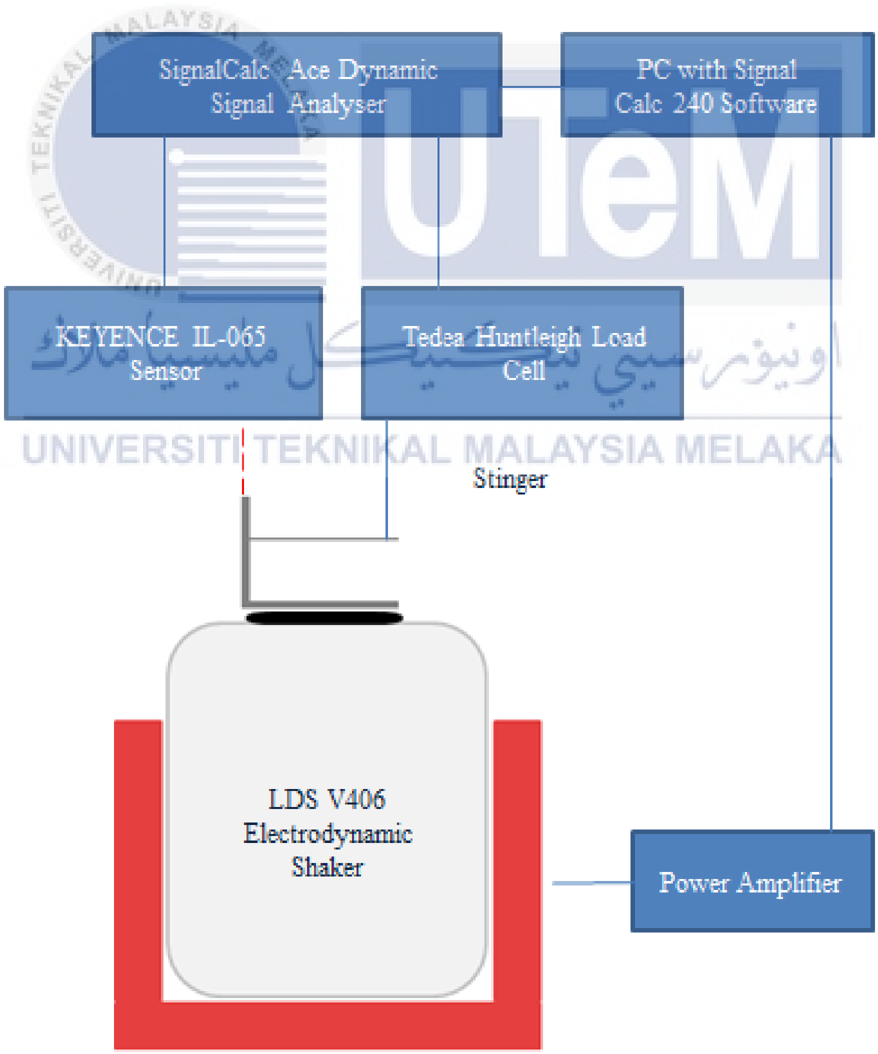

Figure 3.16: Experimental setup for quasi-static measurement.

3.4.1.1 Quasi-static test for linear system

For linear energy harvesting system, the device from Figure 3.11 was measured by using quasi-static measurement in order to obtain the force-deflection that related in the system. The test will be conducted by using different length of the beam, L. The length of the beam will be used in three different configurations, as shown in Table 4.

Table 4: Configurations of length beam.

Configuration	Length of the beam, L
A	90 mm
B	80 mm
C	70 mm

3.4.1.2 Quasi-static test for non-linear system

In non-linear energy harvesting system, the device from Figure 3.13 is tested to obtain the force-deflection characteristic of the mechanism by through quasi-static measurement. The device will be using same length of the beam, L (90 mm), but different in horizontal position, x. Next, the stopper of the device will vary in vertical position, y. Table 5 summarizes the configurations of device in the experiment.

Table 5: Configurations of non-linear device in quasi-static measurement.

Configuration	Length of the beam, *L*	Horizontal position, *x*	Vertical position, *y*
A	90 mm	25 mm	1 mm
	90 mm	35 mm	1 mm
	90 mm	45 mm	1 mm
B	90 mm	25 mm	2 mm
	90 mm	35 mm	2 mm
	90 mm	45 mm	2 mm
C	90 mm	25 mm	3 mm
	90 mm	35 mm	3 mm
	90 mm	45 mm	3 mm

3.4.2 Dynamic measurement

For the dynamic measurement, the energy harvesting device is placed on the ETS shaker and the shaker is connected with ETS amplifier. Figure 3.17 shows an actual photograph of ETS shaker and ETS amplifier. The base of the device is excited from the motion given by ETS Shaker, which is controlled by medallion II controller. In the experiment, the frequency will sweep-up then the amplitude of the base displacement will be varying at certain case. It was kept approximately at desired value by vibration controller.

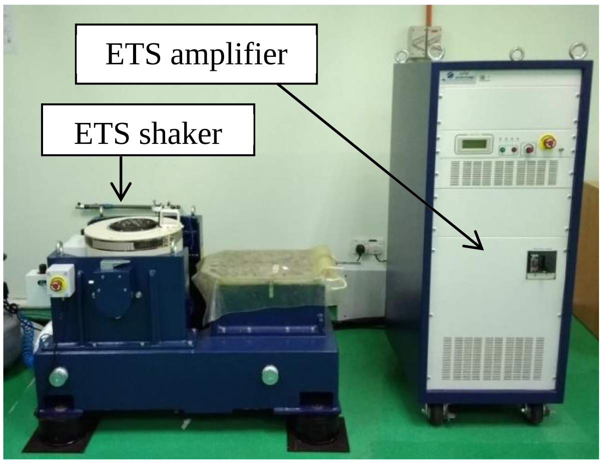

Figure 3.17: Actual photograph ETS amplifier and ETS shaker.

Next, piezoelectric is connected to decade box. TENMA 72-7270 resistance decade box is used as a resistor of any value (within its range) to assist in finding the optimal resistor size for the circuit. TENMA 72-7270 resistance decade box contains resistors of many values accessed *via* mechanical switches, as shown in Figure 3.18.

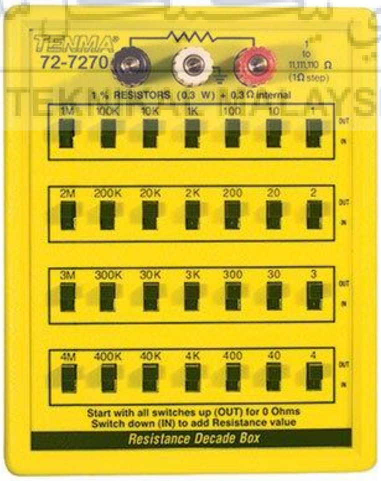

Figure 3.18: TENMA 72-7270 resistance decade box.

In order to calculate the power harvested in device, load resistor, R_L is assumed to be connected to the piezoelectric. The difference in electric potential, V in piezoelectric is recorded by using DI-155 USB data acquisition starter kit.

Then, the average power in sinusoidal AC circuit can be calculated by using Equation (44) due to appearance of electric potential across the piezoelectric transducer when acceleration or mechanical pressure occurs. The damping in the system will change if the resistor in decade box is adjusted.

$$P = \frac{V^2}{2R_L} \tag{44}$$

Lastly, Dytran accelerometer (10 mV/g) is attached with the mass from the device. The accelerometer is used to measure the acceleration of the mass and recorded with the base displacement. Figure 3.19 shows an actual photograph of Dytran accelerometer.

a)

b)

Figure 3.19: a) An actual photograph of Dytran accelerometer and b) close-up view of accelerometer

The experimental setup for dynamic measurement is shown in Figure 3.20.

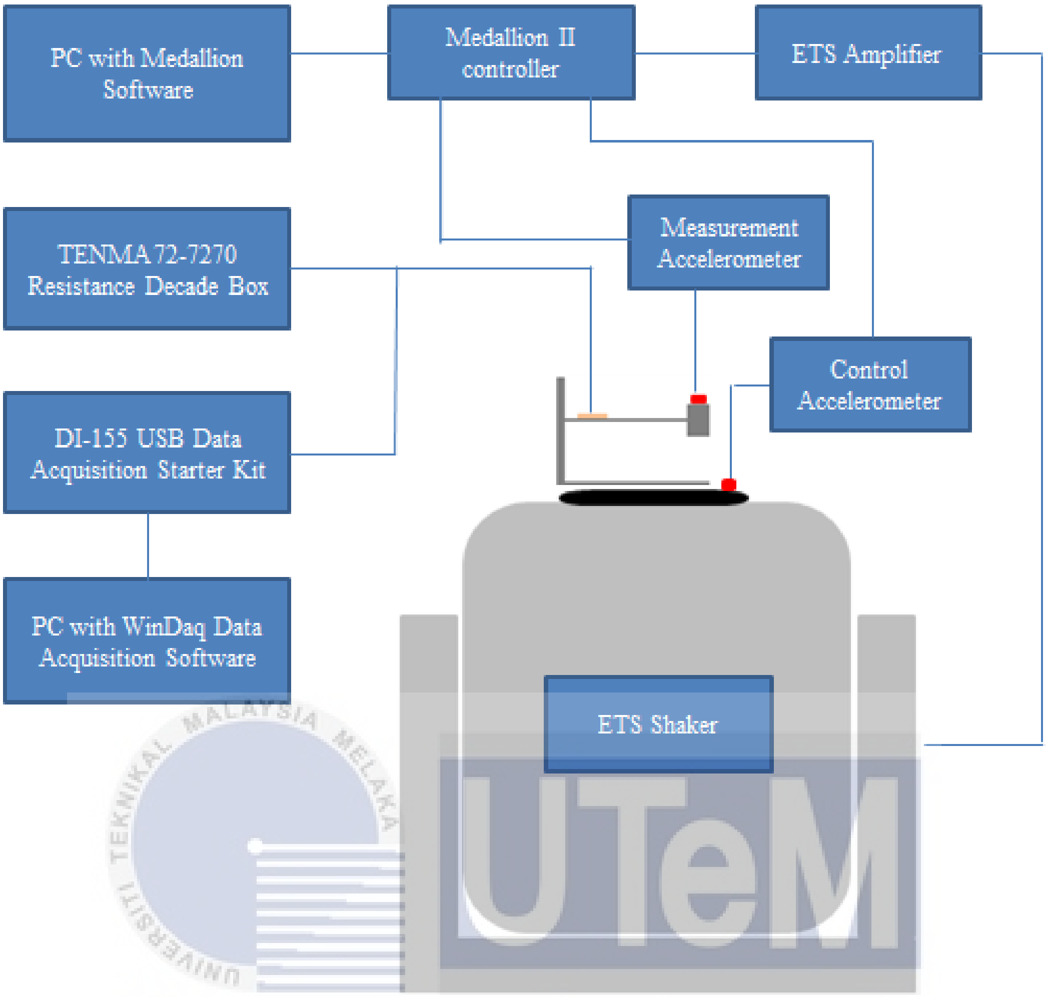

Figure 3.20: The experimental setup of dynamic measurement.

3.4.2.1 Dynamic test for linear system

In this section, linear piezoelectric energy harvesting device is used and the length of the beam, *L* will be fixed at 80 mm. The performance of open circuit and closed circuit linear system will be investigated.

3.4.2.1.1 Dynamic test of open circuit linear system

First, the testing will be run by using linear energy harvesting device. The piezoelectric is attached on the beam and place near to fixed part, as shown in Figure 3.21. For open circuit linear system, the device is placed on the ETS shaker and the test is run without appearance of load resistor, R_L. The voltage against frequency of open circuit linear system is investigated under dynamic measurement setup.

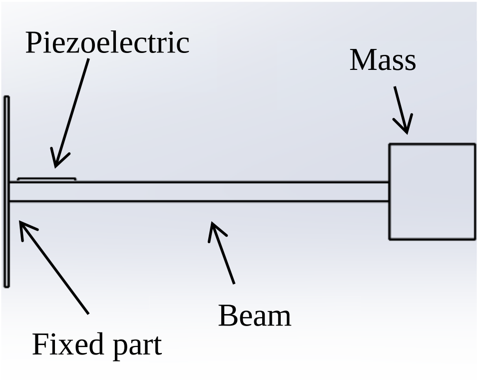

Figure 3.21: Schematic diagram of linear piezoelectric energy harvesting device.

3.4.2.1.2 Dynamic test of closed circuit linear system

For closed circuit linear system, the linear piezoelectric energy harvester, as shown in Figure 3.22 will be test by using different load resistor, R_L, in order to assist in finding maximum power, P for the circuit. Then, TENMA 72-7270 resistance decade box is used as a load resistor of value within 0 MΩ to 4 MΩ. The maximum power against resistance in linear system is investigated under dynamic measurement setup.

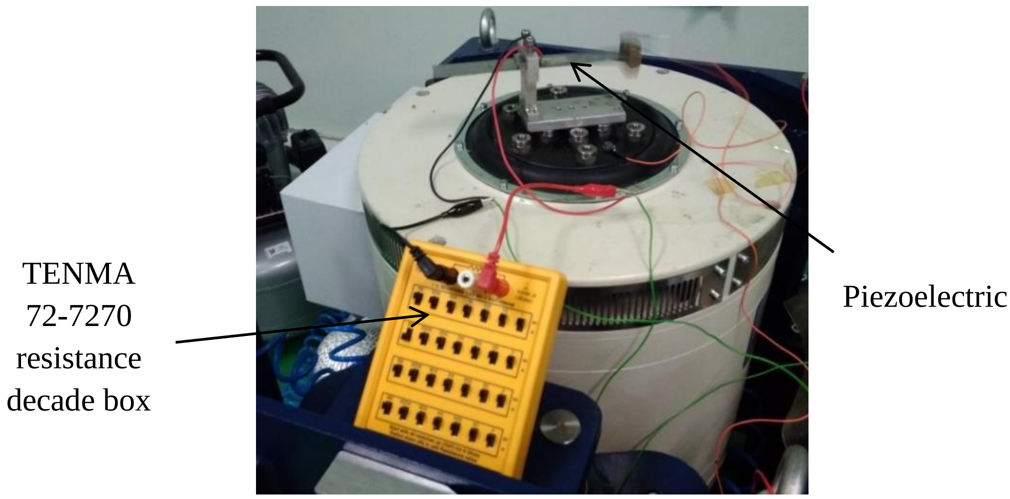

Figure 3.22: Closed circuit linear system under dynamic measurement setup.

3.4.2.2 Dynamic test for non-linear system

Next, a non-linear piezoelectric energy harvesting device is placed on ETS shaker, as shown in Figure 3.23, and it will be test under dynamic measurement.

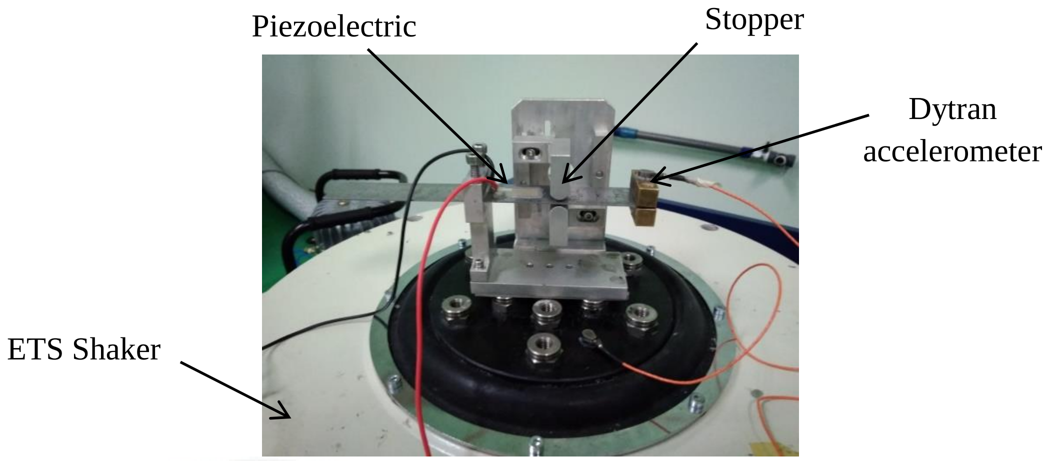

Figure 3.23: A non-linear piezoelectric energy harvesting device on ETS shaker.

The length of beam, L is fixed at 80 mm. An investigation will be made by adjusting the position of stopper and varying the amplitude of the base displacement. First, the stopper is changed in x-direction and fixed in y`-direction. Next, the stopper is fixed in $x$-direction and changed in $y$-direction. Figure 3.24 show the adjustment of stopper in non-linear energy harvester. Lastly, the amplitude of the base displacement will be varied at fixed position of the stopper in x-direction and y`-direction.

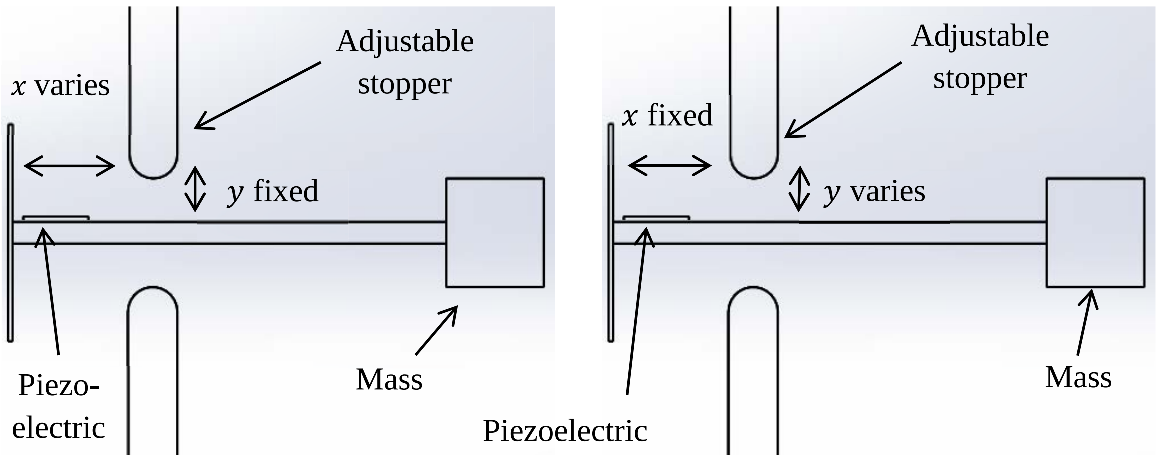

a) x varies and y fixed b) y varies and x fixed

Figure 3.24: The test that will be conducted in non-linear system.

3.4.2.2.1 Dynamic test of open circuit non-linear system

The piezoelectric is attached on the beam and place near to fixed part, as shown in Figure 3.24. For open circuit non-linear system, the device is placed on the ETS shaker and the test is run without appearance of load resistor, R_L. The configuration of the non-linear energy harvesting device in dynamic test for open circuit is shown in Table 6. Then, the voltage against frequency in non-linear system is investigated under dynamic measurement setup.

Table 6: Configuration of open circuit non-linear piezoelectric energy harvester.

Configuration	Type of circuit	Length of the beam, L	Horizontal position, x	Vertical position, y	Amplitude of base displacement
A	Open circuit	80 mm	45 mm	1 mm	1.0 mm
		80 mm	40 mm	1 mm	1.0 mm
		80 mm	35 mm	1 mm	1.0 mm
B	Open Circuit	80 mm	45 mm	1 mm	1.0 mm
		80 mm	45 mm	2 mm	1.0 mm
		80 mm	45 mm	3 mm	1.0 mm
C	Open circuit	80 mm	45 mm	1 mm	1.0 mm
		80 mm	45 mm	1 mm	0.8 mm
		80 mm	45 mm	1 mm	0.6 mm

Varies

3.4.2.2.2 Dynamic test of closed circuit non-linear system

For closed circuit non-linear system, the non-linear piezoelectric energy harvester, as shown in Figure 3.23 will be test by using the optimum resistor from dynamic test for closed circuit linear system (from section 3.4.2.1.2) in order to assist in getting optimum power, *P* for the circuit. The configuration of the non-linear energy harvesting device in dynamic test for closed circuit test is shown in Table 7. The power against resistance in linear system is investigated under dynamic measurement setup.

Table 7: Configuration of closed circuit non-linear piezoelectric energy harvester.

Configuration	Type of circuit	Length of the beam, *L*	Horizontal position, *x*	Vertical position, *y*	Amplitude of base displacement
A	Closed circuit	80 mm	45 mm	1 mm	1.0 mm
		80 mm	40 mm	1 mm	1.0 mm
		80 mm	35 mm	1 mm	1.0 mm
B	Closed Circuit	80 mm	45 mm	1 mm	1.0 mm
		80 mm	45 mm	2 mm	1.0 mm
		80 mm	45 mm	3 mm	1.0 mm
C	Closed circuit	80 mm	45 mm	1 mm	1.0 mm
		80 mm	45 mm	1 mm	0.8 mm
		80 mm	45 mm	1 mm	0.6 mm

Varies

CHAPTER 4

RESULTS AND DISCUSSION

4.1 Experimental results of quasi-static measurement

The quasi-static measurement was conducted for linear and non-linear system as mention in Chapter 3. The device was excited at low frequency (1 Hz) to ensure only small inertia force involved and can be ignored. All the results obtained were plotted using Microsoft Excel in order to obtain the force-deflection graph.

4.1.1 Quasi-static results for linear system

The parameter from Table 4 was used and the effect when using different length of beam, *L* in linear system was studied. The force against deflection graph at three different length of beam was obtained.

4.1.1.1 The effect of different beam length in linear system

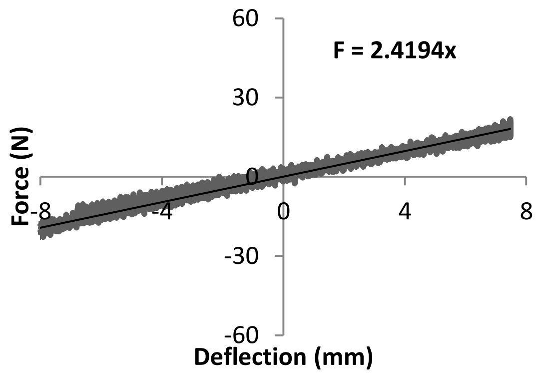

Figure 4.1: Force against deflection graph of linear energy harvester with length of the beam, *L* at 90 mm

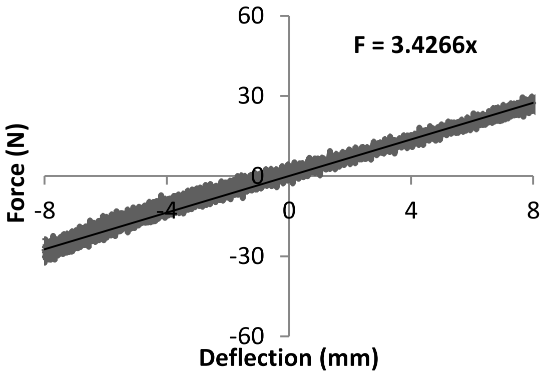

Figure 4.2: Force against deflection graph of linear energy harvester with length of the beam, L at 80 mm

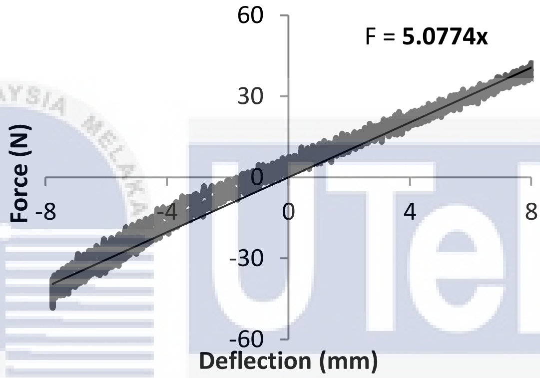

Figure 4.3: Force against deflection graph of linear energy harvester with length of the beam, L at 70 mm

Figure 4.1-4.3 shows the force-deflection of the beam for linear system with three different length of the beam, L (90 mm, 80 mm, and 70 mm). Since, the linear system is a linear function in the form of $F = k_1 x$, the slope of the line was represented as linear stiffness spring constant, k_1. From the equation form Figure 4.1, 4.2 and 4.3, the stiffness was increased as the length of the beam, L decreased. This means that, when the length of the beam, L is decreased, the beam become hard to be deformed. As can be seen, the restoring force of the beam when L at 70 mm is higher rather than L at 90 mm.

4.1.2 Quasi-static results for non-linear system

For non-linear system, the device was tested by using the parameter from Table 5. The effect when using different horizontal position, x and different vertical position, y of the stopper were studied.

4.1.2.1 The effect of horizontal position of stopper

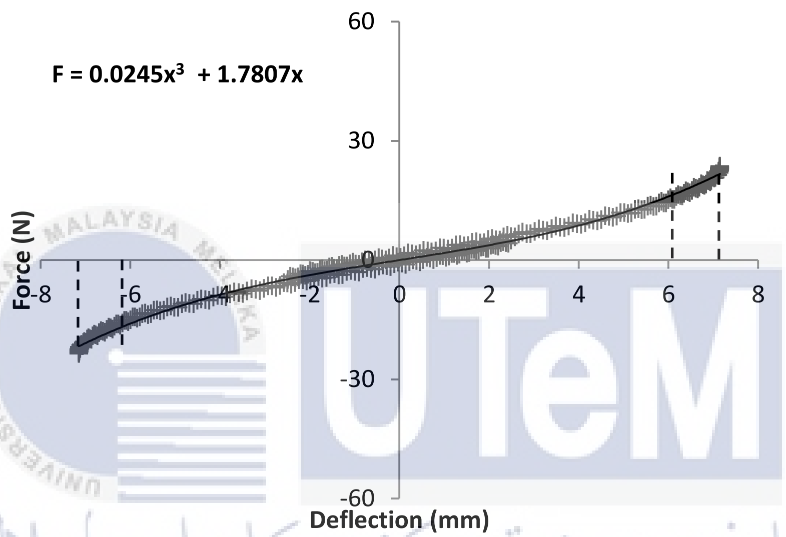

Figure 4.4: Force-deflection curve of non-linear energy harvester with stopper at y = 1 mm and x = 25 mm. Hardening zone (dash).

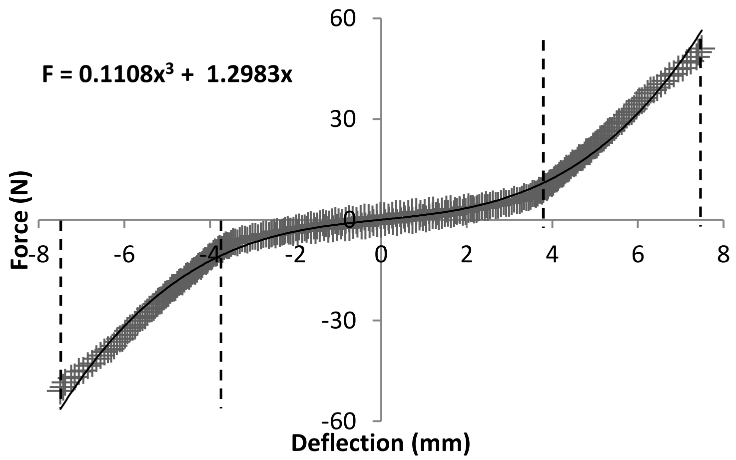

Figure 4.5: Force-deflection curve of non-linear energy harvester with stopper at y = 1 mm and x at 35 mm. Hardening zone (dash).

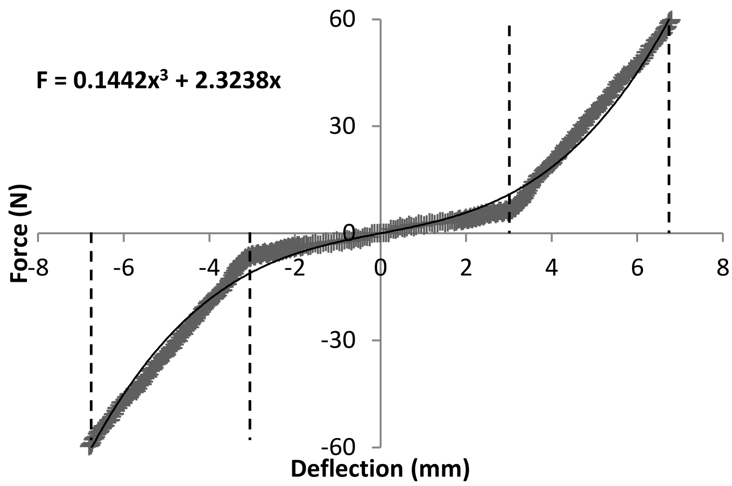

Figure 4.6: Force-deflection curve of non-linear energy harvester with stopper at *y* = 1 mm and *x* at 45 mm. Hardening zone (dash).

Figure 4.4-4.6 show the force-deflection of the beam with three different results when using three different horizontal position, *x* at same vertical position of the stopper, *y* (1 mm). Since, the non-linear system is a cubic function in the form of $F = k_3x^3 + k_1x$, the equation from Figure 4.4, 4.5 and 4.6 shows that, the hardening stiffness, k_3 was increased as the horizontal position of the stopper, *x* increased. This means that, when *x* at 45 mm, the beam able to enter hardening zone earlier than stopper at *x* = 25 mm. Along the experiment, it was observed that, when the stopper was adjusted at higher value in horizontal position, *x*, the beam touches the stopper and move under constrained motion earlier rather than the stopper at lower horizontal position, *x*. Thus, as the horizontal position of the stopper, *x* increased, the beam will hit the stopper earlier and the hardening stiffness, k_3 will increased.

4.1.2.2 The effect of vertical position of stopper

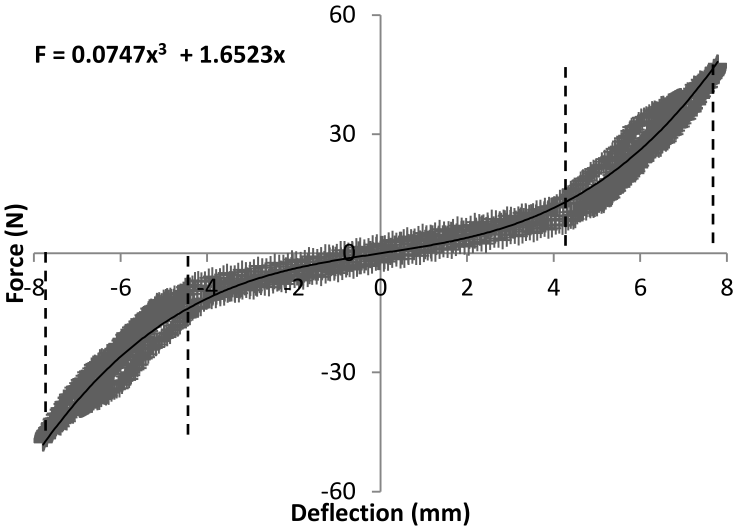

Figure 4.7: Force-deflection curve of non-linear energy harvester with stopper at *x* = 45 mm and *y* = 3 mm. Hardening zone (dash).

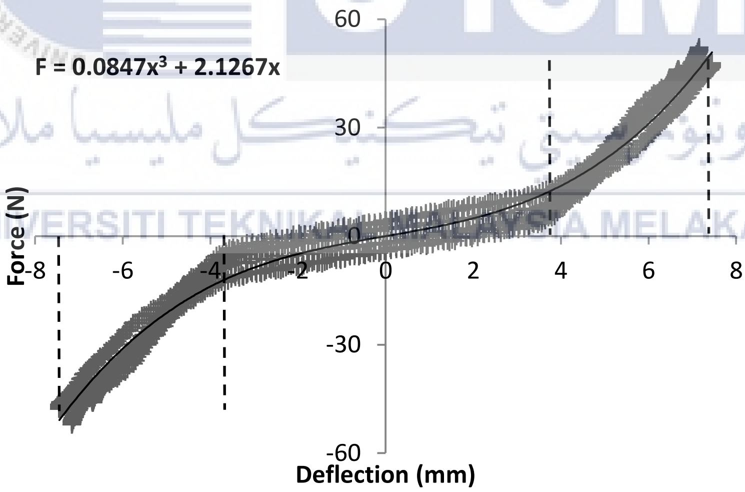

Figure 4.8: Force-deflection curve of non-linear energy harvester with stopper at *x* = 45 mm and *y* = 2 mm. Hardening zone (dash).

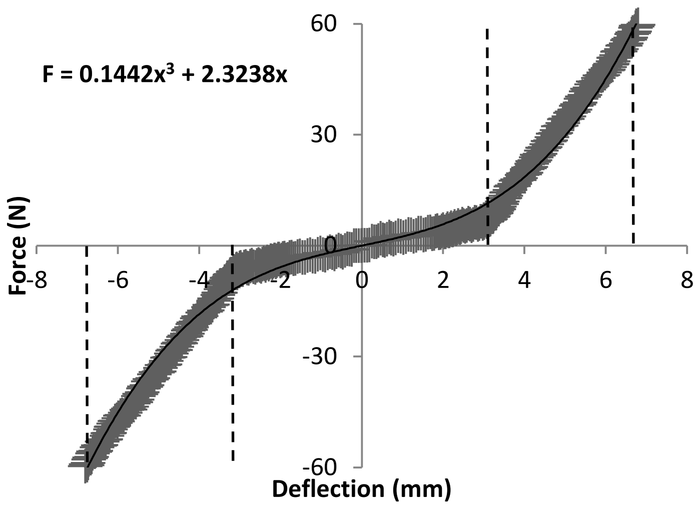

Figure 4.9: Force-deflection curve of non-linear energy harvester with stopper at *x* = 45 mm and *y* at 1 mm. Hardening zone (dash).

Figure 4.7-4.9 shows the force-deflection of the beam with three different results when using three different vertical positions, *y* at same horizontal position, *x* (45 mm) of the stopper. Equation of the trend line from Figure 4.7, 4.8 and 4.9 shows that, the hardening stiffness, k_3 and linear stiffness, k_1 was increased as the vertical position, *y* decreased. Along the experiment, it was observed that, when the stopper was adjusted at lower value in vertical position, *y* (the gap between stopper and beam became closer), the beam able to touch the stopper and move under constrained motion earlier rather than the stopper at higher vertical position, *y*. When gap between beam and stopper became closer (y = 1 mm), the beam able to enter hardening zone earlier rather than stopper at y = 3 mm. Throughout the experiment, as vertical position, *y* decreased, the restoring force of beam was increased and the beam became more harden with increase in value of hardening stiffness, k_3.

4.2 Experimental results of dynamic measurement.

The dynamic measurement was conducted for linear and non-linear system and the base of the device was excited from the motion given by ETS Shaker. The base was excited and frequency was increased from 10 Hz to 40 Hz with increment 0.5 Hz. The measurement was conducted for sweep-up frequency and all the results obtained were plotted using Microsoft Excel to obtain voltage-frequency relation and power-frequency relation.

4.2.1 Dynamic measurement results of linear system

A linear piezoelectric energy harvesting device was tested in dynamic measurement and the length of the beam, L was maintained at 80 mm. The performance of open circuit and closed circuit linear system was investigated.

4.2.1.1 Open circuit performance of linear piezoelectric energy harvester

For open circuit linear system, the piezoelectric was tested without appearance of load resistor, R_L and the voltage produce in circuit was recorded. All the results obtained were plotted using Microsoft Excel and the voltage against frequency graph was obtained.

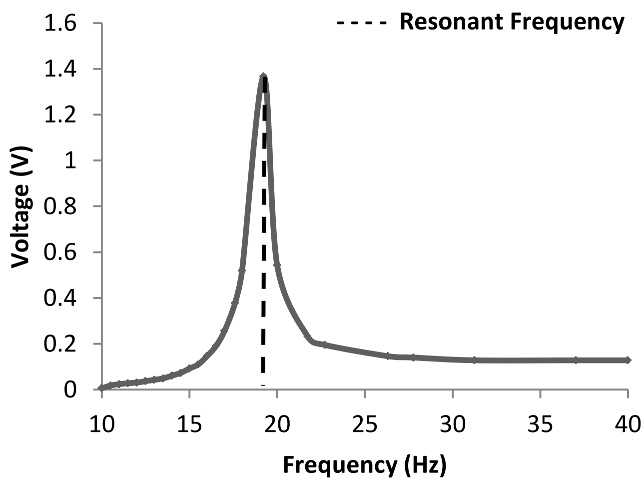

Figure 4.10: A plot of voltage against frequency of open circuit linear system.

Figures 4.10 show the frequency response curve of open circuit voltage for linear energy harvester. The maximum voltage was obtained at 1.4 V when at resonance (19.23 Hz). At resonance, the beam able to deflect at high value but the peak will slightly shift from the excitation frequency due to narrow in frequency range in linear system.

4.2.1.2 Closed circuit performance of linear piezoelectric energy harvester

For closed circuit linear system, the linear piezoelectric energy harvester, as shown in Figure 3.22 was tested by using different load resistor, R_L. The load resistor was increase from 1 MΩ to 4 MΩ with increment 0.5 MΩ. The maximum power against resistance in linear system was obtained under dynamic measurement setup.

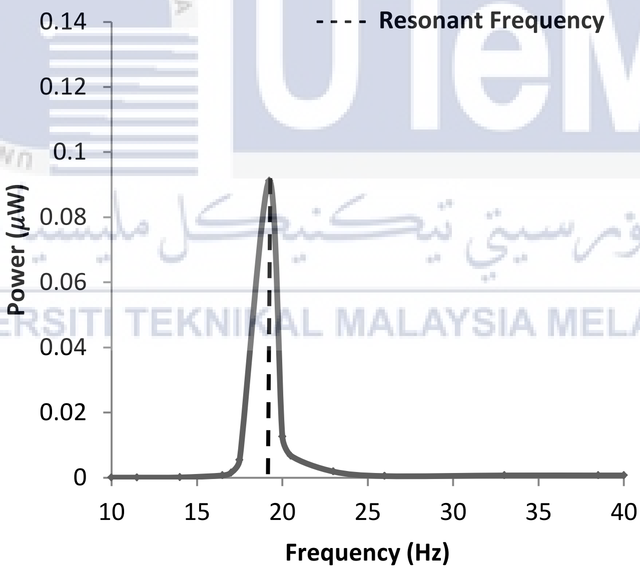

Figure 4.11: The power against frequency graph of closed circuit linear piezoelectric energy harvester with load resistor, R_L at 1.0 MΩ.

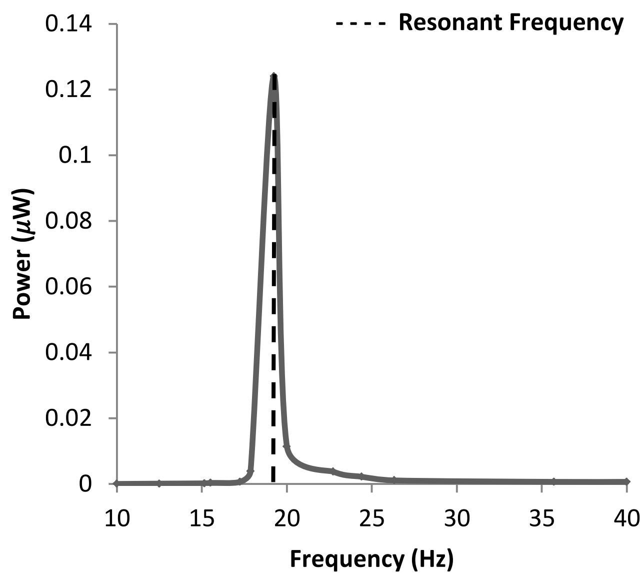

Figure 4.12: The power against frequency graph of closed circuit linear piezoelectric energy harvester with load resistor, R_L at 1.5 MΩ.

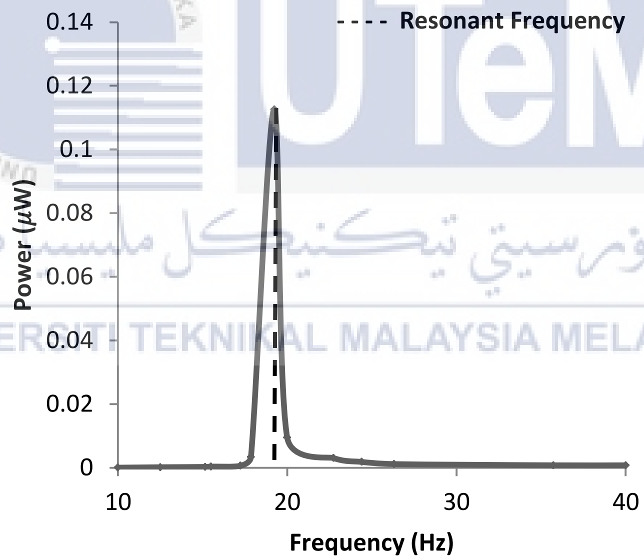

Figure 4.13: The power against frequency graph of closed circuit linear piezoelectric energy harvester with load resistor, R_L at 2.0 MΩ.

Figure 4.11-4.13 shows the frequency responses of closed circuit voltage for linear piezoelectric energy harvester at three different load resistors, R_L (1.0 MΩ, 1.5 MΩ and 2.0 MΩ). All the measured results in Figure 4.11-4.13 show the maximum closed circuit power output with different load resistors, R_L at resonance (19.23 Hz).

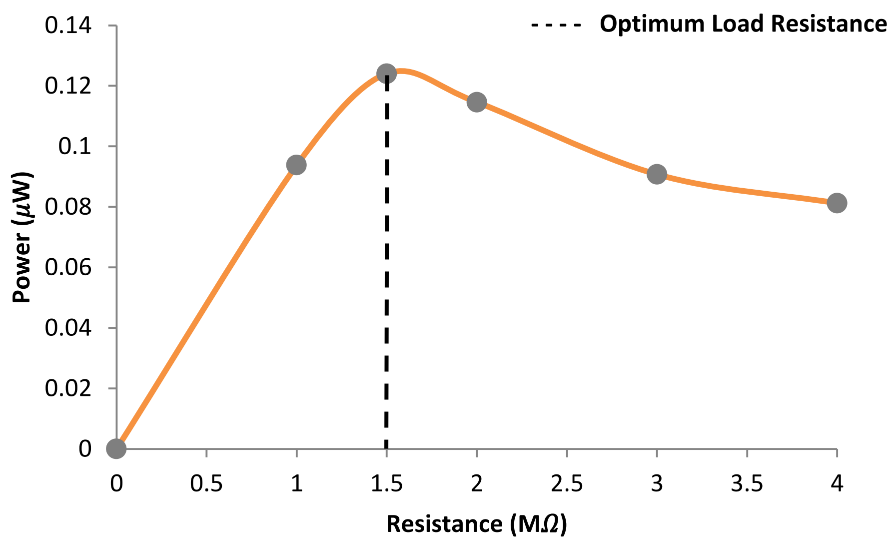

Figure 4.14: Comparison of measured output power of energy harvester as function of load resistor, R_L operating at its experimental resonance frequencies (i.e., maximum closed circuit voltage in Figure 4.11-4.13).

Meanwhile, Figure 4.14 shows the measured output power of closed circuit linear piezoelectric energy harvester as a function of load resistor, R_L operating at the resonance frequencies (the resonance frequency here refers to the experimental frequency having the maximum closed circuit power in Figure 4.11-4.13). The maximum power (0.124 μW) was obtained when the load resistor at 1.5 MΩ. This is due to an equivalent value of resistor in the circuit with the load resistor ($R_i = R_L$). Since the optimum resistance in circuit was found, the load resistor will be used at 1.5 MΩ in closed circuit non-linear system, in order to maximize the power in the circuit.

4.2.2 Dynamic measurement results of non-linear system

In this section, a non-linear piezoelectric energy harvesting device was placed on ETS shaker, as shown in Figure 3.23, and the length of the beam, L was fixed at 80 mm for all parameter under dynamic measurement. The experiment was conducted and the effect of different horizontal position of the stopper, x, different vertical position of the stopper, y and amplitude base displacement was studied. The performance of open circuit and closed circuit non-linear system was investigated.

4.2.2.1 Open circuit performance of non-linear piezoelectric energy harvester

For open circuit non-linear system, without appearance of load resistor, R_L, the device was tested by using the parameter from Table 6. The voltage across in piezoelectric was recorded and the voltage against frequency graph was obtained.

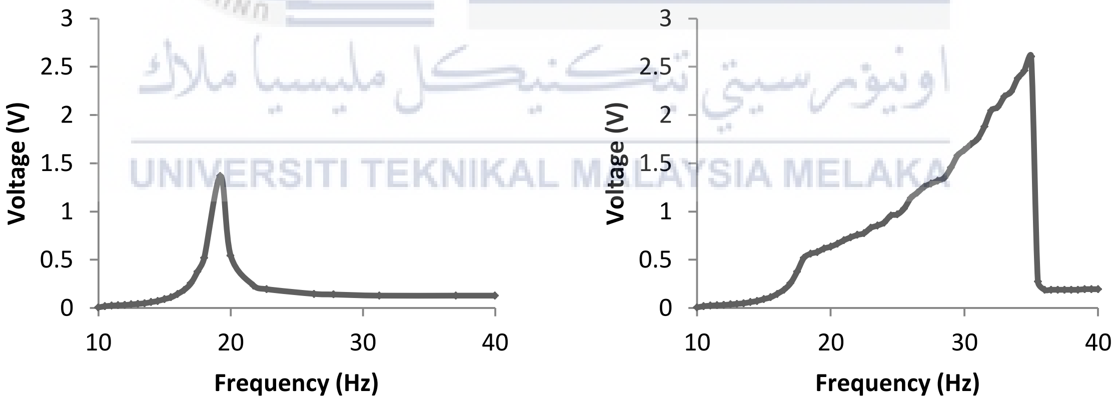

a) b)

Figure 4.15: A plot of power against frequency of a) linear energy harvester and b) hardening response non-linear energy harvester.

Figure 4.15 shows comparison between the bandwidth of linear and non-linear system, which is non-linear system exhibits a good result over a wider frequency range than linear system. Figure 4.15(a) shows a plot of voltage against frequency of linear system at L = 80 mm. Meanwhile, Figure 4.15(b) shows a plot of voltage against frequency of non-linear system at L = 80 mm, stopper at horizontal position, x (45 mm), vertical position, y (1 mm) and amplitude base displacement at 1 mm. For non-linear system, at low excitation level, the frequency response was similar to the response of linear system (Figure 4.15(a)). However, at high excitation level, the response curve was bent to the right, as shown in Figure 4.15(b). Energy harvesting device using hardening mechanism can broaden the frequency response in one mechanism and produce higher voltage output rather device in linear system.

4.2.2.1.1 The effect of horizontal position of the stopper in open circuit non-linear system

Along the experiment, the stopper of device was fixed in vertical position, y (1 mm) and input amplitude base displacement at 1 mm. Then, the stopper of the device varied in three different horizontal position of the stopper, x (45 mm, 40 mm, and 35 mm).

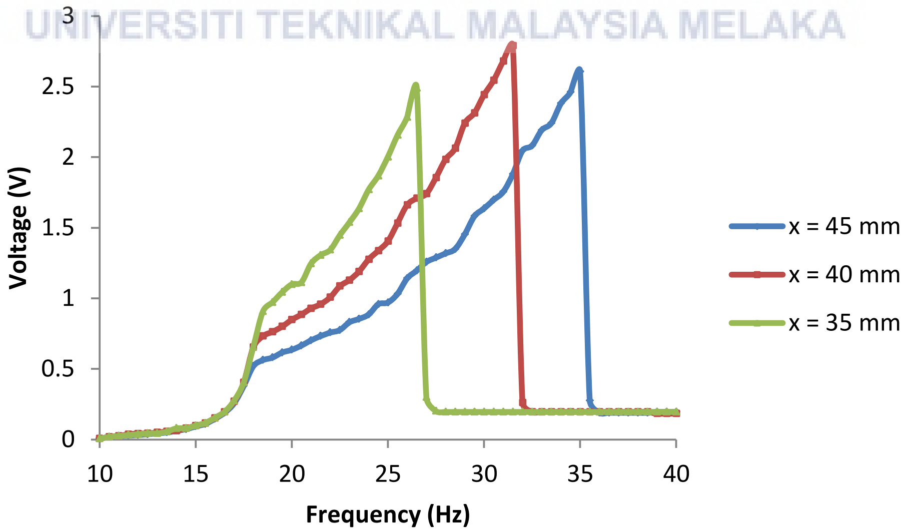

Figure 4.16: Voltage against frequency graph of non-linear piezoelectric energy harvester with fixed vertical position, y (1 mm) and varies in horizontal position, x

Figure 4.16 shows the effect of using different horizontal position of the stopper, *x*. From the results, the maximum voltage was obtained when horizontal position, *x* at 40 mm. When *x* = 40 mm, the stopper was pointed at the middle of the beam (length of the beam, *L* at 80 mm), resulting maximum deflection and maximum voltage output. Next, when the stopper increased in horizontal position, *x*, a wider bandwidth is produced. It was found that, when horizontal position of stopper, *x* at 45 mm, the response curve bent earlier (at low excitation level) and produce wider bandwidth rather than device with stopper *x* at 35 mm. This is because, when the stopper adjusted at higher value in horizontal position, *x*, the beam touches the stopper and move under constrained motion earlier than the stopper at lower horizontal position.

4.2.2.1.2 The effect of vertical position of the stopper in open circuit non-linear system

Along the experiment, the stopper of device was maintained in horizontal position (*x* = 45 mm) and input amplitude base displacement at 1 mm. The device was measured by using three different vertical positions, *y* (1 mm, 2 mm, and 3 mm).

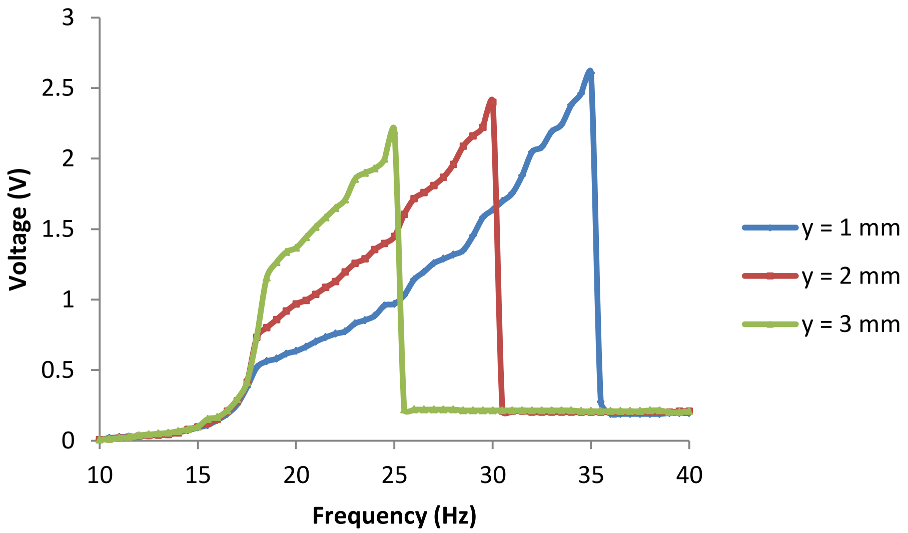

Figure 4.17: Voltage against frequency graph of non-linear piezoelectric energy harvester with fixed horizontal position, *x* (45 mm) and varies in vertical position, *y*.

Figure 4.17 shows the voltage against frequency graph of device at three different vertical position of the stopper, *y* (1 mm, 2 mm and 3 mm). From results, the maximum voltage output was increased when the stopper decreased in vertical position, *y*. This is due to gap between beam and stopper, which is smaller gap able to deflect the beam at high value when move under constrained motion. From Figure 4.17, it is clearly show that when stopper decreased in vertical position, *y*, the bandwidth for open circuit voltage non-linear system exhibits a good result over a wider frequency range. The widest bandwidth was produced when the stopper was adjusted at small gap (*y* = 1 mm), this is because the beam touches the stopper earlier than the stopper at larger gap (*y* = 3 mm). So that, at low excitation level, the response able to shift to right earlier.

4.2.2.1.3 The effect of amplitude base displacement in open circuit non-linear system

In order to investigate the effect of amplitude base displacement, the stopper of device was fixed in horizontal position, *x* (45 mm) and vertical position, *y* (1 mm) but varies in amplitude base displacements (0.6 mm, 0.8 mm and 1.0 mm).

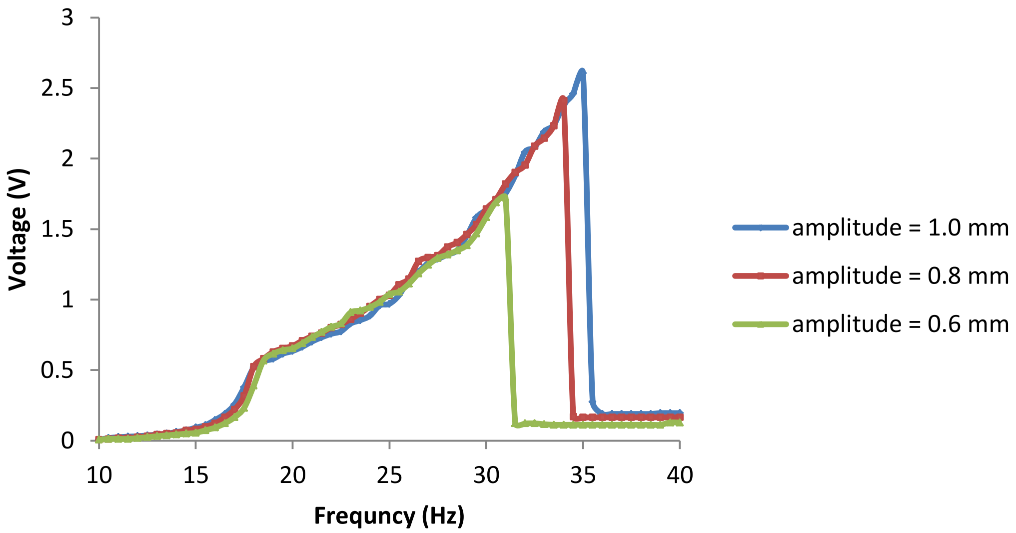

Figure 4.18: Voltage against frequency graph of non-linear energy harvester with stopper fixed at *x* 45 mm and *y* = 1 mm but varies in amplitude base displacement.

As for the device configuration of horizontal position, x (45 mm) and vertical position, y (1 mm), the device easily produced hardening stiffness even at low amplitude base displacement (0.6 mm). This is because of the small gap (y = 1 mm) between the beam and stopper, which is able to make the beam move under constrained motion even at low amplitude base displacement. For the results effect on different amplitude base displacement, an increase in amplitude of base displacement results in an increase in frequency bandwidth and voltage output.

4.2.2.2 Closed circuit performance of non-linear piezoelectric energy harvester

For closed circuit non-linear system, the device was tested by using the parameter from Table 7. Since the optimum power was obtained in closed circuit linear system (section 4.2.1.2), the load resistor was fixed at 1.5 MΩ for all parameter in closed circuit non-linear system. Then, due to appearance of electric potential across the piezoelectric transducer, the voltage against frequency graph and power against frequency graph was obtained.

4.2.2.2.1 The effect of horizontal position of the stopper in closed circuit non-linear system

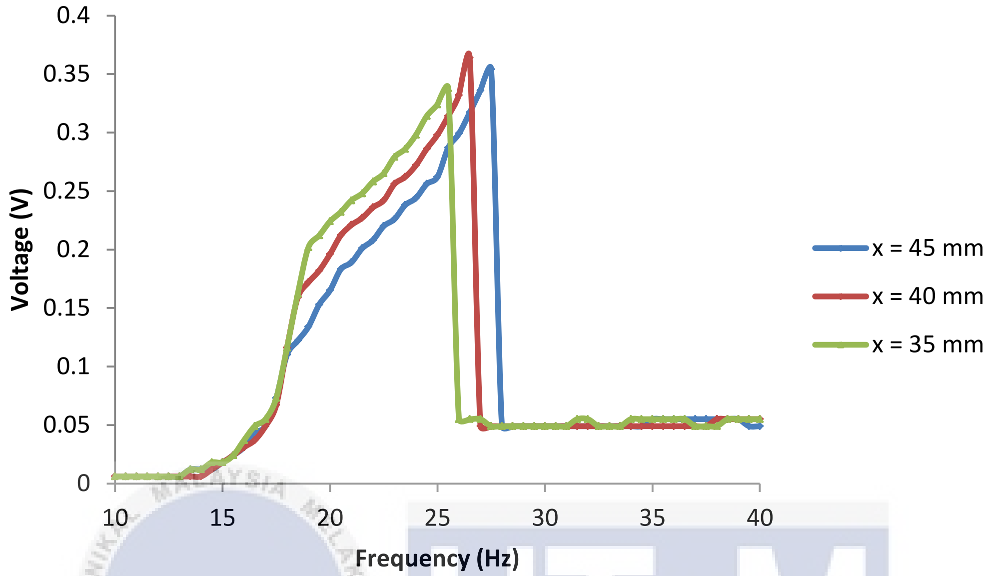

Figure 4.19: Voltage against frequency graph of non-linear piezoelectric energy harvester with fixed in vertical position, *y* (1 mm) and varies in horizontal position, *x*.

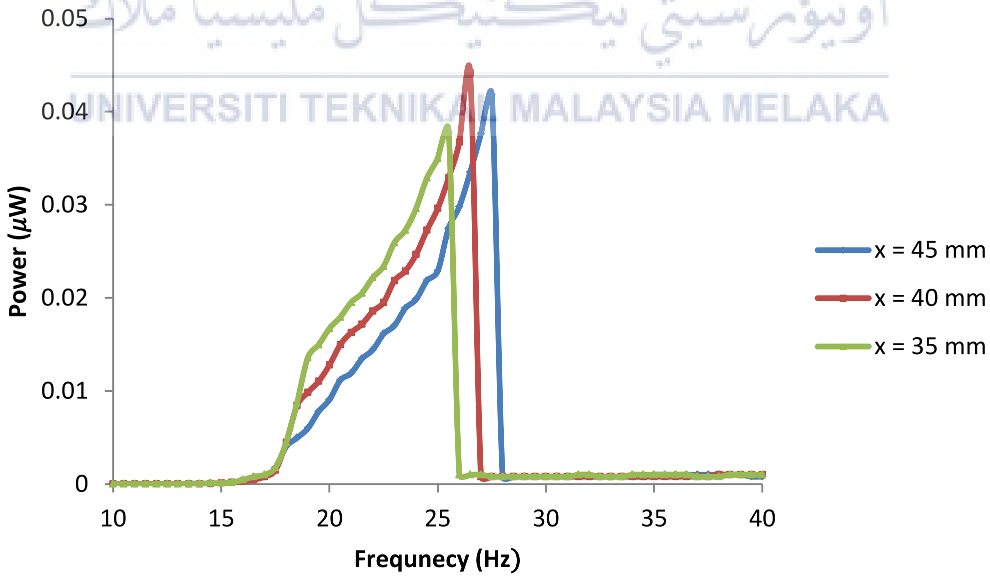

Figure 4.20: Power against frequency graph of non-linear piezoelectric energy harvester with fixed in vertical position, *y* (1 mm) and varies in horizontal position, *x*

Figure 4.19 shows voltage against frequency graph of closed circuit non-linear system when the stopper was adjusted at three different horizontal position, x (35 mm, 40 mm, and 45 mm) under same vertical position, y (1 mm) and same amplitude base displacement (1 mm). The maximum voltage of closed circuit was obtained when stopper in at x = 40 mm. This is due to the stopper was pointed at middle of the beam and resulting maximum deflection and maximum voltage.

Comparison the results from Figure 4.16 and 4.19, it was found that the output voltage of closed circuit non-linear system was lower than open circuit non-linear system. Open circuit non-linear system able to produce higher voltage rather than closed circuit non-linear system. In fact, open circuit voltage is the difference of electrical potential between two terminals of a device when disconnected from any circuit (no load resistor). There is no external load connected in the circuit (no load applied) and no external electric current flows between the terminals. Meanwhile, closed circuit is in a closed state (under load) and voltage drop was occurred.

Figure 4.20 shows power against frequency graph of closed circuit non-linear system when the stopper was adjusted at three different horizontal position, x (35 mm, 40 mm, and 45 mm) under same vertical position, y (1 mm) and amplitude base displacement of the device was fixed at 1 mm. When horizontal position of the stopper, x at 40 mm, the maximum power was obtained due to stopper was pointed at middle of the beam and resulting maximum deflection. An increase in horizontal position of the stopper, results in an increase in frequency bandwidth. This is due to the beam move earlier in constrained motion than the stopper at lower horizontal position.

4.2.2.2.2 The effect of vertical position of the stopper in closed circuit non-linear system

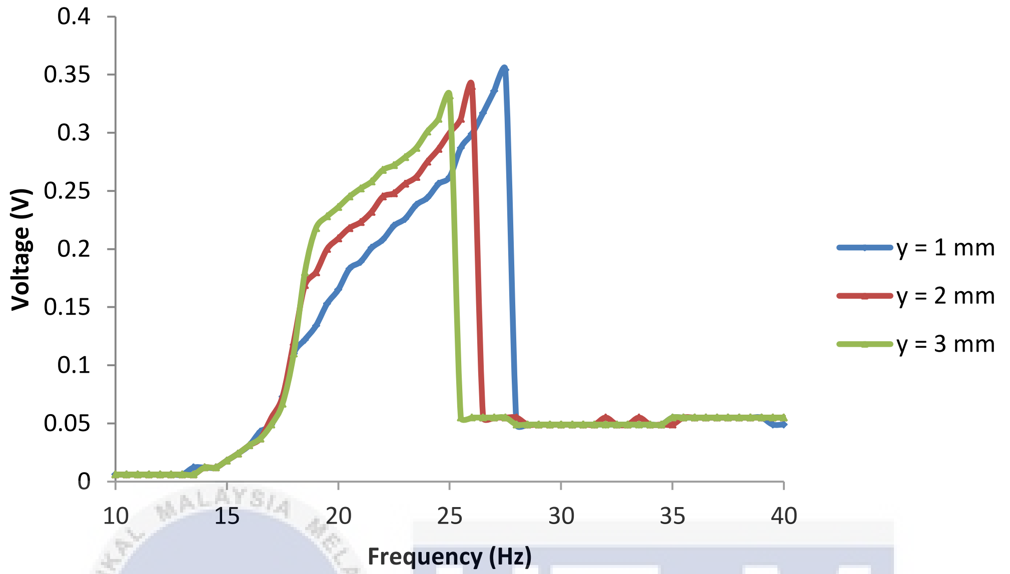

Figure 4.21: Voltage against frequency graph of non-linear piezoelectric energy harvester with fixed in horizontal position, *x* (45 mm) and varies in vertical position, *y*.

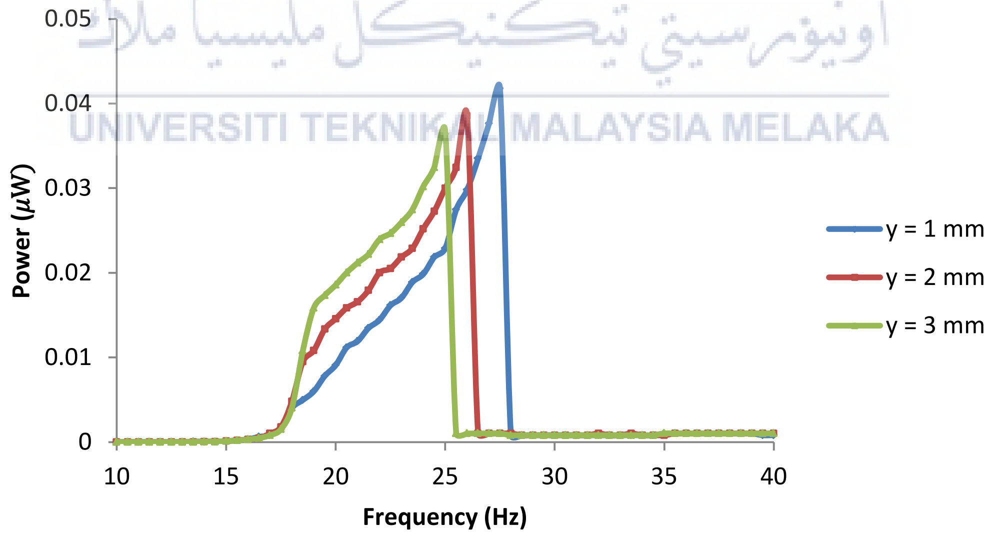

Figure 4.22: Power against frequency graph of non-linear piezoelectric energy harvester with fixed in horizontal position, *x* (45 mm) and varies in vertical position, *y*.

Figure 4.21 shows the voltage against frequency graph of the device when stopper at three different vertical position, y (1 mm, 2 mm and 3 mm) but at same in horizontal position, *x* (45 mm) and fixed in amplitude base displacement (1 mm). Meanwhile, Figure 4.22 shows the power against frequency graph at same configuration of the device used in Figure 4.21. From results, when the stopper decreased in vertical position, *y*, the maximum voltage output was increased. This is because, when the vertical position, *y* is decreased, the gap between beam and stopper will decrease. The smaller gap between beam and stopper, the higher deflection of the beam when move under constrained motion.

Since the power output of the circuit linked with the voltage output, the maximum power output was increased when the stopper decreased in vertical position, *y*. From the Figure 4.21 and 4.22, the lower the gap between the beam and the stopper (vertical position, *y*), the larger the frequency bandwidth produced.

4.2.2.2.3 The effect of amplitude base displacement in closed circuit non-linear system

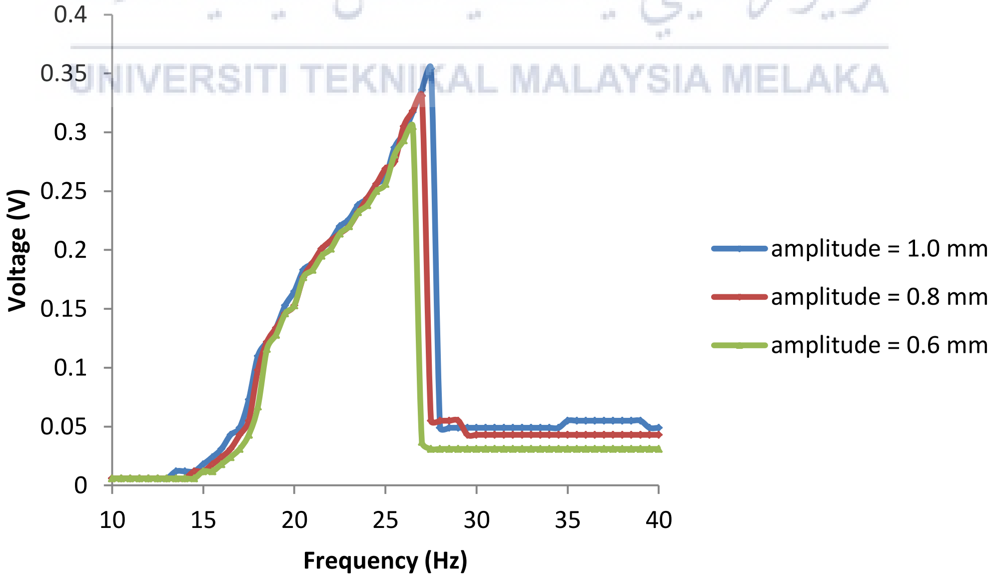

Figure 4.23: Voltage against frequency graph of non-linear piezoelectric energy harvester with fixed in horizontal position, *x* (45 mm), fixed in vertical position, *y* (1 mm) and varies in amplitude base displacement.

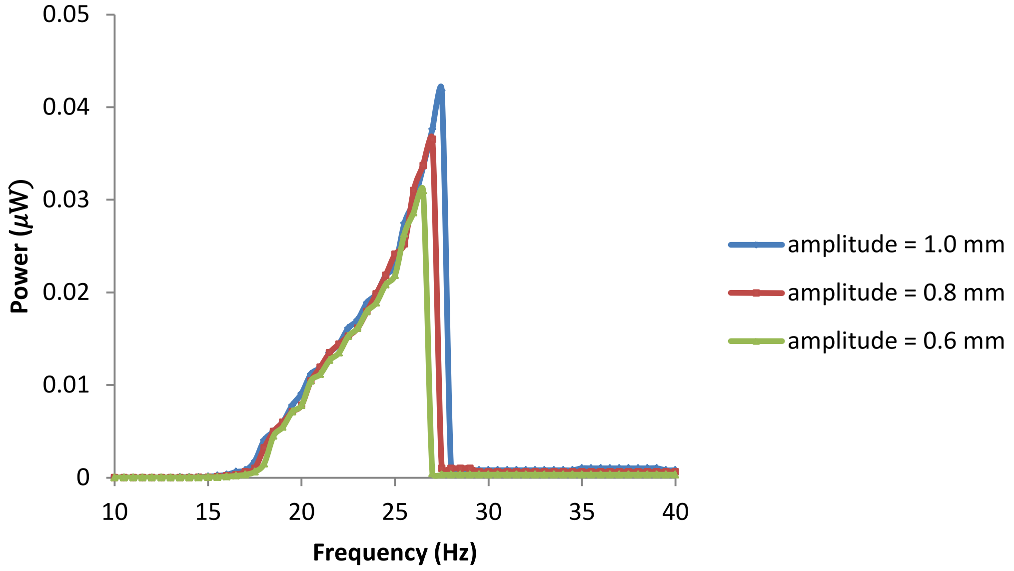

Figure 4.24: Power against frequency graph of non-linear piezoelectric energy harvester with fixed in horizontal position, *x* (45 mm), fixed in vertical position, *y* (1 mm) and varies in amplitude base displacement.

Figure 4.23 and 4.24 show that hardening response able to produce even at low amplitude base displacement (0.6 mm). This is because, the small gap (*y* = 1 mm) between the beam and stopper able make the beam move under constrained motion even at low input amplitude base displacement (0.6 mm). As the input amplitude base displacement increase, frequency bandwidth and voltage also increased. The maximum power output also increased as the input amplitude base displacement increased.

CHAPTER 5

CONCLUSION

5.1 Conclusion from the thesis

In this paper, the state of research on piezoelectric energy harvester has been reviewed. Cantilever geometry (cantilever beam) is suited to use as structure in piezoelectric energy harvesting, especially for mechanical energy harvesting due to their effortless construction and high responsiveness to vibration. The device was attached on the vibration source and several types of configuration of the energy harvester were discussed in order to improve the mechanical-to-electrical conversion efficiency.

This research is focused on the performance of linear and non-linear energy harvesting device on the vibrating source. It also concentrated on stiffness non-linearity in energy harvesting device. The dynamic response of the device in hardening mode showed that the performance of the device depends on the linear and non-linear stiffness and excitation level.

The maximum power output for linear and non-linear devices was investigated and it was found that the maximum power output for non-linear devices occurred at different frequency. From the experimental results, non-linear device provides higher power output and wider bandwidth of power harvested than linear device. Lastly, it was found that, finding an optimum resistance in non-linear system is not as easy as linear system, which is in linear system, maximum power output occurs at the same frequency.

5.2 Recommendations for future work

In order to improve the study of vibration energy harvester, some recommendations for future work are suggested:

a) The position of stopper in vertical or horizontal position and the length of beam were measured by using feeler and ruler. A more systematic way to measure those parameters are needed for a better accuracy in the measurement.

b) Instead of using piezoelectric effect as transduction mechanism in vibration energy harvester, a study on another type of transducer, such as electromagnetic and electrostatic, are suggested to compare with piezoelectric energy harvester.

c) The dimension of piezoelectric was too small. So, a new suitable dimension to fit on the beam for the same piezoelectric that used in the experiment needs to be used for further improvement and optimization a generator to produce maximum output voltage.

d) Since the device able to produce voltage, apply the voltage output to real application such as powering a small Light Emitting Diode (LED) bulb or any electronic devices that used small voltage.

e) Be aware of errors introduced by immediate working environment and protect the experiment from vibrations and electronic noise or other effects from nearby apparatus.

REFERENCES

[1] Andriopoulou, S. (2012). A review on energy harvesting from roads.

[2] Kazmierski & Beeby, S. (2010). Energy harvesting system.

[3] Zhu, D., & Beeby, S. (2010). Kinetic Energy Harvesting, In *Energy harvesting systems*, 1-77.

[4] Williams, C. B., & Yates, R. B. (1996). Analysis of a micro-electric generator for microsystems. *Sensors and actuators A: Physical*, *52*(1-3), 8-11.

[5] Stephen, N. G. (2006). On energy harvesting from ambient vibration. *Journal of sound and vibration*, *293*(1-2), 409-425.

[6] Donelan, J. M., Naing, V., & Li, Q. (2009, January). Biomechanical energy harvesting. In *Radio and Wireless Symposium, 2009. RWS'09. IEEE* (pp. 1-4). IEEE.

[7] Romero, E., Warrington, R. O., & Neuman, M. R. (2009). Energy scavenging sources for biomedical sensors. *Physiological measurement*, *30*(9), R35.

[8] Romero, E., Warrington, R. O., & Neuman, M. R. (2009, September). Body motion for powering biomedical devices. In *Engineering in Medicine and Biology Society, 2009. EMBC 2009. Annual International Conference of the IEEE* (pp. 2752-2755). IEEE.

[9] Starner, T. (1996). Human-powered wearable computing. *IBM systems Journal*, *35*(3/4), 618-629.

[10] Stephen, N. G. (2006). On energy harvesting from ambient vibration. *Journal of sound and vibration*, *293*(1-2), 409-425.

[11] El-Hami, M., Glynne-Jones, P., White, N. M., Hill, M., Beeby, S., James, E., & Ross, J. N. (2001). Design and fabrication of a new vibration-based electromechanical power generator. *Sensors and Actuators A: Physical*, *92*(1-3), 335-342.

[12] Roundy, S. J. (2003). *Energy scavenging for wireless sensor nodes with a focus on vibration to electricity conversion* (Doctoral dissertation, University of California, Berkeley).

[13] Mitcheson, P. D., Green, T. C., Yeatman, E. M., & Holmes, A. S. (2004). Architectures for vibration-driven micropower generators. *Journal of microelectromechanical systems*, *13*(3), 429-440.

[14] Beeby, S. P., Tudor, M. J., Koukharenko, E., White, N. M., O'Donnell, T., Saha, C., & Roy, S. (2004). Micromachined silicon generator for harvesting power from vibrations.

[15] Huang, W. S., Tzeng, K. E., Cheng, M. C., & Huang, R. S.(2003). Design and fabrication of a vibrational micro-generator for wearable MEMS. In *Eurosensors XVII, The 17th European Conference on Solid-State Transducers, University of Minho Guimaraes*, Institute of Electrical and Electronics Engineers.

[16] Perez-Rodriguez, A., Serre, C., Fondevilla, N., Cereceda, C., Morante, J. R., Esteve, J., & Montserrat, J. (2005). Design of electromagnetic inertial generators for energy scavenging applications. *Proc. Eurosensors XIX (Barcelona, Spain)*.

[17] Glynne-Jones, P., Tudor, M. J., Beeby, S. P., & White, N. M. (2004). An electromagnetic, vibration-powered generator for intelligent sensor systems. *Sensors and Actuators A: Physical*, *110*(1-3), 344-349.

[18] Roundy, S., Wright, P. K., & Pister, K. S. (2002, January). Micro-electrostatic vibration-to-electricity converters. In *ASME 2002 International Mechanical Engineering Congress and Exposition* (pp. 487-496). American Society of Mechanical Engineers.

[19] Meninger, S. S. E. (1999). *A low power controller for a MEMS based energy converter* (Doctoral dissertation, Massachusetts Institute of Technology).

[20] Despesse, G., Jager, T., Jean-Jacques, C., Léger, J. M., Vassilev, A., Basrour, S., & Charlot, B. (2005, June). Fabrication and characterization of high damping electrostatic micro devices for vibration energy scavenging. In *Proc. Design, Test, Integration and Packaging of MEMS and MOEMS* (pp. 386-390).

[21] Lovinger, A. J. (1983). Ferroelectric polymers. *Science*, *220*(4602), 1115-1121.

[22] Nye, J. F. (1985). *Physical properties of crystals: their representation by tensors and matrices*. Oxford university press.

[23] Warner, A. W., Berlincourt, D., Meitzler, A. H., Tiersten, H. F., Coquin, G. A., & Welsh, I. F. S. (1988). *IEEE standard on piezoelectricity (ANSI/IEEE standard 176-1987)*. Technical report, The Institute of Electrical and Electronics Engineers, Inc.

[24] Matoroc, M. (1996). Piezoelectric ceramics databook for designers. *Morgan Matoroc Ltd*.

[25] Gonzalez, J. L., Rubio, A., & Moll, F. (2001, October). A prospect on the use of piezoelectric effect to supply power to wearable electronic devices. In *Proceedings of the International Conference on Materials Engineering Resources (ICMR)* (pp. 202-206).

[26] Cavallier, B., Nouira, H., Foltête, E., Hirsinger, L., & Ballandras, S. (2005). Energy Storage Capacity of Vibrating Structure: application to a Shock System, Symposium on Design, Test, Integration and Packaging of MEMS/MOEMS (DTIP 2005), Montreux, Switzerland. *Proceedings of DTIP 2005*, pp-391.

[27] Roundy, S., & Zhang, Y. (2005, February). Toward self-tuning adaptive vibration-based microgenerators. In *Smart Structures, Devices, and Systems II* (Vol. 5649, pp. 373-385). International Society for Optics and Photonics.

[28] Leland, E. S., & Wright, P. K. (2006). Resonance tuning of piezoelectric vibration energy scavenging generators using compressive axial preload. *Smart Materials and Structures*, *15*(5), 1413.

[29] Eichhorn, C., Goldschmidtboeing, F., & Woias, P. (2008). A frequency tunable piezoelectric energy converter based on a cantilever beam. *Proceedings of PowerMEMS*, *9*(12), 309-312.

[30] Morris, D. J., Youngsman, J. M., Anderson, M. J., & Bahr, D. F. (2008). A resonant frequency tunable, extensional mode piezoelectric vibration harvesting mechanism. *Smart Materials and Structures*, *17*(6), 065021.

[31] Youngsman, J. M., Luedeman, T., Morris, D. J., Anderson, M. J., & Bahr, D. F. (2010). A model for an extensional mode resonator used as a frequency-adjustable vibration energy harvester. *Journal of Sound and Vibration*, *329*(3), 277-288.

[32] Wu, X., Lin, J., Kato, S., Zhang, K., Ren, T., & Liu, L. (2008). A frequency adjustable vibration energy harvester, In *Proceedings Power MEMS*, 245-248.

[33] Challa, V. R., Prasad, M. G., Shi, Y., & Fisher, F. T. (2008). A vibration energy harvesting device with bidirectional resonance frequency tunability. *Smart Materials and Structures*, *17*(1), 015035.

[34] Reissman, T., Wolff, E. M., & Garcia, E. (2009, April). Piezoelectric resonance shifting using tunable nonlinear stiffness. In *Active and Passive Smart Structures and Integrated Systems 2009* (Vol. 7288, p. 72880G). International Society for Optics and Photonics.

[35] Zhu, D., Roberts, S., Tudor, J., & Beeby, S. (2008). Closed loop frequency tuning of a vibration-based micro-generator.

[36] Wu, W. J., Chen, Y. Y., Lee, B. S., He, J. J., & Peng, Y. T. (2006, March). Tunable resonant frequency power harvesting devices. In *Smart Structures and Materials 2006: Damping and Isolation* (Vol. 6169, p. 61690A). International Society for Optics and Photonics.

[37] Peters, C., Maurath, D., Schock, W., Mezger, F., & Manoli, Y. (2009). A closed-loop wide-range tunable mechanical resonator for energy harvesting systems. *Journal of Micromechanics and Microengineering*, *19*(9), 094004.

[38] MacCurdy, R. B., Reissman, T., & Garcia, E. (2008, April). Energy management of multi-component power harvesting systems. In *Active and Passive Smart Structures and Integrated Systems 2008* (Vol. 6928, p. 692809). International Society for Optics and Photonics.

[39] Challa, V. R., Prasad, M. G., & Fisher, F. T. (2009). A coupled piezoelectric–electromagnetic energy harvesting technique for achieving increased power output through damping matching. *Smart materials and Structures*, *18*(9), 095029.

[40] Tadesse, Y., Zhang, S., & Priya, S. (2009). Multimodal energy harvesting system: piezoelectric and electromagnetic. *Journal of Intelligent Material Systems and Structures*, *20*(5), 625-632.

[41] Yang, Z., & Yang, J. (2009). Connected vibrating piezoelectric bimorph beams as a wide-band piezoelectric power harvester. *Journal of Intelligent Material Systems and Structures*, *20*(5), 569-574.

[42] Shahruz, S. M. (2006). Design of mechanical band-pass filters for energy scavenging. *Journal of sound and vibration*, *292*(3-5), 987-998.

[43] Shahruz, S. M. (2006). Limits of performance of mechanical band-pass filters used in energy scavenging. *Journal of sound and vibration*, *293*(1-2), 449-461.

[44] Xue, H., Hu, Y., & Wang, Q. M. (2008). Broadband piezoelectric energy harvesting devices using multiple bimorphs with different operating frequencies. *IEEE transactions on ultrasonics, ferroelectrics, and frequency control*, *55*(9).

[45] Liu, J. Q., Fang, H. B., Xu, Z. Y., Mao, X. H., Shen, X. C., Chen, D., & Cai, B. C. (2008). A MEMS-based piezoelectric power generator array for vibration energy harvesting. *Microelectronics Journal*, *39*(5), 802-806.

[46] Lee, D. G., Carman, G. P., Murphy, D., & Schulenburg, C. (2007, June). Novel micro vibration energy harvesting device using frequency up conversion. In *Solid-State Sensors, Actuators and Microsystems Conference, 2007. TRANSDUCERS 2007. International* (pp. 871-874). IEEE.

[47] Kulah, H., & Najafi, K. (2008). Energy scavenging from low-frequency vibrations by using frequency up-conversion for wireless sensor applications. *IEEE Sensors Journal*, *8*(3), 261-268.

[48] Mann, B. P., & Sims, N. D. (2009). Energy harvesting from the nonlinear oscillations of magnetic levitation. *Journal of Sound and Vibration*, *319*(1-2), 515-530.

[49] Stanton, S. C., McGehee, C. C., & Mann, B. P. (2009). Reversible hysteresis for broadband magnetopiezoelastic energy harvesting. *Applied Physics Letters*, *95*(17), 174103.

[50] Lin, J. T., Lee, B., & Alphenaar, B. (2010). The magnetic coupling of a piezoelectric cantilever for enhanced energy harvesting efficiency. *Smart materials and Structures*, *19*(4), 045012.

[51] Ramlan, R., Brennan, M. J., Mace, B. R., & Kovacic, I. (2010). Potential benefits of a non-linear stiffness in an energy harvesting device. *Nonlinear dynamics*, *59*(4), 545-558.

[52] Erturk, A., Hoffmann, J., & Inman, D. J. (2009). A piezomagnetoelastic structure for broadband vibration energy harvesting. *Applied Physics Letters*, *94*(25), 254102.

[53] Erturk, A., & Inman, D. J. (2008). Issues in mathematical modeling of piezoelectric energy harvesters. *Smart Materials and Structures*, *17*(6), 065016.

[54] Gammaitoni, L., Neri, I., & Vocca, H. (2009). Nonlinear oscillators for vibration energy harvesting. *Applied Physics Letters*, *94*(16), 164102.

[55] Cottone, F., Vocca, H., & Gammaitoni, L. (2009). Nonlinear energy harvesting. *Physical Review Letters*, *102*(8), 080601.

[56] Moehlis, J., DeMartini, B. E., Rogers, J. L., & Turner, K. L. (2009, January). Exploiting nonlinearity to provide broadband energy harvesting. In *ASME 2009 Dynamic Systems and Control Conference* (pp. 119-121). American Society of Mechanical Engineers.

[57] Ferrari, M., Ferrari, V., Guizzetti, M., Andò, B., Baglio, S., & Trigona, C. (2009). Improved energy harvesting from wideband vibrations by nonlinear piezoelectric converters. *Procedia Chemistry*, *1*(1), 1203-1206.

[58] McInnes, C. R., Gorman, D. G., & Cartmell, M. P. (2008). Enhanced vibrational energy harvesting using nonlinear stochastic resonance. *Journal of Sound and Vibration*, *318*(4-5), 655-662.

[59] Wellens, T., Shatokhin, V., & Buchleitner, A. (2003). Stochastic resonance. *Reports on progress in physics*, *67*(1), 45.